ARTERIAL HYPOXIA IN ATHEROSCLEROSIS

ARTERIAL HYPOXIA IN HYPERGLYCEMIC ACCELERATED ATHEROSCLEROSIS

By: ALEXANDRA BRUTON, BMSc.

A Thesis Submitted to the School of Graduate Studies in Partial Fulfilment of the Requirements for the Degree Master of Science

McMaster University MASTER OF SCIENCE (2020) Hamilton, Ontario

(Medical Sciences)

TITLE: Arterial Hypoxia in Hyperglycemic Accelerated Atherosclerosis

AUTHOR: Alexandra Bruton, BMSc. (University of Western Ontario)

SUPERVISOR: Dr. G. H. Werstuck

NUMBER OF PAGES: CLX, 160

LAY ABSTRACT

Individuals with diabetes have elevated blood glucose levels which can damage blood vessels throughout the body. This damage can result in the development of cardiovascular diseases. The vasa vasorum is a distinct microvessel network that surrounds the walls of large arteries. Damage to the vasa vasorum can result in decreased oxygen supply to the artery wall, triggering low oxygen environments and accelerated atherosclerosis development. In this study we aim to investigate the mechanisms associated with high glucose induced vasa vasorum damage. Results demonstrate reduced vessel formation of human endothelial cells in high glucose conditions. This decrease correlates with advanced glycation end products and oxidative stress inducing a decreased expression of vascular endothelial growth factor A, a known stimulator of vessel formation. Understanding of the unorthodox pathways of atherosclerosis in diabetes will facilitate the development of new and more effective treatment strategies for this ongoing epidemic.

ABSTRACT

Individuals with diabetes mellitus (DM) have a 2 to 4-fold increased risk of cardiovascular diseases (CVD) compared to those without DM. A contributing factor to the development of CVD is atherosclerosis, a chronic inflammatory disease causing plaque build-up in medium to larger arteries. Increasing evidence suggests that hypoxia within the arterial wall is known to promote atherosclerosis, however the underlying mechanisms remain unclear. Our lab has previously shown that hyperglycemic APOE-deficient mice have impaired angiogenesis of the aortic vasa vasorum, increased arterial hypoxia, elevated vascular inflammation and accelerated atherosclerosis development at 15 weeks of age compared to normoglycemic APOE-deficient controls. The objective of this study is to elucidate the mechanisms associated with these differences, specifically the reductions in vasa vasorum. The effects of hyperglycemia and specific interventions to modulate endoplasmic reticulum stress (4-phenylbutyric acid (4PBA)), oxidative stress (n-acetyl-cysteine (NAC)) and advanced glycation end products (pyridoxamine (PX)) are examined *in vivo* and *in vitro*.

Results demonstrate that human cardiac microvascular endothelial cells (HMVEC-Cs) have reduced angiogenesis in high glucose compared

to normal glucose conditions in both hypoxic and normoxic environments. This may be associated with reduced expression of vascular endothelial growth factor A (VEGF-A). Treatment with PX or NAC in hypoxic, high glucose conditions increased the angiogenesis and expression of VEGF-A in HMVEC-Cs. Pilot studies suggest that PX, NAC or 4PBA supplementation are well tolerated in drinking water using STZ mouse models. Future studies should assess the direct effects of each of the chemical interventions on vasa vasorum angiogenesis, arterial hypoxia and atherosclerosis. These results suggest that oxidative stress and advanced glycation end products play a more significant role in reducing microvessel angiogenesis *in vitro*. Understanding of the non-canonical pathways of atherosclerosis progression in the presence of DM will facilitate the development of novel and more specific treatments for this ongoing epidemic.

ACKNOWLEDGEMENTS

I would like to thank numerous individuals for their support and continual guidance with this thesis project. Firstly, I would like to thank my supervisor Dr. G. H. Werstuck. Despite limited experience in the research field prior to my graduate degree, he gave me the chance I knew that I deserved. This initial vouch of confidence allowed me to grow into an independent, motivated and hardworking researcher. For this I will be forever grateful. Further, I would like to thank him for his unconditional care and direction with this project and with my work. Without him none of this would have been possible.

Secondly, I would like to thank my committee members, Dr. Hertzel Gerstein and Dr. Judy West-Mays, for the time they spent with me amending my mistakes and motivating me to pursue my goals. Both brought different perspectives and clinical opinions to my research that allowed me to think outside of the box, examine the bigger picture of my research and drive creativity and innovation.

Thirdly, I would like to thank my colleagues at the time, including Dr. Monica De Paoli, Lauren Mastrogiacomo, Sarvatit Patel and Dr. Daniel Venegas. They constantly supported me through the ups and downs of my degree, giving me much needed advice and guidance to succeed with this

project. I could not have asked for more understanding, respectful and enjoyable colleagues, more importantly friends, to be around each day. I wish them the best of luck with their individual endeavours as they continue to strive towards their research and individual goals.

Fourthly, I would like to thank our lab technician Dr. Peter Shi who was an essential member of this project. Not only did he help me with the technical aspects of my thesis, but he consistently assisted with some of the more difficult tasks I faced. He created a positive work environment, with open communication in case any issues arose.

Finally, I would like to thank my support system outside of academia, including my parents, Linda and Stephen Bruton, and my friends. With their encouragement and enthusiasm I have grown into a more well-rounded individual ready to tackle any future problems I face.

TABLE OF CONTENTS

LIST OF FIGURES

LIST OF TABLES

LIST OF ABBREVIATIONS AND SYMBOLS

4PBA	4-Phenyl-Butyric Acid
AGEs	Advanced Glycation End Products
ANOVA	Analysis of Variance
APOE	Apolipoprotein E
$APOE^{-/-}$	Apolipoprotein E Deficient
BCA	Bicinchoninic Acid
CANTOS	Canakinumab, Anti-Inflammatory Thrombosis Outcome Study
CBP	CREB-Binding Protein
cDNA	Complementary Deoxyribonucleic Acid
CHOP	C/EBP Homologous Protein
Csf1r	Colony Stimulating Factor 1 Receptor
CVD	Cardiovascular Disease
DAB	3,3'-Diaminobenzidine
Dll4	Delta Like Ligand 4
DM	Diabetes Mellitus
DN	Diabetic Nephropathy
DNA	Deoxyribonucleic Acid
DR	Diabetic Retinopathy

EDTA	Ethylenediaminetetraacetic Acid
eNOS	Endothelial Nitric Oxide Synthase
ER	Endoplasmic Reticulum
FDA	Food and Drug Administration
GAPDH	Glyceraldehyde 3-Phosphate Dehydrogenase
GFAT	Glutamine Fructose-6 Phosphate Amidotransferase
GLUT1	Glucose Transporter 1
GRP78	Glucose Regulated Protein 78
GRP94	Glucose Regulated Protein 94
HbA_{1c}	Hemoglobin A1C
HBP	Hexosamine Biosynthesis Pathway
HDL	High Density Lipoprotein
HFD	High Fat Diet
HG	High Glucose
HIF	Hypoxia Inducible Family
HMVEC-C	Human Cardiac Microvascular Endothelial Cells
HRE	Hypoxia Response Element
ICAM-1	Intercellular Adhesion Molecule 1
IgG	Immunoglobulin G
IL-1	Interleukin-1
iNOS	Inducible Nitric Oxide Synthase

IP	Intraperitoneal
LAD	Left Anterior Descending
LDL	Low Density Lipoprotein
MI	Myocardial Infarction
N_2	Nitrogen
NAC	N-Acetyl-Cysteine
NaOH	Sodium Hydroxide
NG	Normal Glucose
NLRP3	NLR Family Pyrin Domain Containing 3
NO	Nitric Oxide
NRP-1	Neuropilin 1
O_2	Oxygen
oxLDL	Oxidized Low Density Lipoprotein
PBS	Phosphate Buffered Saline
PCR	Polymerase Chain Reaction
PHD	Prolyl Hydroxylase
PMA	Phorbol 12-Myristate 13-Acetate
PMAr	Phorbol 12-Myristate 13-Acetate Rested
PX	Pyridoxamine
qPCR	Real-Time Polymerase Chain Reaction
RAGE	Receptor for Advanced Glycation End Products

RNA	Ribonucleic Acid
RNS	Reactive Nitrogen Species
ROS	Reactive Oxygen Species
SDS-PAGE	Sodium Dodecyl Sulfate Polyacrylamide Gel Electrophoresis
SEM	Standard Error of the Mean
SMC	Smooth Muscle Cell
STZ	Streptozotocin
T1DM	Type 1 Diabetes Mellitus
T2DM	Type 2 Diabetes Mellitus
TAG	Triacylglycerol
tAUC	Trapezoidal Area Under the Curve
Ub	Ubiquitinate
UDP-GlcNAc	UDP-*N*-Acetyl Glucosamine
UPR	Unfolded Protein Response
VCAM-1	Vascular Adhesion Molecule 1
VEGF	Vascular Endothelial Growth Factor
VEGFR	Vascular Endothelial Growth Factor Receptor
VHL	Von Hippel-Lindau Tumor Suppressor
VLDL	Very Low Density Lipoprotein
WT	Wildtype

DECLARATION OF ACADEMIC ACHIEVEMENT

This study has utilized an *in vitro* assay system to elucidate the potential mechanisms associated with hyperglycemic induced damage to microvessels. It has found reduced angiogenesis of human cardiac microvascular endothelial cells in high glucose, normal oxygen or reduced oxygen conditions. This reduction in low oxygen conditions, has been associated with hyperglycemic interference of VEGF-A and VEGFR-2 expression. This interference is most likely a result of oxidative stress or advanced glycation end products, as inhibitors of these pathways elevated tube formation back to normal glucose conditions. Pilot studies with *in vivo* administration of each of the chemical inhibitors (4PBA, NAC or PX) were well tolerated in STZ-APOE$^{-/-}$ mice, a DM atherosclerosis prone model.

In vitro and *in vivo* work conducted in this thesis was completed by Alexandra Bruton with some assistance. Dr. Peter Shi expanded and cryopreserved HMVEC-Cs for cell culture use, and assisted with harvesting and tissue collection. Dr. Daniel Venegas helped with breeding strategies, before passing on the colony. He also bred and monitored the APOE colony, providing mice when needed for *in vivo* experiments and breeding purposes.

1.0. INTRODUCTION

1.1. Diabetes Mellitus

1.1.1. Definitions, Diagnosis, Therapies and Epidemiology

Diabetes mellitus (DM) is a chronic metabolic disease characterized by impaired insulin secretion by pancreatic β cells[1]. DM may also be accompanied by a decreased response to the action of insulin in peripheral tissues, such as adipose or muscle, termed insulin resistance. Although all types of DM involve metabolic dysfunction, their individual etiologies differ. Type 1 DM (T1DM), previously known as insulin dependent or juvenile DM, is an autoimmune disorder characterized by the destruction of pancreatic β cells by immune cells[1]. This disease results in decreased β cell mass and deficient insulin secretion[1]. T1DM accounts for approximately 5-10% of all diagnosed cases of DM[2]. In contrast, type 2 DM (T2DM), previously known as non-insulin dependent or adult onset DM, occurs as a result of insulin resistance in peripheral tissues as well as insufficient insulin secretion[2]. T2DM accounts for 90-95% of all cases of DM[2]. Although different types of DM exist, the clinical definition of all forms is hyperglycemia, described as consistently elevated blood glucose levels.

The clinical criteria for diagnosing DM in humans is a fasting plasma glucose level ≥ 7.0 mmol/L, a 2-hour plasma glucose level in a 75-

gram oral glucose tolerance test ≥ 11.1 mmol/L, a random plasma glucose level ≥ 11.1 mmol/L, or a glycated hemoglobin A_{1c} (HbA_{1c}) measurement ≥ 6.5%[2]. HbA_{1c} evaluates average blood glucose levels over a period of approximately three months prior to the test. This is advantageous to clinicians for measuring chronic hyperglycemia[2]. Individuals with slightly elevated blood glucose levels, such as a fasting plasma glucose level of 6.1 to 6.9 mmol/L or an HbA_{1c} measurement of 6% to 6.4% are diagnosed with pre-diabetes[2]. It is important to identify pre-diabetic patients as they also have an increased risk for the development of DM and associated complications of DM.

Despite a wide variety of medication and lifestyle therapies for the management of DM, there is currently no cure. Exogenous insulin can be supplied through insulin injections, continuous subcutaneous insulin infusions with an insulin pump or a closed-loop insulin delivery system, termed an artificial pancreas[3]. Other medications include metformin, glucagon-like peptide-1 receptor agonists and sodium-glucose co-transporter 2 inhibitors[3]. Lifestyle management can include dietary and exercise plans, as well as reducing blood pressure and stress levels[3]. Despite considerable advances in the present treatment options for patients with DM, there are limitations to their effectiveness. This includes

difficulties maintaining acceptable glycemic control while limiting extreme blood glucose variation over time.

The prevalence of diagnosed T1DM and T2DM patients in Canada is approximately 10%. However, evaluations including undiagnosed T2DM and pre-diabetic patients estimate this value to be up to 28%[3]. Diabetes Canada predicts a continual increase in disease diagnosis, reaching a prevalence rate of 32% by 2028[3]. These increasing prevalence rates of DM represent a significant healthcare and economic burden. Specifically, Diabetes Canada estimates a current direct healthcare cost of $14 billion, increasing to $39 billion by 2028[3].

1.1.2. Generalized Diabetic Complications

Generally the complications of DM are separated into two groups: acute and chronic. Acute complications are short-term emergencies and include diabetic ketoacidosis and hyperosmolar hyperglycemic non-ketotic state[38]. Diabetic ketoacidosis occurs due to decreased glycogen storage and increased lipolysis[38]. As more triglycerides are hydrolyzed by the liver, free fatty acids are converted into acidic ketone bodies[39]. This increase in ketones can lead to acidic blood, termed metabolic acidosis[39]. In contrast, hyperosmolar hyperglycemic non-ketotic state occurs due to chronically elevated glucose levels, resulting in severe dehydration[38].

Chronic complications of DM are long-term consequences that lead to irreparable damage to the body and organ systems. Despite current therapeutic approaches, DM patients still have an increased risk of developing chronic complications such as retinopathy, nephropathy, neuropathy and cardiovascular disease.

Diabetic Retinopathy (DR) is a complication of hyperglycemia that can be divided into three stages[4]. Mild to moderate non-proliferative DR is the earliest stage of DR caused by damage to retinal pericytes[4]. Apoptosis of pericytes, specialized cells that maintain the structure of retinal blood vessels, by hyperglycemia can lead to capillary outpouching and microaneurysm formation[40]. The second stage, severe non-proliferative DR, is characterized by further weakening of blood vessels and endothelial damage[40]. Severe non-proliferative DR results in vessel occlusion, retinal ischemia and tissue hypoxia[40]. The final stage, termed proliferative DR, occurs due to extensive retinal ischemia resulting in increased vascular endothelial growth factor (VEGF) expression leading to retinal angiogenesis[4,40]. Newly synthesized blood vessels are abnormally delicate causing blood leakage, scar tissue formation and retinal detachment leading to distorted vision or complete vision loss[40].

Diabetic Nephropathy (DN) involves damage to the blood vasculature of the kidney as a result of high glucose concentrations damaging endothelial cells. The pathophysiology of DN includes glomerular mesangial cell expansion, thickening of the glomerular basement membrane and glomerular sclerosis[41]. DN can lead to proteinuria, and overall reduced kidney filtration and function[41].

Diabetic Neuropathy involves hyperglycemic induced damage to small blood vessels supplying peripheral nerves[5]. This damage can impact blood supply and oxygen levels in neurons causing long-term nerve degeneration[5].

Cardiovascular Disease (CVD) is a complication of DM resulting from hyperglycemic induced damage to cardiac blood vessels and nerves[6]. Individuals with DM have a 2 to 4-fold increased risk of CVD compared to those without DM, even after controlling for modifiable risk factors such as dyslipidemia[6]. CVDs include systolic and diastolic heart failure, myocardial infarction (MI), stroke, heart valve disease, cardiomyopathies, deep vein thrombosis and pulmonary embolism.

Other chronic complications of DM include peripheral vascular disease, skin conditions, cataracts, hypertension and impaired wound healing[3].

1.1.3. Vascular Diabetic Complications

Traditionally, the chronic complications of DM on the blood vasculature have been divided into two categories: macrovascular and microvascular. Macrovascular complications include structural and functional alterations to the large blood vessels such as atherosclerosis, leading to an increased risk for MI or stroke[7]. In contrast, microvascular complications include disruptions to capillary networks associated with the development of DN and DR[8]. Accumulating evidence suggests that these two groups are in fact closely related. For example, a meta-analysis of 20 epidemiological studies showed that T1DM and T2DM patients with any degree of DR had a 2 to 4-fold increased risk of future ischemic cardiovascular events, compared to those without DR[9]. Further, the risk of cardiovascular events increased with the degree of DR[9]. A better understanding of the associations between macrovascular and microvascular complications in DM will facilitate the development of new treatments strategies.

1.2. Vasculature and Atherosclerosis

1.2.1. Blood Vessel Structure and Function

Blood vessels make up a large portion of the human anatomy, playing an extensive role in homeostasis and oxygen transport. Blood vessels vary greatly in size and type, however arteries generally have three distinct layers: the tunica intima, tunica media and tunica adventitia[42]. The tunica intima is the innermost layer of arteries, consisting of a simple squamous layer of endothelial cells, a fibrous basement membrane and a subendothelial layer of elastic fibers[42]. This layer is in direct contact with the blood and is the site of monocyte trafficking and extravasation through increased endothelial adhesion molecule expression[42]. Below this layer is the tunica media, primarily made of smooth muscle cells, elastic fibers and collagen. The function of the tunica media, in conjunction with smooth muscle cells, is to regulate the blood flow, blood pressure and tone of the vessels by dilation and constriction to widen or narrow the vessel diameter[42]. The external layer, termed the tunica adventitia, is composed of collagen and elastic fibers. Its role is mainly structural, anchoring arteries to their respective organs[42].

1.2.2. Canonical Atherosclerosis Theory

Atherosclerosis is a chronic inflammatory disease involving plaque build-up in medium to larger arteries that can result in disrupted blood flow[10]. The etiology of atherosclerosis is complex, influenced by genetic, environmental and metabolic dysfunction[11].

The earliest detectable change in the development of atherosclerosis is the occurrence of fatty streaks[12]. These initial streaks are the result of a focal increase in lipoproteins in the tunica intima of arteries[13]. Lipoproteins contain an inner fat core and an outer lipid membrane containing proteins[14]. There are four major classes of lipoproteins: chylomicrons, very low-density lipoprotein (VLDL), low-density lipoprotein (LDL) and high-density lipoprotein (HDL)[14]. Each of these particles play a role in lipid transport, metabolism and regulation by the liver. Briefly, VLDL and chylomicrons facilitate the delivery of triacylglycerol (TAG) to cells of the body through the conversion of TAG to fatty acids[14]. In comparison, LDL delivers cholesterol to cells via LDL receptor-mediated endocytosis[14]. This is important for the synthesis of lipid membranes. Finally, HDL is involved in reverse cholesterol transport, allowing excess cholesterol to be brought back to the liver for elimination.

Normally, there is a homeostatic balance between plasma LDL and subendothelial LDL[12]. However, LDLs modified through glycation or

oxidation become trapped, resulting in endothelial cell activation[10]. Endothelial activation is characterized by a loss of vascular wall integrity and an increased expression of leukocyte adhesion molecules, including intercellular adhesion molecule-1 (ICAM-1) and vascular cell adhesion molecule-1 (VCAM-1) on the endothelial cell surface[11]. Monocytes and T cells are then recruited to the vessel wall releasing pro-inflammatory cytokines. These monocytes differentiate into macrophages, which uptake oxidized LDLs and become foam cells[11]. Foam cells secrete cytokines that stimulate smooth muscle cell migration and proliferation, collagen accumulation and fibrous cap formation contributing to plaque build-up[11]. Ultimately, foam cells can undergo apoptosis, resulting in the formation of a necrotic core within the developing lesion. This process determines the development of unstable lesions which are generally defined by a large necrotic core and thin fibrous cap. Although the fibrous collagen cap seals the lesion, proteases such as metalloproteinases can degrade collagen[12]. This weakens the fibrous cap promoting plaque rupture and thrombus formation[12]. The formation of a thrombus can partially or fully occlude arteries leading to acute infarction. Partially occluding blood clots can erode leading to acute infarction at various secondary sites downstream. DM is a significant independent risk factor for the development of atherosclerosis through various biochemical pathways (**Figure 3**).

Figure 1. Canonical Atherosclerosis Model.

Atherosclerosis typically occurs at the site of bifurcations or curvature points of vessels and begins with a stressor initiating endothelial cell injury. Endothelial cell activation increases the expression of endothelial adhesion molecules (ICAM-1, VCAM-1, P-selectin and E-selectin) which allow circulating leukocytes to bind and extravasate into the vascular wall. Endothelial activation also increases the permeability of endothelial cells, allowing low-density lipoproteins (LDLs) to enter into the vascular wall, become modified through glycation or oxidation (oxLDLs) and get trapped in the intima layer. Inside the wall, monocytes differentiate into tissue specific macrophages, uptake trapped modified low-density lipoproteins and become foam cells. Foam cells release cytokines that induce the migration of smooth muscle cells (SMCs) up into the subendothelial layer where they start to produce collagen and form the fibrous cap. Foam cells can undergo apoptosis and form the necrotic core of the developing lesion. Unstable plaques, characterized by thin fibrous caps and large necrotic cores, are prone to rupture leading to thrombus formation. Thrombi can partially or fully occlude blood vessels leading to acute MI or stroke at the primary site. Further, partially occluding thrombi can rupture, travel through the vasculature and initiate acute MI or stroke in various secondary sites downstream.

Image adapted from Wallert, M., Schmölz, L., Galli, F., Birringer, M., & Lorkowski, S.[70]

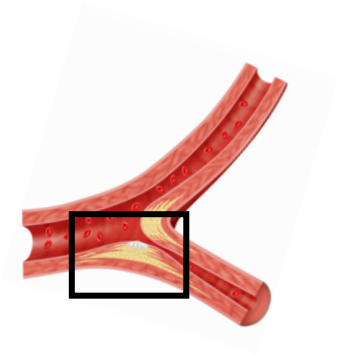

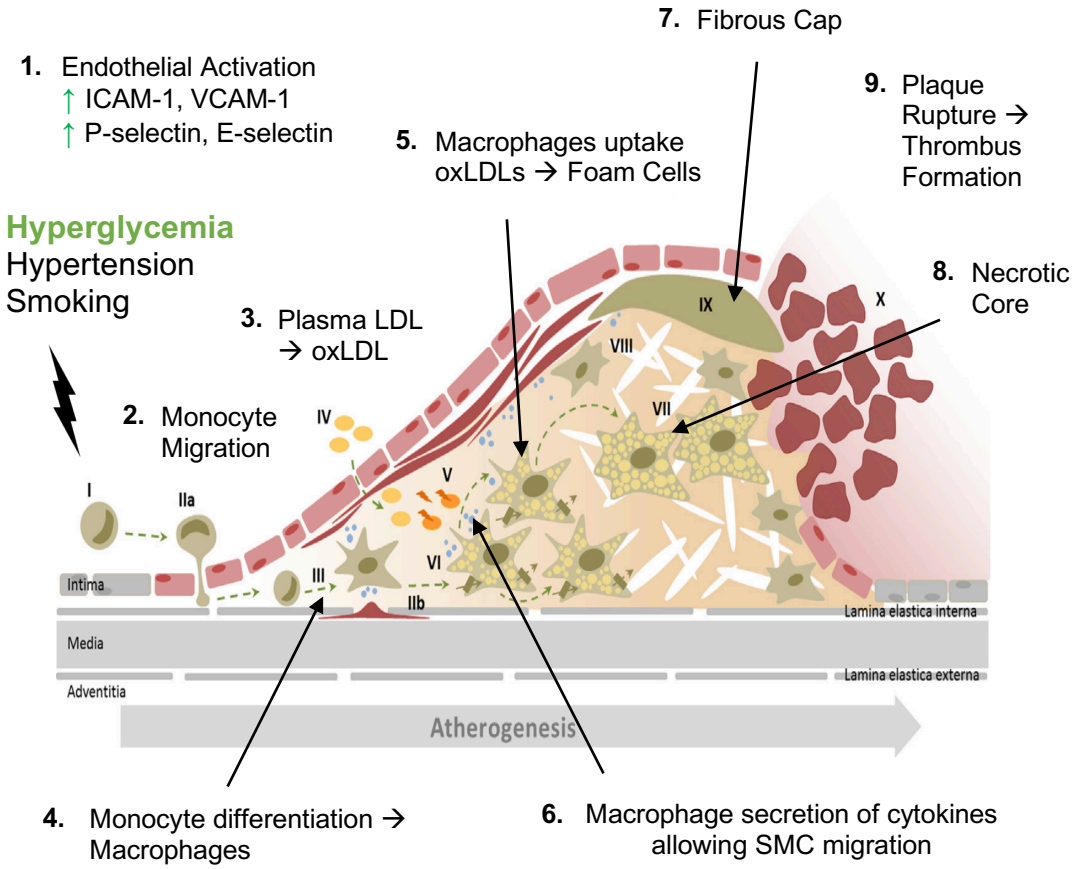
7. Fibrous Cap
1. Endothelial Activation
↑ ICAM-1, VCAM-1
↑ P-selectin, E-selectin
9. Plaque Rupture → Thrombus Formation
5. Macrophages uptake oxLDLs → Foam Cells
Hyperglycemia
Hypertension
Smoking
8. Necrotic Core
3. Plasma LDL → oxLDL
2. Monocyte Migration
IX
X
VIII
VII
IV
V
I
IIa
VI
III
IIb
Intima
Media
Adventitia
Lamina elastica interna
Lamina elastica externa
Atherogenesis
4. Monocyte differentiation → Macrophages
6. Macrophage secretion of cytokines allowing SMC migration

1.2.3. Anoxemia Atherosclerosis Theory

The canonical atherosclerosis model (**Figure 1**) is the widely accepted pathway for atherosclerosis development in current research. This model emphasizes atherosclerosis development through a lipid-driven macrovascular mechanism, however it does not consider the development of atherosclerosis in patients with normal LDL cholesterol levels. As a matter of fact, studies show that approximately 50% of patients without cardiovascular risk factors, such as dyslipidemia, still have subclinical arterial calcification[15]. Further, this model fails to consider the relationship between both macrovascular and microvascular disease, as well as other mechanisms including inflammation and tissue hypoxia that could drive atherosclerosis development. Therefore, it is important to assess other less commonly accepted pathways of atherosclerosis development such as the “anoxemia theory.”

The anoxemia theory states that any imbalance in the supply or demand of oxygen within the arterial wall plays a role in the progression of atherosclerosis[71]. This is relevant to the canonical model of atherosclerosis due to the increased thickening of the arterial wall resulting in hypoxia, a low oxygen environment. Our previous and current experiments focus on oxygen supply to the aorta by examining the aortic vasa vasorum, a small microvascular capillary bed that surrounds the

walls of large arteries. We also study oxygen demand by examining changes in arterial inflammation. Using this analysis, a potential reduction of accelerated atherosclerosis induced by DM could aim at 1) increasing aortic oxygen supply by elevating vasa vasorum angiogenesis or 2) reducing aortic oxygen demand by attenuating arterial wall inflammation.

1.2.4. Oxygen Supply – Vasa Vasorum

The vasa vasorum is a distinct microvascular capillary network that surrounds the walls of large vessels[16, 17]. The literal translation of vasa vasorum is “vessels of the vessels” and therefore, by definition, it is the place where the microvasculature and macrovasculature meet. The role of these microvessels is to remove waste products and deliver nutrients and oxygen to the cells of the macrovasculature[16]. Typically, small vessels depend on diffusion to transport waste products and nutrients. However, large vessels with a luminal diameter greater than 0.5 mm cannot depend on diffusion alone[18]. For example, the tunica intima thickens normally when vessels grow (termed diffuse intimal thickening) leading to hypoxia. As a result, vasa vasorum undergo angiogenesis in order to increase vascularization and eliminate oxygen deficiency of the surrounding cells[16]. Although normal vascular growth can stimulate angiogenesis of the vasa vasorum, additional stimuli such as inflammation and vascular wall

thickening in atherogenesis can also trigger the cascade. Despite a relationship between vasa vasorum growth and vascular wall thickening in atherosclerosis, it is still unclear whether vasa vasorum angiogenesis plays a causal role in atherosclerotic lesion development or if lesion progression drives angiogenesis.

1.2.5. Vasa Vasorum in Atherosclerosis

Previous studies have examined vasa vasorum angiogenesis in atherosclerosis in the absence of hyperglycemia[30,43]. These studies found increased angiogenesis of the vasa vasorum, structured in dense plexuses, around coronary arteries with extensive atherosclerosis[30,43]. This rapid angiogenesis, similar to that in proliferative DR, creates delicate and immature microvessels susceptible to hemorrhage[44]. Although most research accepts the infiltration of inflammatory cells through luminal endothelial cell adhesion molecule expression, others have proposed that increased density of adventitial vasa vasorum could act as conduits for further inflammatory cell infiltration in advanced atherosclerosis[18]. Despite a known relationship between vasa vasorum angiogenesis and atherosclerosis in the absence of hyperglycemia, little was known about vasa vasorum angiogenesis and atherosclerosis in the presence of hyperglycemia prior to our previous studies[31].

1.2.6. Vasa Vasorum in Hyperglycemic Accelerated Atherosclerosis

Vasa vasorum angiogenesis and atherosclerosis progression was examined in our lab using diabetic, atherosclerosis prone mice. Results showed an initial, significant reduction in the aortic vasa vasorum density of hyperglycemic APOE-deficient mice at 15 and 20 weeks of age compared to normoglycemic APOE-deficient controls[31]. These results correlated with a significantly increased aortic sinus lesional area, lesional volume and necrotic core at 15 weeks of age in hyperglycemic APOE-deficient mice compared to normoglycemic APOE-deficient controls[31]. Despite early reductions in angiogenesis of the aortic vasa vasorum in hyperglycemic APOE-deficient mice, results showed elevated aortic hypoxia marker staining (hypoxia-inducible factor 1-alpha, HIF-1α) with a relative, significant deficiency in aortic angiogenesis stimulator staining (vascular endothelial growth factor A, VEGF-A)[31]. These results contrast those seen in mice without hyperglycemia[30]. This suggests that 1) in addition to affecting the microvessels of other tissues, such as the retina in DR, hyperglycemia impairs normal vasa vasorum angiogenesis and 2) increased angiogenesis of the vasa vasorum is not required for the development of atherosclerosis[31]. The reason for the disconnect between high HIF-1α and low VEGF-A in this experiment still remains unclear[31].

These findings were further confirmed by evaluating the intima-media and adventitial vasa vasorum density in autopsied human left anterior descending (LAD) coronary arteries[45]. Results demonstrated a significant reduction in the vasa vasorum density of patients with DM compared to those without DM[45]. Further, a significant negative correlation between post-mortem whole blood HbA_{1c} measurements and vasa vasorum density was identified, with higher HbA_{1c} levels resulting in lower vasa vasorum densities of the LAD coronary artery[45].

Figure 2. Vasa Vasorum Angiogenesis in Atherosclerosis.

The relationship between vasa vasorum angiogenesis and atherosclerosis progression depends on glycemic control. Under normoglycemic conditions, increased inflammation rapidly drives adventitial vasa vasorum angiogenesis, increasing inflammatory cell infiltration, hemorrhage and advanced atherosclerosis development. In hyperglycemic conditions, with chronically elevated blood glucose levels, hyperglycemic induced vasa vasorum damage reduces vasa vasorum angiogenesis increasing arterial wall hypoxia and driving accelerated atherosclerosis progression compared to normoglycemic conditions.

Image adapted from Jenkins, N. The Vasa Vasorum.[73]

i. Normoglycemic Atherosclerosis

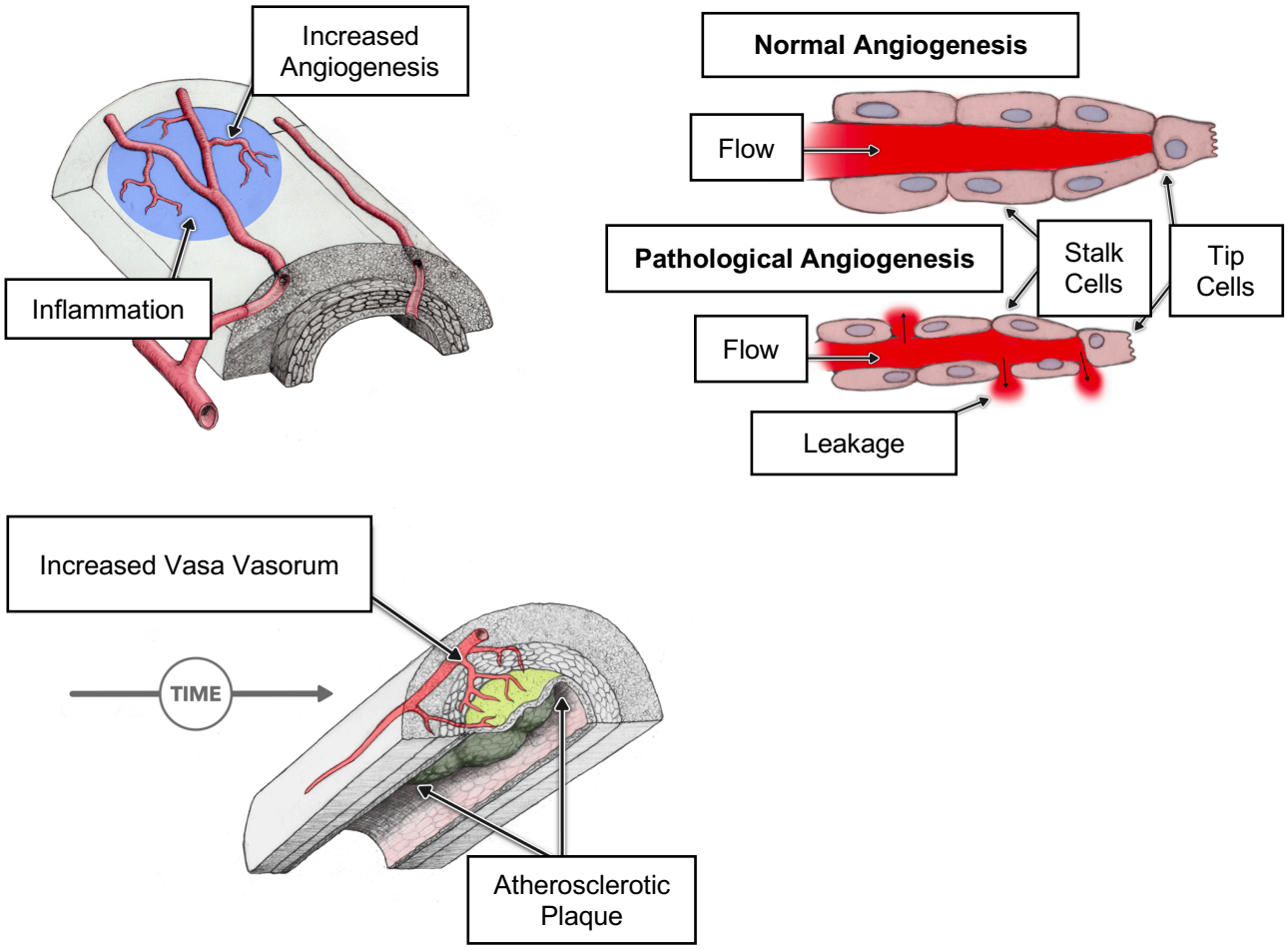

ii. Hyperglycemic Accelerated Atherosclerosis

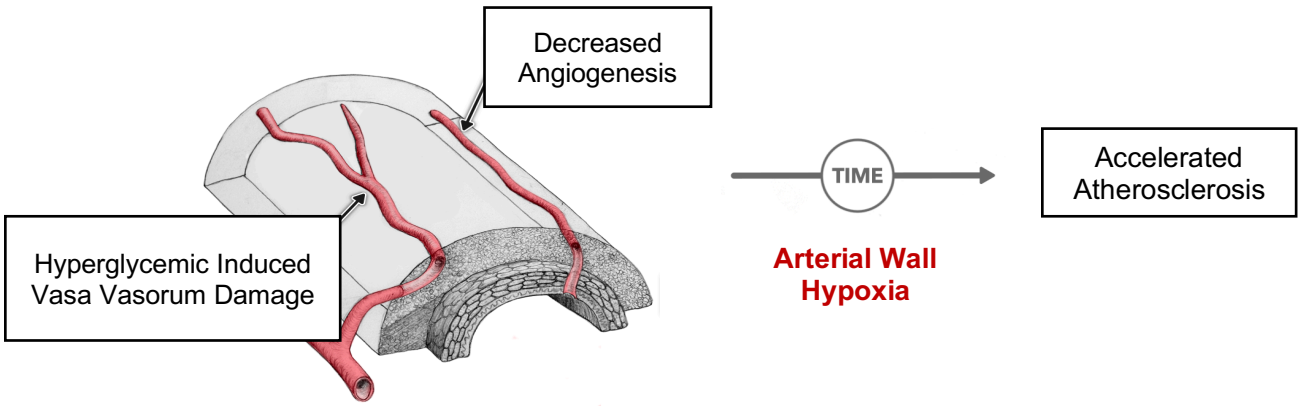

1.2.7. Oxygen Demand – Inflammation

Oxygen homeostasis can be disrupted by increasing oxygen consumption. This can occur in atherosclerosis through the infiltration and accumulation of metabolically active inflammatory cells inside the arterial wall. Inflammatory cells utilize oxygen as energy, and in inflammatory conditions release cytokines causing a hypoxic microenvironment.

Recent studies have examined the relationship between atherosclerosis development and inflammation by investigating the NLR pyrin domain containing 3 (NLRP3)[37]. NLRP3 is a component of an inflammasome that senses signals released from apoptotic or damaged cells to activate caspase-1[37]. Caspase-1 cleaves precursors of inflammatory cytokines such as IL-1β, causing inflammation[37]. NLRP3 and atherosclerosis has been investigated in mice, with findings showing that NLRP3 silencing results in decreased plaque size[37]. The CANTOS trial showed that inhibition of IL-1β through a monoclonal antibody can protect humans from cardiovascular events[38].

1.2.8. Mechanisms of Vascular Dysfunction in DM

Since associations between microvascular and macrovascular pathologies exist[9], researchers hypothesize that vascular beds are a continuum of one another[19]. This suggests that any damage to either the

macrovasculature or microvasculature can lead to damage in the other. For example, animal studies of atherosclerosis found impairment in the coronary microvasculature[19]. These findings indicate that microvascular disease may be able to predict future macrovascular outcomes and that a common unified pathway for DM-induced vascular damage could exist. DM is known to activate pathways that could lead to microvascular injury. These involve advanced glycation end products, endoplasmic reticulum stress or oxidative stress[20, 21].

Advanced Glycation End Products (AGEs): AGEs are formed through the non-enzymatic Maillard reaction between reducing sugars, such as glucose and fructose, with free amino groups of proteins or other biomolecules[20,46]. Once generated these heterogeneous complexes have a variety of deleterious effects related to CVD. These include 1) cross linking with collagen to induce vascular and cardiac tissue stiffening 2) binding to receptors of AGEs (RAGEs) in tissues causing activation of inflammatory pathways, reduction of nitric oxide (NO) biosynthesis inducing endothelial activation, and the production of reactive oxygen species (ROS) increasing oxidative stress 3) glycating LDLs which promote oxidation of LDL and 4) binding to DNA resulting in genetic mutations[46]. Commonly modified proteins include fibrinogen, albumin,

immunoglobulins and collagen resulting in impaired fibrinolysis, platelet aggregation, immune suppression and atherosclerosis respectively[20]. The role of AGEs in CVD has been studied extensively, especially in relation to DM. For example, higher levels of plasma AGEs have been found in T1DM patients with fatal or non-fatal CVD[47]. This may explain hyperglycemic accelerations in atherosclerosis progression and may present as an important target for reducing CVD outcomes. A commonly used inhibitor of AGE formation is pyridoxamine (PX), a vitamin B_6 derivative that scavenges protein carbonyls and improves cell survival[23]. Supplementation with PX has been shown to attenuate DR in rats[24]. In accordance with these studies, streptozotocin (STZ)-induced hyperglycemic APOE-deficient mice receiving PX by gavage treatment have attenuated aortic atherosclerosis[48]. Currently, the effects of PX on the vasa vasorum in DM is not known.

Oxidative Stress: Although oxygen metabolism is important for efficient aerobic energy production, cells must limit the presence of damaging oxygen metabolites including ROS. ROS, such as peroxides and superoxide, are capable of damaging cells and are generated in diabetic conditions by 1) the electron transport chain of mitochondria 2) the Maillard reaction forming AGEs and 3) membrane bound NADPH

oxidase[20,49]. An imbalance in ROS generation and endogenous antioxidants leads to oxidative stress which can promote vascular complications and atherosclerosis development. For example, oxidative stress induces endothelial nitric oxide synthase (eNOS) dysfunction, where eNOS produces reactive nitrogen species (RNS) instead of the potent vasodilator NO[50]. Therefore, reducing oxidative stress by inhibiting ROS or RNS generation, increasing exogenous antioxidants or increasing a product required for endogenous antioxidant production could be useful in preventing hyperglycemic accelerated atherosclerosis. A commonly used antioxidant used to reduce oxidative stress levels is n-acetyl-cysteine (NAC). NAC increases intracellular cysteine levels, an amino acid important in glutathione formation[25]. Glutathione neutralizes ROS, acting as an essential endogenous antioxidant[69]. Studies demonstrate that along with providing benefit in diets[25], intraperitoneal (IP) injection of NAC reduces atherosclerosis in APOE-deficient mice fed a high fat diet (HFD)[51]. NAC also reduces glycemia and atherogenic index in STZ rats[52]. Currently, the effects of NAC on the vasa vasorum in DM is unknown.

Endoplasmic Reticulum (ER) Stress: The ER is a membranous organelle that plays a role in secretory biomolecule trafficking. Proteins are folded and covalently modified in the ER into their native form. When there

is an imbalance in processing and the amount of unfolded proteins exceeds protein folding capacity, misfolded proteins accumulate in the ER lumen causing ER stress and activation of the unfolded protein response (UPR) pathway[26]. The adaptive branch of the UPR pathway alleviates ER stress first by 1) decreasing the influx of new proteins into the ER lumen, thereby inhibiting protein translation 2) increasing the expression of active chaperones to fold misfolded proteins, including glucose regulated proteins 78 and 94 (Grp78 and Grp94) and 3) degrading misfolded proteins[53]. Chronic ER stress activates the pro-apoptotic branch of the UPR pathway mediating apoptosis through C/EBP homologous protein (CHOP)[53]. Current research implicates a role of ER stress in hyperglycemic conditions through the hexosamine biosynthesis pathway (HBP)[53]. Under normal conditions, approximately 2-5% of glucose is shunted into the HBP to produce UDP-*N*-acetyl glucosamine (UDP-GlcNAc) through the rate limiting enzyme Glutamine Fructose-6 Phosphate Amidotransferase (GFAT)[53]. UDP-GlcNAc is a key substrate for *N*- and *O*- linked protein glycosylation. Increased glucose influx into the HBP promotes ER stress and the development of atherosclerosis due to impaired *N*-linked glycosylation[53]. A commonly used agent to investigate ER stress is the ER stress inhibitor 4-phenyl-butyric acid (4PBA)[26]. 4PBA, an FDA approved drug for the treatment of urea cycle abnormalities, can

act as a chemical chaperone that alleviates prolonged ER stress and UPR pathway activation[26]. 4PBA treatment has been shown to significantly reduce atherosclerotic lesional area and necrotic core size in low-density lipoprotein receptor deficient mice fed a HFD[54]. However, the effects of 4PBA on the vasa vasorum in DM have not been studied.

Figure 3. Mechanisms of Vascular Dysfunction in DM.

Pathways involved in diabetic vascular dysfunction and atherosclerosis progression include endoplasmic reticulum (ER) stress, oxidative stress and advanced glycation end products (AGEs). **ER stress:** Hyperglycemia increases the influx of glucose into the hexosamine biosynthesis pathway (HBP), leading to impaired *N*-linked glycosylation and an accumulation of misfolded proteins in the ER lumen. ER stress activates the unfolded protein response (UPR) pathway. Failure of adaptive UPR pathway activation to suppress ER stress leads to pro-apoptotic UPR pathway activation causing apoptosis and inflammation. **Oxidative stress:** Hyperglycemia interferes with mitochondrial metabolism increasing reactive oxygen species (ROS) and reactive nitrogen species (RNS) generation. Increased ROS and RNS relative to endogenous antioxidants leads to oxidative stress, uncoupling of endothelial nitric oxide synthase (eNOS), endothelial dysfunction and prolonged vasoconstriction. **AGEs:** Hyperglycemia increases the amount of reducing sugars, which enter through the Maillard reaction to form heterogenous AGEs. AGEs cross link with collagen inducing vascular stiffness, bind to AGE receptors (RAGEs) inducing endothelial activation and promote LDL glycation and oxidation. Each individual pathway can feedback onto one another, resulting in disease progression such as atherosclerosis.

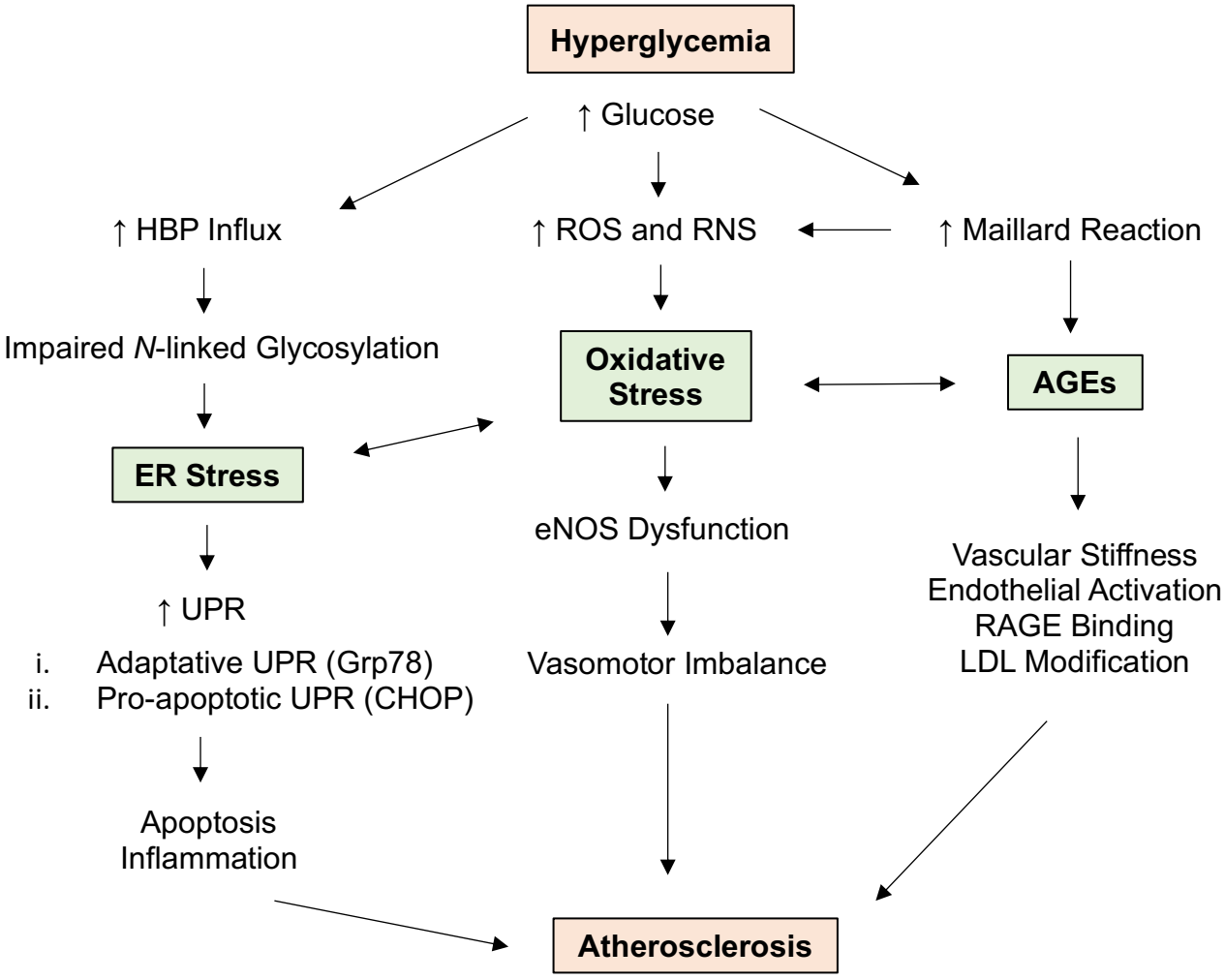
Hyperglycemia
↑ Glucose
↑ HBP Influx
↑ ROS and RNS
↑ Maillard Reaction
Impaired *N*-linked Glycosylation
Oxidative Stress
AGEs
ER Stress
eNOS Dysfunction
Vascular Stiffness
Endothelial Activation
RAGE Binding
LDL Modification
↑ UPR
i. Adaptative UPR (Grp78)
ii. Pro-apoptotic UPR (CHOP)
Vasomotor Imbalance
Apoptosis
Inflammation
Atherosclerosis

1.3. Hypoxia

1.3.1. Hypoxic-Mediated Angiogenesis

Angiogenesis is defined as the formation of new vessels from pre-existing vessels and is upregulated by a variety of angiogenic stimulators including inflammation, mechanical stress and hypoxia. It is important to distinguish angiogenesis from other forms of vessel formation including vasculogenesis, defined as *de novo* vessel formation.

In order to meet the metabolic demands of tissues in hypoxic conditions, additional blood vessels must be produced through angiogenesis. This pathway is mediated through an α,β-heterodimer of two DNA binding proteins called the hypoxia-inducible factor (HIF). Under normoxic conditions, HIF-1α is post translationally modified by prolyl hydroxylases (PHDs), allowing the Von Hippel-Lindau (VHL) E3 ubiquitin ligase to recognize, complex to and eliminate it through proteasomal degradation. Under hypoxic conditions, PHD activity is inhibited, resulting in the accumulation of HIF-1α. HIF-1α dimerizes with HIF-1β and translocates to the nucleus[22]. The HIF-1α/HIF-1β complex then binds to hypoxia response elements (HREs) within the promoters of specific hypoxia inducible genes and with the additional binding of CREB-binding protein and p300 co-activators causes increased expression of genes associated with angiogenesis, glucose metabolism and cell growth[22].

Hypoxia inducible genes include VEGF, inducible nitric oxide synthase (iNOS), VEGF receptor-1 (VEGFR-1) and glucose transporter-1 (GLUT1).

The HIF family includes two additional isoforms, HIF-2α and HIF-3α. Research suggests similarities between HIF-1α and HIF-2α, both binding to HREs and increasing the expression of hypoxia inducible genes[55]. In contrast, HIF-3α, a more distantly related isoform, has been shown to decrease the expression of hypoxia inducible gene expression[55]. Despite function and sequence similarities between HIF-1α and HIF-2α, their roles are non-redundant[55]. This is demonstrated by whole body knockouts of each individual isoform. Constitutive HIF-1α knockout in mice results in consistent lethality at embryonic day 10.5 due to cardiovascular and neural fold defects[56]. Whereas constitutive HIF-2α knockout in mice causes either 1) embryonic lethality at embryonic day 12.5 due to vascular defects 2) neonatal death due to impaired lung development or 3) death at 1-2 months of age due to ROS imbalance[56]. These differences highlight the non-redundant, essential role each HIF isoform plays during development[56]. Generally, HIF-1α drives the initial response and HIF-2α drives the chronic response to hypoxia[56].

Figure 4. Hypoxia Inducible Factor (HIF) Pathway.

The hypoxia-inducible factor (HIF) pathway is mediated through an α,β-heterodimer of two DNA binding proteins called the hypoxia-inducible factor (HIF). Under normoxic conditions, HIF-1α is post translationally modified by prolyl hydroxylases (PHDs), allowing the Von Hippel-Lindau (VHL) E3 ubiquitin ligase to recognize, complex to, ubiquitinate (Ub) and eliminate it through proteasomal degradation. Under hypoxic conditions, PHD activity is inhibited, resulting in the accumulation of HIF-1α. HIF-1α dimerizes with HIF-1β and translocates to the nucleus. The HIF-1α/HIF-1β complex then binds to hypoxia response elements (HREs) within the promoters of specific hypoxia inducible genes and with the additional binding of CREB-binding protein (CBP) and p300 co-activators causes increased expression of genes associated with angiogenesis, cell growth and glucose metabolism.

Image created in BioRender (2020).

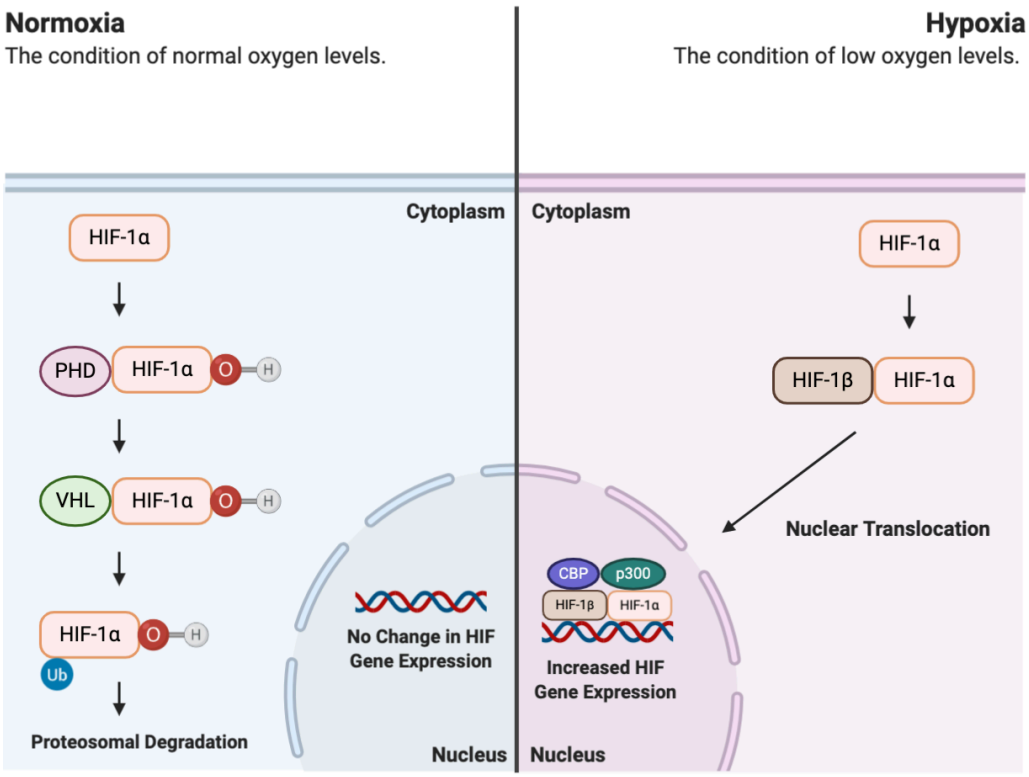
Normoxia
The condition of normal oxygen levels.
Hypoxia
The condition of low oxygen levels.
Cytoplasm
Cytoplasm
HIF-1α
PHD
HIF-1α
O
H
VHL
HIF-1α
O
H
HIF-1α
O
H
Ub
Proteosomal Degradation
No Change in HIF
Gene Expression
Nucleus
HIF-1α
HIF-1β
HIF-1α
Nuclear Translocation
CBP
p300
HIF-1β
HIF-1α
Increased HIF
Gene Expression
Nucleus

1.3.2. Vascular Endothelial Growth Factor (VEGF)

VEGF is a signaling molecule, produced by many cells including macrophages, platelets and tumour cells, used to promote vascular growth[27]. The VEGF family includes VEGF-A, B, C, D, E and placental growth factor 1 and 2[28]. Different isoforms of VEGF exist due to alternative splicing, resulting in molecules with diverse solubilities and binding affinities (**Figure 5**). The most potent and extensively studied homolog is VEGF-A[28]. VEGFs transduce their signal via membrane bound, endothelial specific tyrosine kinase receptors: VEGFR-1, VEGFR-2, and VEGFR-3[29]. VEGFR-2 is the primary receptor for VEGF-A binding. Despite having a weaker binding affinity for VEGF-A, VEGFR-2 has a 10-fold stronger downstream angiogenic signal. VEGFR-2 also has a co-receptor termed neuropilin-1 (NRP-1)[58]. Constitutive NRP-1 knockout in mice causes embryonic death due to severe vascular defects[58]. In contrast, mice with genetically altered NRP-1, which no longer binds VEGF-A, survive into adulthood and develop normal blood vessels[58]. This demonstrates the essential role of NRP-1 co-receptor in controlling VEGFR-2 binding to VEGF-A, not just binding VEGF-A itself[58]. In contrast, VEGFR-1 acts as a decoy receptor, binding VEGF-A with high affinity but with little downstream angiogenic effects[29]. VEGFR-1 also presents in a soluble form acting to increase VEGF-A sequestering from VEGFR-2[29].

VEGF signalling through VEGFR binding promotes the activation of endothelial cells inducing angiogenesis towards hypoxic regions[29].

Further variants of VEGF-A exist due to alternative splicing of VEGF-A exons 6 and 7[57]. These include VEGF-A_{165}, the most extensively studied isoform of VEGF-A, VEGF-A_{121}, VEGF-A_{145}, VEGF-A_{148}, VEGF-A_{183}, VEGF-A_{189}, and VEGF-A_{206}. Each VEGF-A variant has a different domain size, defined by the amount of amino acids used to form them[57]. Recently, VEGF-A_{165} has been found to have two additional families which differ only by their carboxy-terminal six amino acids[57]. These include VEGF-A_{165}a and VEGF-A_{165}b. VEGF-A_{165}a binding to VEGFR-2 is robust, with stable and persistent receptor tyrosine kinase phosphorylation (pro-angiogenic form). In contrast, VEGF-A_{165}b prevents the binding of NRP-1 co-receptor to VEGFR-2, leading to unstable and transient receptor tyrosine kinase phosphorylation (anti-angiogenic form)[57]. These variants of VEGF-A_{165} can be utilized to study possible alterations to the balance between pro-angiogenic and anti-angiogenic forms of VEGF-A_{165}, specifically if VEGF-A_{165} gene expression appears unaffected under distinct conditions.

Figure 5. Families of Vascular Endothelial Growth Factor (VEGF).

Ligand, receptor and function for VEGF-A, B, C, D and E.

Ligand	Receptor	Function
VEGF-A	VEGFR-1, VEGFR-2, NRP-1	Angiogenesis
VEGF-B	VEGFR-1	Unknown
VEGF-C + D	VEGFR-2, VEGFR-3	Lymphangiogenesis
VEGF-E (Viral)	VEGFR-2	Angiogenesis

1.3.3. Paracrine and Autocrine Endothelial Angiogenesis

Paracrine signalling refers to the communication between one cell, which produces a secreted factor, and a neighbouring target cell which binds and responds to the secretion. Since endothelial cells do not produce VEGF under basal conditions, the binding and angiogenic response of VEGF to VEGFR-2 depends on other cell types through paracrine signalling mechanisms. Although angiogenesis is driven primarily by paracrine interactions, hypoxic and pathological conditions have been shown to induce VEGF gene expression in endothelial cells[59]. This novel pathway, termed an autocrine mechanism, suggests that endothelial cells may be able to produce their own VEGF which is secreted to act back on itself[59]. Both of these pathways are important to consider as hyperglycemic vasa vasorum damage induces a hypoxic environment, driving VEGF expression. Determining the cellular sources of VEGF in and around the atherosclerotic lesion is important to explain reduced aortic VEGF-A found in hyperglycemic APOE-deficient mice[31].

After VEGF-VEGFR-2 interactions, endothelial cells select which cells migrate out of the vessel during angiogenesis producing a tip cell. This selection is mediated by the Notch signaling cascade[66-67]. Notch ligands, such as delta-like ligand 4 (Dll4), are increased in the selected tip cells compared to surrounding endothelial cells [29, 66]. This causes the cell

to produce filopodia, a cytoplasmic projection, towards the VEGF-A rich source[67]. Increased Dll4 in tip cells activates notch receptors in neighbouring cells forming stalk cells. Stalk cells produce fewer filopodia, are more proliferative than migratory and form the lumen of new vessels[67].

1.3.4. Aberrant Angiogenesis in DM

Depending upon the tissue and severity of the disease, the effects of hyperglycemia on the microvasculature can lead to excessive or attenuated angiogenesis. Specifically, excessive angiogenesis exists in proliferative DR due to retinal ischemia[66,40]. Despite eliminating low oxygen concentrations, rapid angiogenesis results in leaky, immature vascular structures, enhancing hard exudate leakage into the retina[40,68]. In comparison, attenuated angiogenesis is present in non-proliferative DR and wound healing of DM patients. Studies on hyperglycemic mice show a reduced release of VEGF from fibroblasts compared to wildtype (WT) mice, leading to decreased recruitment of cells to injured tissues[66]. The concurrent existence of both pro-angiogenic and anti-angiogenic responses in DM has been termed the “angiogenesis paradox.” This paradox is highlighted by the fact that treatments for proliferative DR involve anti-VEGF medications, whereas application of VEGF facilitates wound healing[66]. An understanding of the angiogenic outcome in the

aortic vasa vasorum in DM will facilitate a clearer understanding of the development of macrovascular disease stemming from microvascular damage.

2.0. RATIONALE, HYPOTHESIS & OBJECTIVES

2.1. Rationale

The prevalence of DM is increasing dramatically around the world and the majority of DM mortality is determined by DM-induced CVD[3]. This is resulting in a significant global healthcare and economic burden. A better understanding of the mechanisms by which DM promotes the development and progression of CVD will lead to new and more effective treatments for this epidemic.

2.2. Hypothesis

We hypothesize that hyperglycemic-associated arterial hypoxia – which can arise from decreasing oxygen supply by reduced vasa vasorum density or by increasing oxygen demand through increased inflammation – promotes atherosclerosis.

2.3. Research Objectives

1. To investigate the effects of hyperglycemia and hypoxia on the angiogenesis of human microvascular endothelial cells using *in vitro* tube formation assays.

2. To investigate the mechanisms by which hyperglycemia and hypoxia promote atherosclerosis.
3. To develop and characterize a novel transgenic mouse model to study the effect of modulating VEGF-A levels on vasa vasorum angiogenesis and on the development of atherosclerosis in hyperglycemic and normoglycemic mice.

3.0. METHODOLOGY

3.1. In Vitro

3.1.1. Cell Types

i. Human Cardiac Microvascular Endothelial Cells (HMVEC-Cs)

HMVEC-Cs are primary human microvascular endothelial cells isolated from donated tissue after permission and informed consent. Donor specific characteristics for those cells utilized in the following experiments include:

Age: 34 Y **Sex:** FEMALE **Virus Testing:** NEGATIVE

Since it is not an immortalized cell line, HMVEC-Cs are more physiologically comparable to *in vivo* endothelial cells even though its cells are isolated from a single patient and contain cells that do not specifically originate from the vasa vasorum.

ii. THP-1 Monocytes

THP-1 monocytes constitute an immortalized cell line derived from a child with acute monocytic leukemia. These cells can be differentiated into macrophages for the *in vitro* study of macrophage physiology and function.

3.1.2. Tissue Culture – Normoxic Incubator

Many publications disregard information on the normoxic oxygen concentrations of their cell culture work. In these studies, cells were incubated in a normoxic incubator at 5% CO_2 and 37°C. The partial pressure of oxygen (pO_2) value is around 18.6% (141 mmHg) in a standard incubator, which compares to approximately 20.9% (159 mmHg) in the input air[66]. Although this difference exists, the pO_2 in biological tissues vary greatly. Since great variation does exist, a normoxic condition for an individual tissue or cell should be termed a physioxic condition. For example, the longitudinal pressure gradient of O_2 within blood vessels ranges from 90 mmHg at the arterial end, to 30 mmHg at the venous end[66]. Normoxic incubators can therefore be considered a hyperoxic environment for a variety of cells. This limitation is important to consider when analyzing the *in vitro* results.

3.1.3. Alamar Blue Assay

Human cardiac microvascular endothelial cells (HMVEC-Cs) (Lonza, Walkersville, USA) were cultured using EBM-2 Basal Medium supplemented with EGM-2MV SingleQuots Kit (Lonza, Walkersville, USA). EBM-2 Basal Medium contains approximately 5.6 mM glucose, which is an ideal glucose concentration for normoglycemic studies. Cells were

trypsinized, counted and resuspended with EBM-2 Basal Medium to a final concentration of 2.0 x 10^4 cells per 100 µL. 2.0 x 10^4 cells were added to each well in a 96-well plate and left for 24 hours to adhere. After 24 hours, increasing concentrations of glucose up to 45 mM or chemical interventions (4PBA, PX or NAC) dissolved and neutral buffered in EBM-2 Basal Medium were added to each well. Cells were incubated in a normoxic (5% CO_2 and 37°C) or hypoxic (1% O_2, 5% CO_2 and 37°C) incubator for 18 hours. 10% v/v alamarBlue reagent (Bio-Rad, Mississauga, Canada) was added to each well for 4 hours. Absorbance was measured at 570 nm and 600 nm to calculate the percent difference in reduction between treated and control cells (5.6 mM glucose or 0 mM mannitol). Mannitol was used as an osmotic control. Data was expressed as an arbitrary unit in which the control group value equals 1. This assay was used to determine the viability of HMVEC-Cs in increasing concentrations of glucose and chemical interventions in normoxic and hypoxic environments. Toxicity thresholds were calculated, based on significant reductions in cell viability compared to controls, to determine maximum concentrations for use on HMVEC-Cs *in vitro.*

3.1.4. Tube Formation Assay

HMVEC-Cs were cultured using EBM-2 Basal Medium supplemented with EGM-2MV SingleQuots Kit. HMVEC-Cs were cultured until passage 4, as literature suggests endothelial cells should be used between passage 2 and passage 6 for optimal endothelial tube formation[32]. Cells were incubated with Calcein AM (2 µg/mL) for 30 minutes, a cell permeable dye that binds to calcium and results in green fluorescent staining. Cells were trypsinized, counted and resuspended with EBM-2 Basal Medium to a final concentration of 6.0×10^4 cells per 200 µL. Ice cold BD Matrigel Basement Membrane (100 µL) was added to each well in a 48 well-plate using refrigerated tips and solidified in a normoxic incubator (5% CO_2 and 37°C) for 30 minutes. 6.0×10^4 cells were added to each well, followed by glucose treatments (with or without chemical interventions) and incubated for 18 hours in a normoxic (5% CO_2 and 37 °C) or hypoxic (1% O_2, 5% CO_2 and 37°C) incubator. Tubes were imaged using a Brightfield microscope and fluorescent imager with Infinity camera under 4X magnification. Images were quantified using WimTube Image Analyzer to determine the total number of microvascular tubes formed. The microvascular tubes formed parameter is defined as the total number of endothelial tubes produced on the matrix per image.

3.1.5. THP-1 Macrophage Differentiation

THP-1 human monocytes (American Type Culture Collection) were cultured using RPMI 1640 Medium (Thermo Fisher Scientific, Canada) supplemented with 10% fetal bovine serum (FBS) and antibiotics, containing approximately 11.1 mM glucose. Suspension cells were counted and resuspended with sterile filtered no glucose RPMI 1640 Medium (Thermo Fisher Scientific, Canada) with 5 mM glucose added to a final concentration of 2.0×10^5 cells per 1.0 mL. 1.0×10^6 cells were added to each well in a 6-well plate. THP-1 monocytes were treated with 100 nM phorbol 12-myristate 13-acetate (PMA) for 72 hours to allow differentiation into adherent macrophages. After 72 hours, medium with PMA was aspirated and cells were left to rest in no glucose RPMI 1640 Medium with 5 mM glucose added, for 5 days to produce PMA rested (PMAr) macrophages. Literature suggests that PMAr macrophages are similar to primary macrophages in their morphology, resistance to apoptosis and number of mitochondria[33]. PMAr cells were then treated with glucose (final glucose concentration of 5 mM or 35 mM) and placed in a normoxic or hypoxic incubator for 24 hours. Cells were collected for subsequent downstream applications including qPCR.

3.1.6. Total RNA Isolation and Real-Time Reverse Transcription–PCR

HMVEC-Cs were cultured using EBM-2 Basal Medium supplemented with EGM-2MV SingleQuots Kit (Lonza, Walkersville, USA). Cells were trypsinized, counted and resuspended with EBM-2 Basal Medium to a final concentration of 1.5 x 10^5 cells per 1.0 mL. 1.5 x 10^5 cells were added to each well in a 12-well plate and left for 24 hours to adhere. HMVEC-Cs monolayers were treated to a final concentration of 35 mM or 5 mM glucose and PX (1.0 mM), NAC (5.0 mM) or 4PBA (1.0 mM) for 18 hours. Monolayers were incubated in both a normoxic and hypoxic incubator (1% O_2, 5% CO_2 and 37°C). 1% O_2 inside the chamber was validated after a 2-hour purge with N_2 and 1-hour purge with 1% O_2 gas mixture (Air Liquide, Ontario, Canada) using an O_2 sensor. Sensor measurements recorded 1 ± 0.2% O_2. After an exposure time of 18 hours, total RNA was extracted using TRIzol (Invitrogen, Canada) according to manufacturer's protocol. RNA concentration and purity were measured using a NanoDrop. 1 µg of RNA was used to synthesize cDNA using the High-Capacity cDNA Reverse Transcription Kit (Applied Biosystems, Canada) according to manufacturer's protocol. cDNA product was subjected to real-time PCR (Applied Biosystems) using *Power* SYBR Green PCR Master Mix (Applied Biosystems) with specific forward and reverse primers (**Table 1**). GAPDH and β-actin were used as

housekeeping controls. Delta delta C_t analysis was completed to determine the relative fold change between control and treated groups. Data was expressed as an arbitrary unit in which the control group value equals 1. Melt curves were analyzed to confirm the absence of DNA contamination or primer dimer formation.

Gene	Forward Primer (5' – 3')	Reverse Primer (5' – 3')
VEGF-A	CACTGCCTGGAAGATTCA	TGGTTTCAATGGTGTGAGGA
VEGFR-1	TCTCACACATCGACAAACCAATACA	GGTAGCAGTACAATTGAGGACAAGA
VEGFR-2	GCAGGGGACAGAGGGACTTG	GAGGCCATCGCTGCACTCA
iNOS	GTTTCTGGCAGCAGCGGCTC	GCTCCTCGCTCAAGTTCAGC
eNOS	TGGACCTGGATACCCGGAC	TGGTGACTTTGGCTAGTCGGT
IL-1β	GTCAGCTCTCTCCTTTCA	AATGTGGCCGTGGTTTCT
CHOP	TGCCTTTCTCTTCGGACACT	TGTGACCTCTGCTGGTTCTG
VEGF-A_{165}	CCCACTGAGGAGTCCAACATC	AAGGCCCACAGGGATTTTCTT
VEGF-A_{189}	CCCACTGAGGAGTCCAACATC	AAGGCCCACAGGGAACGC
VEGF-A_{165}a	GAGCAAGACAAGAAAATCCC	CCTCGGCTTGTCACATCTG
VEGF-A_{165}b	GAGCAAGACAAGAAAATCCC	GTGAGAGATCTGCAAGTACG
β-actin	ACCGAGCGCGGCTACAG	CCTAATGTGACGCACGATTTC
GAPDH	GGATTTGGTCGTATTGGG	GGAAGATGGTGATGGGATT

Table 1. Human Real-Time Reverse Transcription–PCR Primers. Forward and reverse primers for human genes examined using qPCR in HMVEC-Cs and PMAr THP-1 differentiated macrophages.

3.2. In Vivo

3.2.1. Hypoxyprobe – Examination of Early Hypoxia

Five week old female APOE$^{-/-}$ mice were placed on a standard chow diet and randomized to one of two treatment groups. Hyperglycemia (HG) was induced in one group by IP administration of five low-dose streptozotocin (STZ) injections (50 mg/kg), followed by a rest week. The injections were then repeated for a second round using the same therapeutic scheme. The second normoglycemic (NG) group was given two sets of five IP injections of citrate buffer over the same three week period. STZ-HG mice were confirmed as hyperglycemic at week 8 after saphenous vein fasted blood glucose measurements confirmed a level > 15 mM. Enrolled mice were sacrificed at 10 weeks of age. Two hours prior to sacrifice, mice received IP injections with 60 mg/kg pimonidazole hydrochloride (Hypoxyprobe™-1; Hypoxyprobe Inc., Burlington, MA). Mice were anaesthetized with isoflurane, flushed with 1X PBS, and tissues were perfusion-fixed with 10% neutral buffered formalin. Plasma and tissue samples were collected from each mouse for further examination.

3.2.2. 4PBA, NAC, PX – Chemical Interventions

Five week old female APOE$^{-/-}$ mice were placed on a standard chow diet and randomized into various treatment groups. HG was induced

by IP administration of five low-dose streptozotocin (STZ) injections (50 mg/kg), followed by a rest week. The injections were then repeated for a second round using the same therapeutic scheme. NG mice were given two sets of five IP injections of citrate buffer over the same three week period. STZ-HG mice were confirmed as hyperglycemic at week 8 after saphenous vein fasted blood glucose measurements confirmed a level > 15 mM. At 8 weeks of age HG and NG mice started treatment with 4PBA (1 g/kg bw/day), NAC (250 mg/kg bw/day), PX (250 mg/kg bw/day) or no treatment in their drinking water until sacrifice at 16 weeks of age. 4PBA, NAC or PX drinking water was prepared with autoclaved sterile tap water and neutral buffered, as required, with NaOH after the addition of each chemical. Neutral pH was confirmed after addition of NaOH with pH indicator paper. NAC and PX required buffering due to their acidic properties. Midpoint blood glucose and body weight measurements were taken at 12 weeks of age. Prior to sacrifice, a glucose tolerance test was completed on all mice by IP injecting a 10% w/v glucose solution in PBS and measuring fasting tail blood glucose level at 0, 30, 60 and 120 minutes. Area under the curve was calculated using the trapezoidal method (tAUC) with a baseline set at y = 0.

3.2.3. Tissue Collection of Mouse Samples

Cardiac puncture blood was collected and placed in EDTA tubes. A small subset of blood was placed in a 1.5 mL Eppendorf tube. Blood samples were centrifuged at 6000 rpm for 5 minutes in a cold room to isolate serum. Serum samples were transferred to another 1.5 mL Eppendorf tube, and centrifuged at 12000 rpm for 5 minutes in a cold room to isolate plasma. Samples were stored in -80^{o}C freezer. Perigonadal adipose, liver, left kidney and pancreas was collected and weighed. Various other organs were collected but not weighed including brain, heart, aorta, small intestine, muscle, lung, eye and spleen.

3.2.4. Immunofluorescent and Immunohistochemistry Staining

Upon excision of the heart and ascending aorta, the apex of the heart was sectioned transversely, and the remaining cardiac tissue was processed and embedded in paraffin. Using the valve leaflets as a point of orientation, 5 μm serial sections of the aortic root were collected and stained. Serial sections were collected on ten individual microscope slides to obtain side by side aortic sections 50 μm apart. Immunohistochemistry was performed using a primary mouse monoclonal antibody against pimonidazole hydrochloride (Hypoxyprobe™-1; Hypoxyprobe Inc., Burlington, MA), an indicator of hypoxia. A secondary biotin conjugated

anti-mouse reagent, streptavidin peroxidase and DAB (Dako, Burlington, ON) chromogenic substrate were used. Immunofluorescence was performed using a primary mouse monoclonal antibody against HIF-1α (Novus Biologicals, Oakville, ON), an indicator of hypoxia. Fluorescence was assessed using secondary antibodies tagged with Alexa 488. Non-specific staining was controlled by incubating serial aortic cross-sections with pre-immune IgG.

3.2.5. Plasma Analysis

Four hour fasting blood glucose levels were measured in mice using a glucometer (OneTouch Verio Flex) with blood collected from the saphenous vein. Fasting plasma triglyceride and cholesterol was measured using Infinity colorimetric assays (Thermo Scientific).

3.2.6. Imaging and Quantification

Microscope images were captured with an Olympus DP72 digital camera. Immunohistochemistry staining was quantified using a colour deconvolution plugin on ImageJ. Immunofluorescent staining was quantified on ImageJ. Positively stained areas of the aortic intima were defined as a percentage relative to the intima area selected.

3.2.7. Masson's Trichrome and Atherosclerosis Quantification

Masson's Trichrome (Sigma-Aldrich, Canada) staining was used on serial sections of the aortic root to quantify atherosclerosis. ImageJ was used to calculate the total lesion area at increasing distances from the aortic sinus. Lesional volume was calculated by examining the area under the curve of lesional area versus distance from the aortic sinus.

3.2.8. Inducible VEGF (iVEGF)

3.2.8.1. $APOE^{-/-}$ $iCRE^{+/-}$ ROSA26-FLOXSTOP-$VEGF_{164}^{+/-}$

ROSA26-FLOXSTOP-$VEGF_{164}$ mice (Nagy Lab, Toronto, ON) were crossed with Tg(Csf1r-cre/Esr1*)1Jwp/J and $APOE^{-/-}$ (JAX, USA) mice to obtain $APOE^{-/-}$ $iCRE^{+/-}$ ROSA26-FLOXSTOP-$VEGF_{164}^{+/-}$ mice. These mice carry the gene encoding the tamoxifen inducible Cre/Esr1* recombinase under the control of the macrophage-specific colony stimulating factor 1 receptor (Csf1r) promoter. Once activated by tamoxifen, Cre/Esr1* recombinase excises the floxed STOP to induce a conditional upregulation of vascular endothelial growth factor ($VEGF_{164}$). These mice have a complete knockout of APOE, the gene responsible for apolipoprotein E production, leading to poor lipoprotein clearance, increased plasma cholesterol levels and spontaneous atherosclerosis progression beginning at approximately 8 weeks of age.

3.2.8.2. Genotyping

Small mouse tail clippings were collected, digested using a lysis buffer and incubated on a heating block at 60°C for 90 minutes, followed by 90°C for 10 minutes. Polymerase chain reaction (PCR) was then used with specific forward and reverse primers complementary to the gene of interest (**Table 2**). Following amplification, PCR products were run on a 1.5% agarose gel, stained with ethidium bromide and photographed for documentation. Genotypes of interest were determined based on a DNA ladder to compare PCR product sizes (**Figure 6**).

Gene	Forward Primer (5' – 3')	Reverse Primer (5' – 3')
ROSA26-WT	AAAGTCGCTCTGAGTTGTTAT	GGAGCGGGAGAAATGGATATG
ROSA26-TG	AAAGTCGCTCTGAGTTGTTAT	GCGAAGAGTTTGTCCTCAACC
APOE	GCCTAGCCGAGGGAGAGCCG TGTGACTTGGGAGCTCTGCAGC	GCCGCCCCGACTGCATCT
CSF1R iCRE	AGATGCCAGGACATCAGGAACCTG	ATCAGCCACACCAGACACAGAGATC

Table 2. Mouse Genotyping Primers. Forward and reverse primers for mouse genotyping.

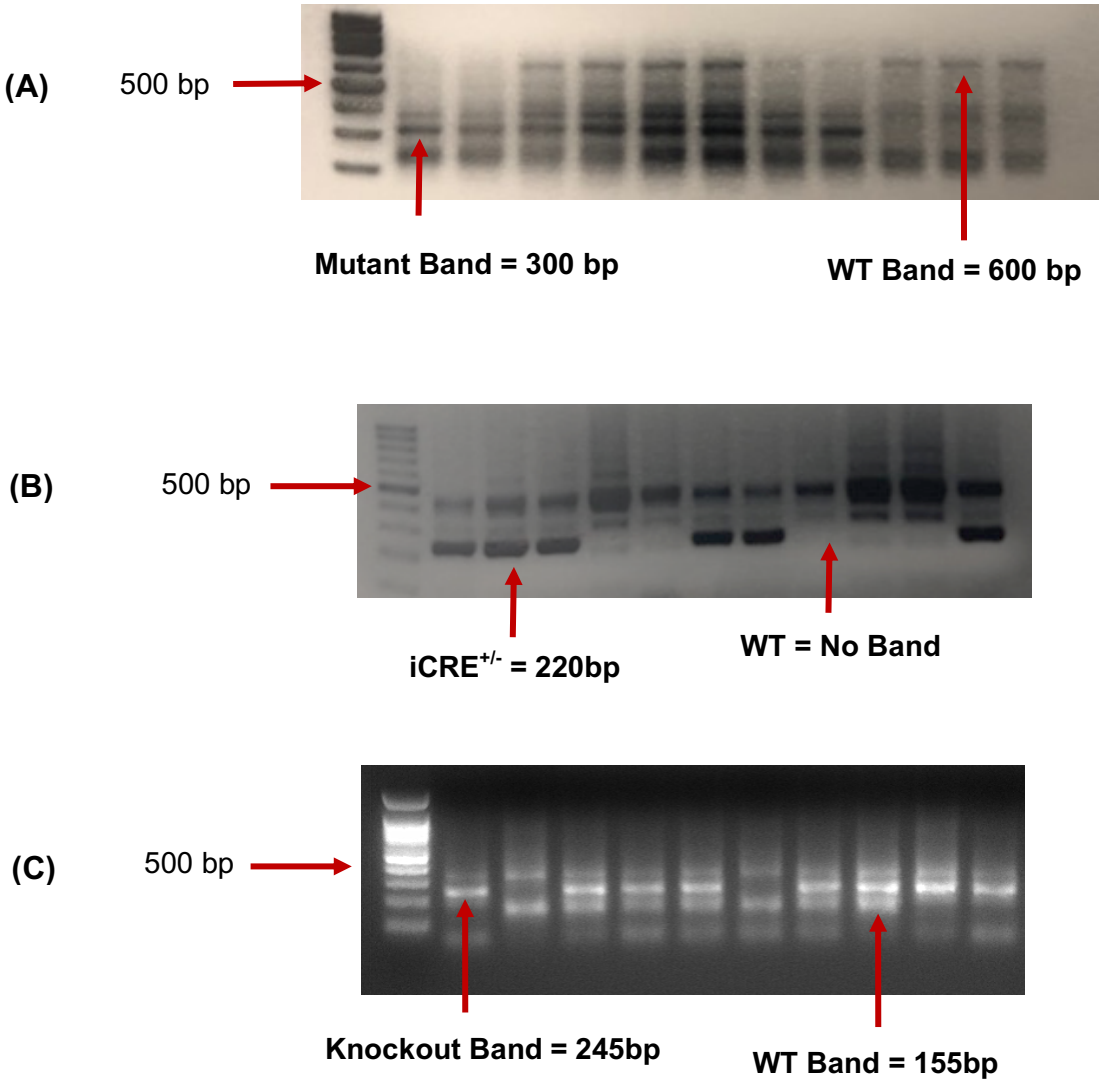

Figure 6. Band Identification for Mouse Genotyping.

1.5% agarose gels with DNA ladder for identification of base pair size for **(A)** ROSA26 **(B)** CSFR1 iCRE and **(C)** APOE.

3.2.8.3. Peritoneal Macrophage Extraction

APOE$^{-/-}$ iCRE$^{+/-}$ ROSA26-FLOXSTOP-VEGF$_{164}$$^{+/-}$ mice were IP injected once a day with tamoxifen (75 mg/kg bw/day) dissolved in corn oil or corn oil as a control for 5 consecutive days. One week after final tamoxifen injection, mice were IP injected once with 1.0 mL 10% w/v thioglycolate. After 4 days, mice were anaesthetized with isoflurane, followed by cervical dislocation. 10.0 mL of warmed 5 mM EDTA-PBS was injected into the peritoneum and the abdomen was massaged to dislodge peritoneal macrophages. Cell suspension was removed from abdomen, centrifuged and plated in DMEM with 20% FBS. After 2 hours of normoxic incubation, media was aspirated to remove contaminating red blood cells and macrophages collected for downstream analysis of VEGF expression.

Gene	Forward Primer (5' – 3')	Reverse Primer (5' – 3')
VEGF-A	CTGTGCAGGCTGCTGTAAGG	GTTCCCGAAACCCTGAGGAG
GAPDH	ACCACAGTCCATGCCATCAC	CACCACCCTGTTGCTCTAGCC

Table 3. Mouse Real-Time Reverse Transcription–PCR Primers.
Forward and reverse primers for mouse genes examined using qPCR in extracted peritoneal macrophages.

3.2.8.4. Western Blot – Confirmation of VEGF overexpression

Total protein lysates were separated using SDS-PAGE and transferred to a nitrocellulose membrane. Protein of interest was detected with a primary antibody against VEGF-A (Boster Bio, PA1080) and β-actin (Sigma-Aldrich). Blots were then incubated with a secondary antibody conjugated to horseradish peroxidase and imaged with a chemiluminescence detection system. Bands were quantified by densitometry using ImageJ and graphed relative to β-actin.

3.3. STATISTICAL ANALYSIS

Data was analyzed by an unpaired t-test, one- or two-way ANOVA followed by a multiple comparison test for all groups using GraphPad Prism. Data is expressed as arithmetic means ± SEM. For all experiments, a *p* value of 0.05 or less was considered statistically significant. Significance was also recorded for *p* values falling below 0.01, 0.001, and 0.0001.

4.0. RESULTS

4.1. Hyperglycemia Impairs the Angiogenesis of HMVEC-Cs in Normoxic Conditions using the Tube Formation Assay

Tube formation assays were used to assess the effects of hyperglycemia on HMVEC-C angiogenesis. This assay utilizes a basement membrane like matrix, allowing endothelial cells to migrate and form tube like capillary structures. These structures mimic *in vivo* angiogenesis[72]. Angiogenesis quantification in distinct experimental groups can be calculated by counting the total number of microvascular tubes formed per imaged well using WimTube Image Analyzer. Results demonstrate a significant reduction in HMVEC-C angiogenesis in elevated glucose conditions compared to normoglycemic controls in normoxia (**Figure 7**). This effect is dose dependent with increasing glucose resulting in a larger decrease in the number of tubes formed (**Figure 7D**).

To determine if the observed effect on angiogenesis was a result of a general decrease in HMVEC-C viability, cell monolayers were cultured for 24 hours in the presence of 5.6 mM, 15 mM, 25 mM, 35 mM or 45 mM glucose under normoxic (**Figure 8A**) or hypoxic (**Figure 8B**) conditions. Viability was assessed using the alamarBlue assay, which measures the chemical reduction of growth media, resulting from cellular growth and

proliferation. No significant differences in HMVEC-C viability was observed under any of the tested hyperglycemic glucose conditions compared to normoglycemic glucose controls (5.6 mM). Mannitol was utilized in a subset of cells as an osmotic control. Mannitol is a sugar alcohol used clinically as an osmotic diuretic and is not converted to glucose. Mannitol controls are useful to differentiate effects due to hyperglycemia or due to osmolality resulting in shrinkage and death of cells via osmosis. These results suggest HMVEC-C survival in hyperglycemic conditions with normal or reduced oxygen partial pressure.

Based on these results, 35 mM glucose was selected as the hyperglycemic concentration for subsequent *in vitro* experiments. This value was selected as it yielded the greatest significant decrease in total tube formation compared to normoglycemic controls. Glucose concentrations beyond 35 mM showed no significant difference compared to 35 mM glucose (**Figure 7D**). Further, 35 mM glucose is representative of hyperglycemic blood glucose measurements in streptozotocin (STZ) injected mice, our *in vivo* model of DM in subsequent experiments. These findings demonstrate a detrimental, negative effect of high glucose on the angiogenesis of endothelial cells *in vitro* and can be used as a quantitative assay to further elucidate the mechanisms associated with this damage.

Figure 7. Hyperglycemia is associated with impaired microvascular tube formation of HMVEC-Cs cultured for 18 hours in a normoxic environment in the presence of the indicated glucose concentrations. (A) Images taken using Brightfield microscope with Infinity camera under 4X magnification. Scale bar = 1000 μm. **(B)** Images taken using fluorescent imager with Infinity camera under 4X magnification. Cells stained with Calcein AM. Scale bar = 1000 μm. **(C)** Angiogenesis quantification by WimTube Image Analyzer, *n* = 4 per group. **(D)** Mean number of tubes ± SEM, *n* = 4 per group. Significance calculated using a one-way ANOVA followed by a multiple comparison test. *$p < 0.05$, **$p < 0.01$, ****$p < 0.0001$ relative to 5.6 mM glucose. $^{\#\#}p < 0.01$ relative to 15 mM glucose. $^{+}p < 0.05$ relative to 25 mM glucose.

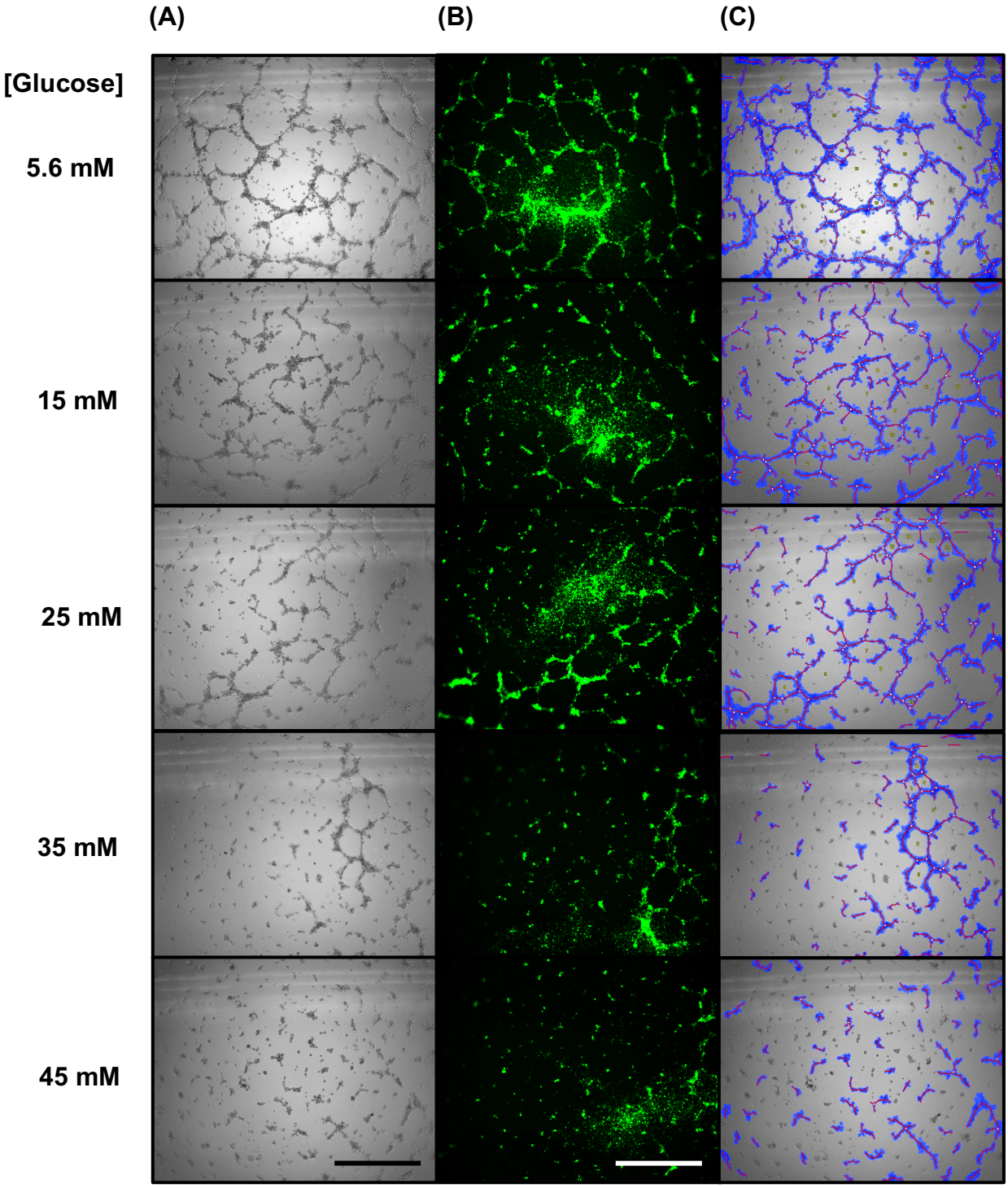
(A)
(B)
(C)
[Glucose]
5.6 mM
15 mM
25 mM
35 mM
45 mM

(D)

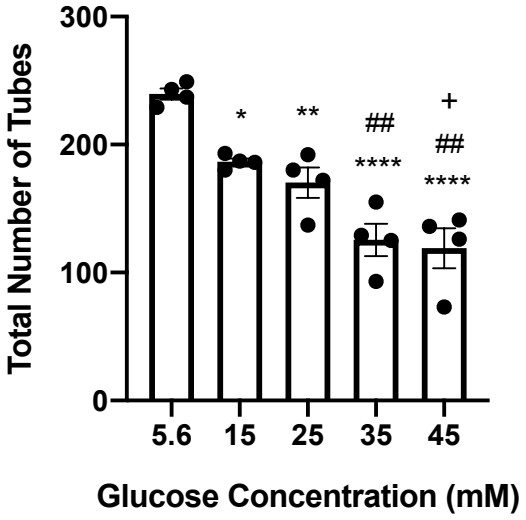
300
200
100
0
Total Number of Tubes
*
**
##
****
+
##
****
5.6
15
25
35
45
Glucose Concentration (mM)

Figure 8. Increasing concentrations of glucose and mannitol have no effect on decreasing HMVEC-C monolayer viability, cultured for 24 hours in (A) normoxic or (B) hypoxic (1% O_2) conditions. Cell viability was calculated using the alamarBlue assay. Absorbance was measured at 570 nm and 600 nm to calculate the percent difference of treated HMVEC-Cs relative to untreated controls (5.6 mM glucose, 0 mM mannitol). Data is expressed as a mean ± SEM, *n* = 3 – 4 per group. Significance calculated using a two-way ANOVA followed by a multiple comparison test.

(A)

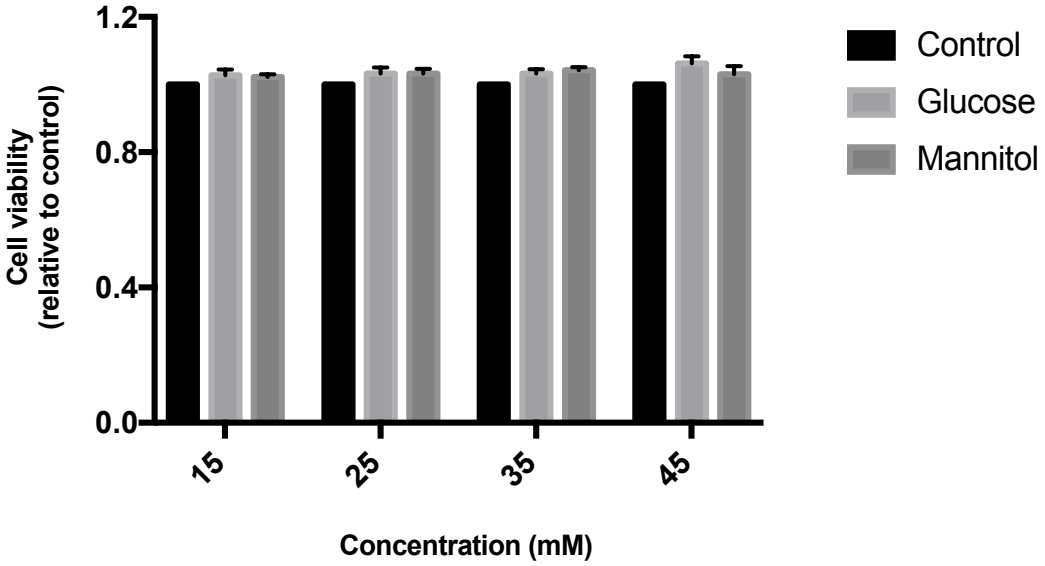
1.2
0.8
0.4
0.0
Cell viability
(relative to control)
15
25
35
45
Concentration (mM)
Control
Glucose
Mannitol

(B)

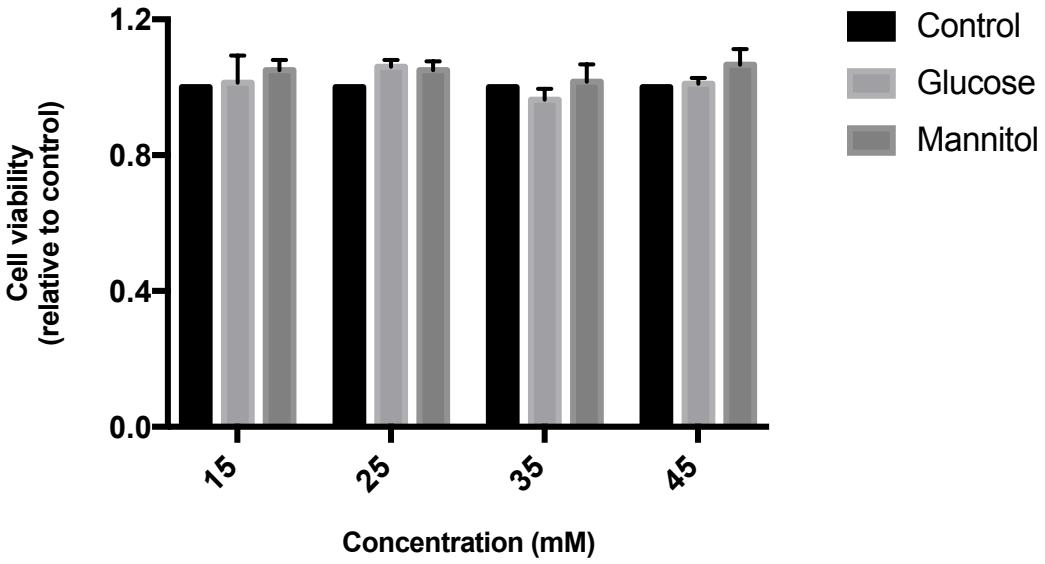
1.2
0.8
0.4
0.0
Cell viability
(relative to control)
15
25
35
45
Concentration (mM)
Control
Glucose
Mannitol

4.2. NAC or PX Rescues Hyperglycemic Impaired HMVEC-C Angiogenesis in Hypoxic Conditions

To further elucidate the mechanisms associated with hyperglycemic induced reductions to HMVEC-C angiogenesis (**Figure 7**), cultured HMVEC-Cs were treated with small molecule interventions to attenuate ER stress, oxidative stress and AGE pathways (4-phenyl-butyric acid (4PBA), n-acetyl-cysteine (NAC) and pyridoxamine (PX), respectively).

Identification of maximum toxicity thresholds for each of the chemical interventions selected was completed using the alamarBlue assay. This was accomplished by treating HMVEC-Cs with 4PBA from 0 mM to 8 mM, PX from 0 mM to 8 mM or NAC from 0 mM to 32 mM for 24 hours in normoxia. Results show HMVEC-C viability was not significantly reduced by chemical concentrations up to 8 mM 4PBA, 2 mM PX or 8 mM NAC. These thresholds were used to determine *in vitro* dosing for subsequent HMVEC-C tube formation assays with treatment (**Figure 9**).

Tube formation assays were then completed in normal (5.6 mM) or high glucose (35 mM) with each of the chemical interventions at concentrations below their calculated HMVEC-C toxicity threshold. Treatment with high glucose in both normoxic and hypoxic conditions significantly reduced HMVEC-C total tube formation, similar to previous findings (**Figure 7**). However, the protective impact of each of the

interventions on HMVEC-C angiogenesis differed in hypoxia versus normoxia. Under normoxic conditions, treatment with 4PBA, NAC or PX did not significantly rescue hyperglycemic impaired HMVEC-C tube formation (**Figure 10A-C**). In contrast, under hypoxic conditions, treatment with PX or NAC significantly increased the total tube formation of HMVEC-Cs in hyperglycemia back to normoglycemic levels (**Figure 10A and C**). 4PBA had no effect on rescuing hyperglycemic impaired angiogenesis of HMVEC-Cs in hypoxic environments (**Figure 10B**). Further, hypoxia elevated the total number of tubes formed in all conditions relative to normoxic environments (**Figure 10A-C**).

This data suggests a potential negative effect of oxidative stress and AGEs, more than ER stress, on hyperglycemic induced reductions in HMVEC-Cs angiogenesis.

Figure 9. The effect of increasing concentrations of (A) 4PBA (B) NAC or (C) PX on HMVEC-C monolayer viability cultured for 24 hours in a normoxic incubator. Cell viability was measured using the alamarBlue assay. Absorbance was measured at 570 nm and 600 nm to calculate the percent difference of treated relative to untreated HMVEC-Cs. Data expressed as the mean ± SEM, *n* = 4 per group. Significance calculated using a two-way ANOVA followed by a multiple comparison test. **p < 0.01, *** p < 0.001, ****p < 0.0001.

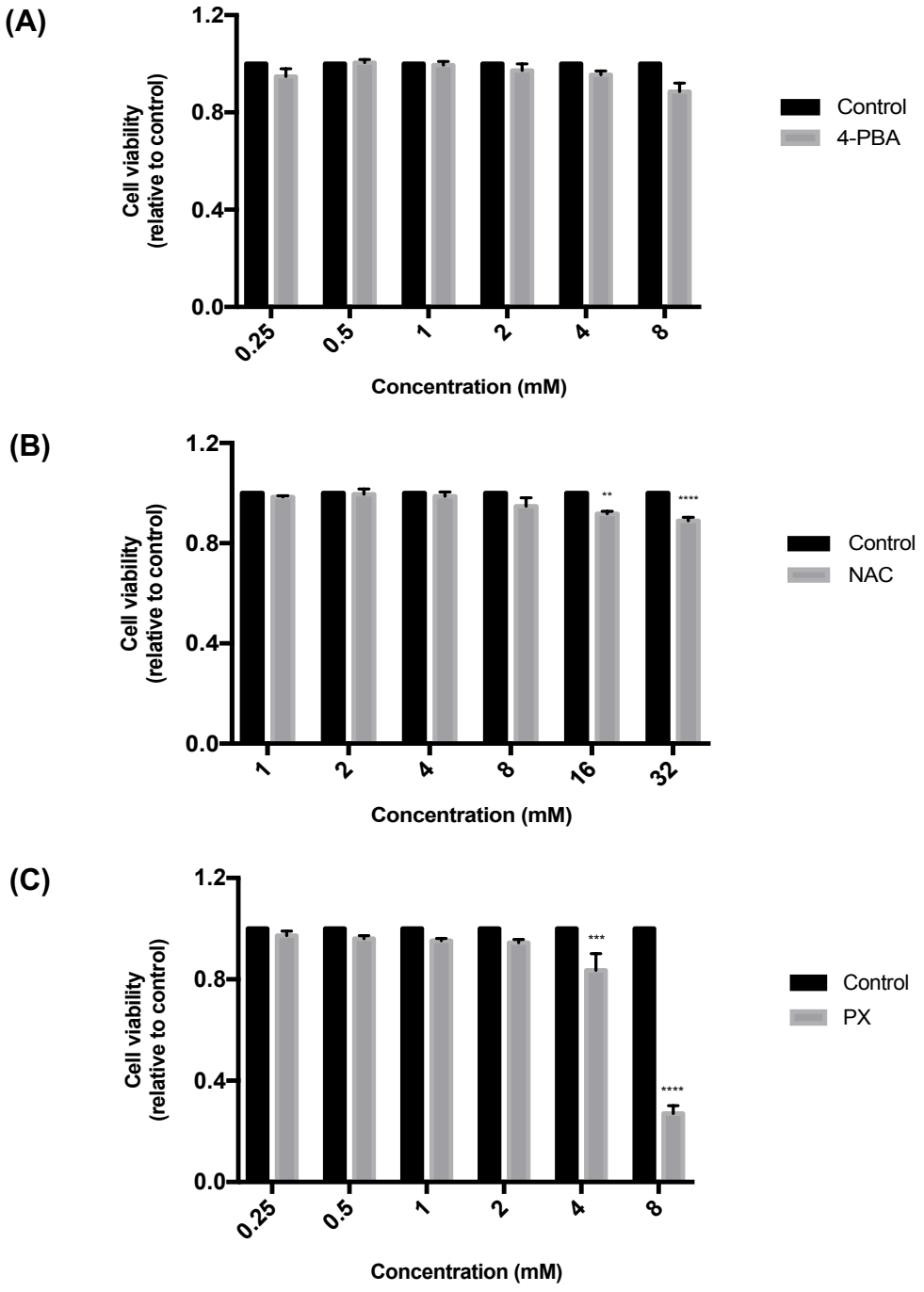
(A)
1.2
0.8
0.4
0.0
Cell viability
(relative to control)
0.25
0.5
1
2
4
8
Concentration (mM)
Control
4-PBA
(B)
1.2
0.8
0.4
0.0
Cell viability
(relative to control)
**
****
1
2
4
8
16
32
Concentration (mM)
Control
NAC
(C)
1.2
0.8
0.4
0.0
Cell viability
(relative to control)
***
****
0.25
0.5
1
2
4
8
Concentration (mM)
Control
PX

Figure 10. Effect of (A) 4PBA (B) PX or (C) NAC on hyperglycemic induced HMVEC-C angiogenic damage in normoxic and hypoxic (1% O_2) conditions. Images taken using a Brightfield microscope under 4X magnification with Infinity Camera. Quantification of the mean number of microvascular tubes formed ± SEM using WimTube Image Analyzer, *n* = 3 – 6 per group. Hypoxic and normoxic data plotted on the same graph for side by side comparison. However, significance calculated separately using a one-way ANOVA followed by a multiple comparison test. *p < 0.05, **p < 0.01, ***p < 0.001, ****p < 0.0001. $ represents groups that are not significantly different from either the NG or untreated HG groups.

(A)

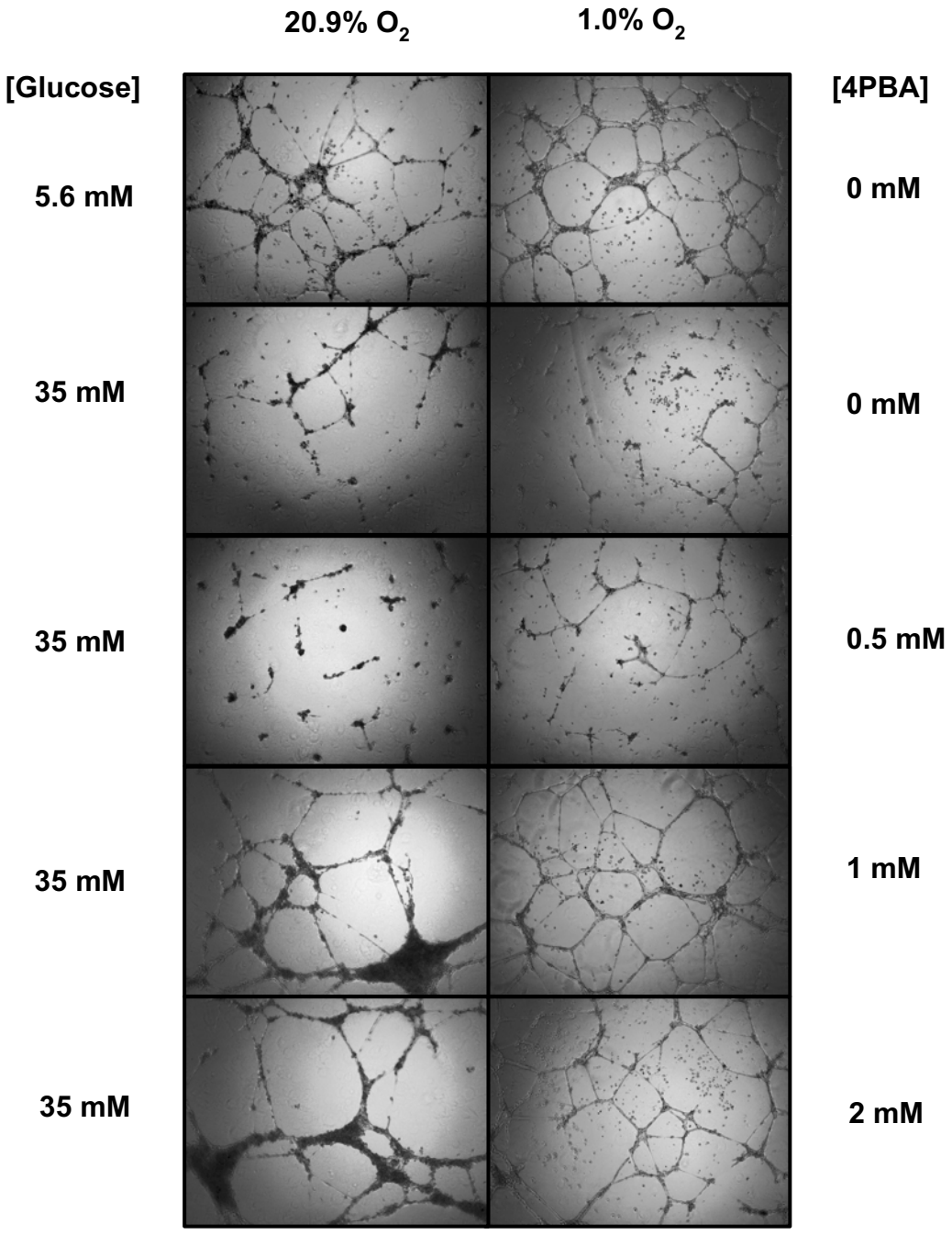
20.9% O_2
1.0% O_2
[Glucose]
[4PBA]
5.6 mM
0 mM
35 mM
0 mM
35 mM
0.5 mM
35 mM
1 mM
35 mM
2 mM

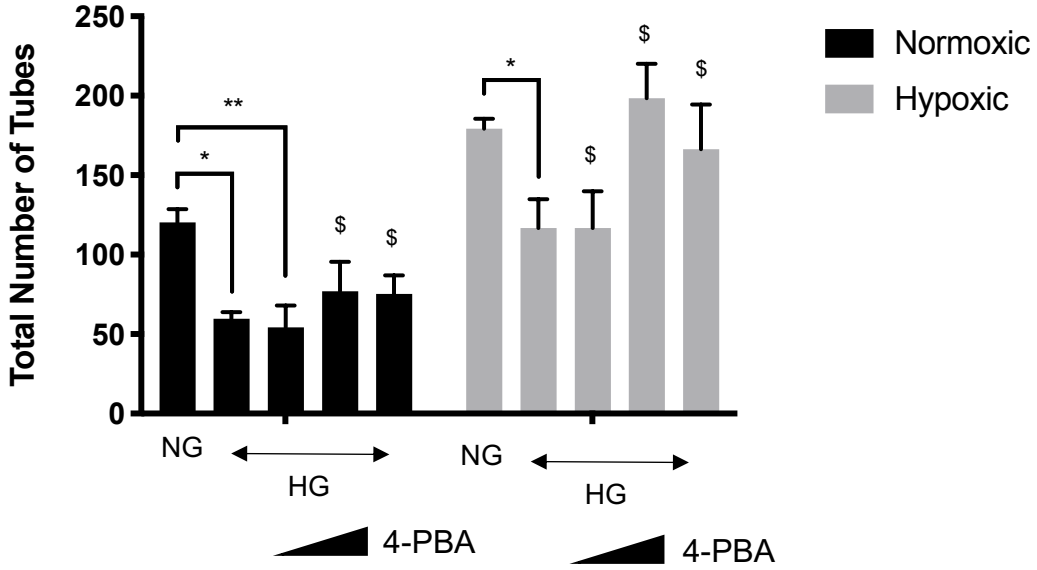
Total Number of Tubes
250
200
150
100
50
0
**
*
$
$
*
$
$
Normoxic
Hypoxic
NG
HG
4-PBA
NG
HG
4-PBA

(B)

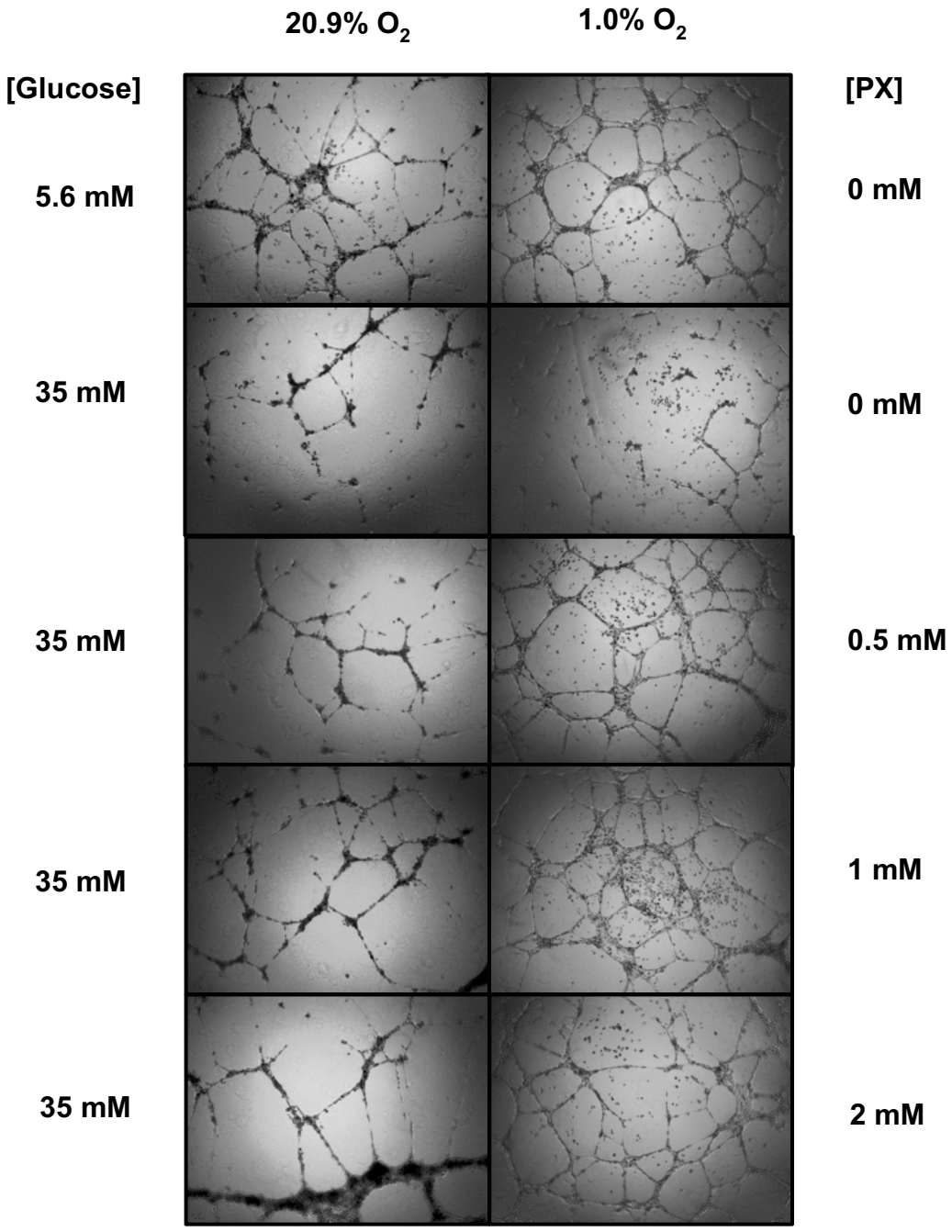
20.9% O2
1.0% O2
[Glucose]
[PX]
5.6 mM
0 mM
35 mM
0 mM
35 mM
0.5 mM
35 mM
1 mM
35 mM
2 mM

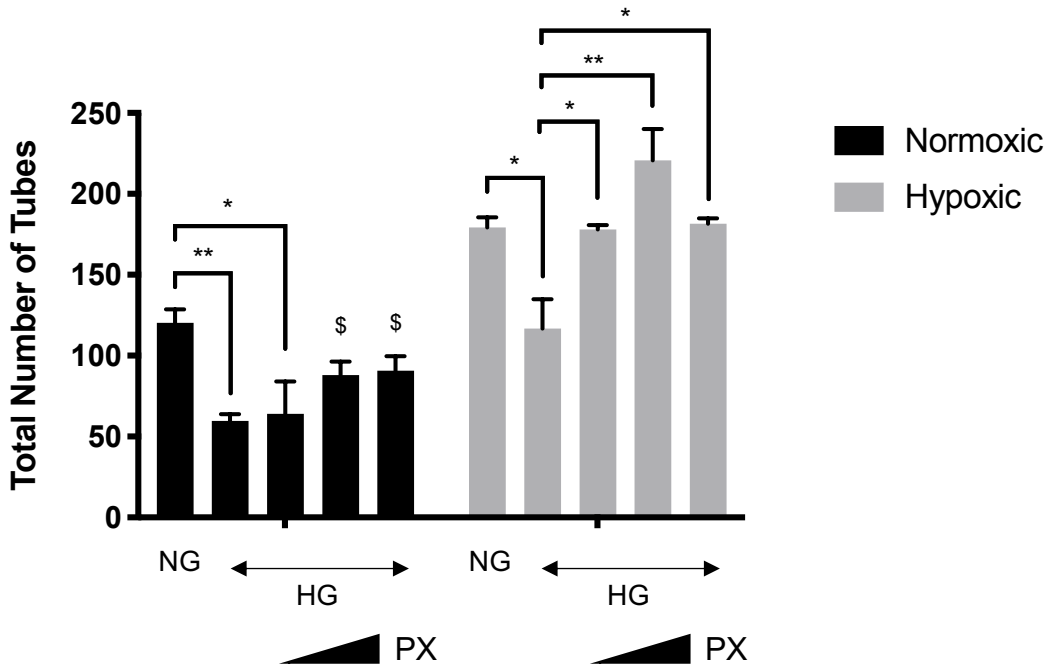
Total Number of Tubes
250
200
150
100
50
0
*
**
*
*
**
*
$
$
NG
HG
PX
NG
HG
PX
Normoxic
Hypoxic

(C)

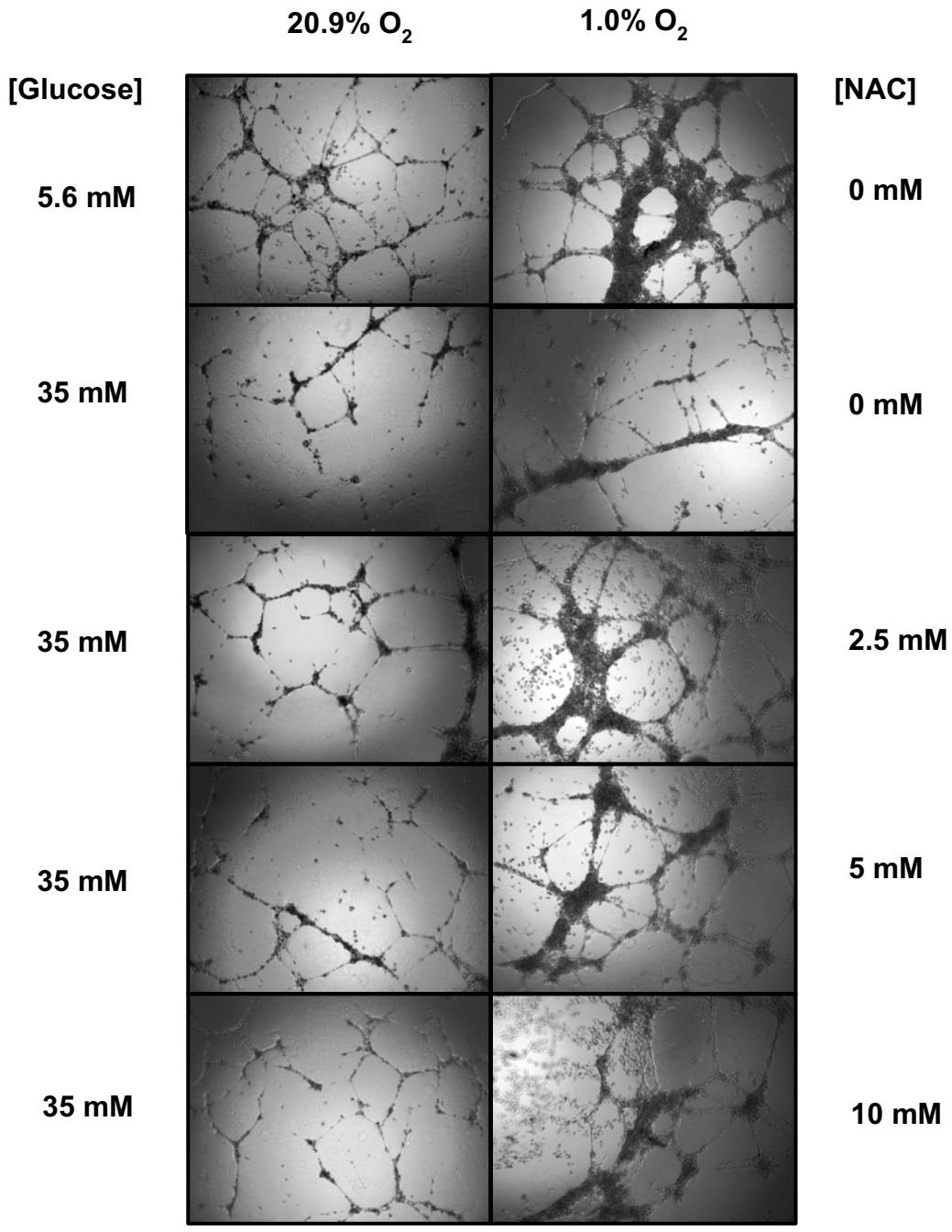
20.9% O2
1.0% O2
[Glucose]
[NAC]
5.6 mM
0 mM
35 mM
0 mM
35 mM
2.5 mM
35 mM
5 mM
35 mM
10 mM

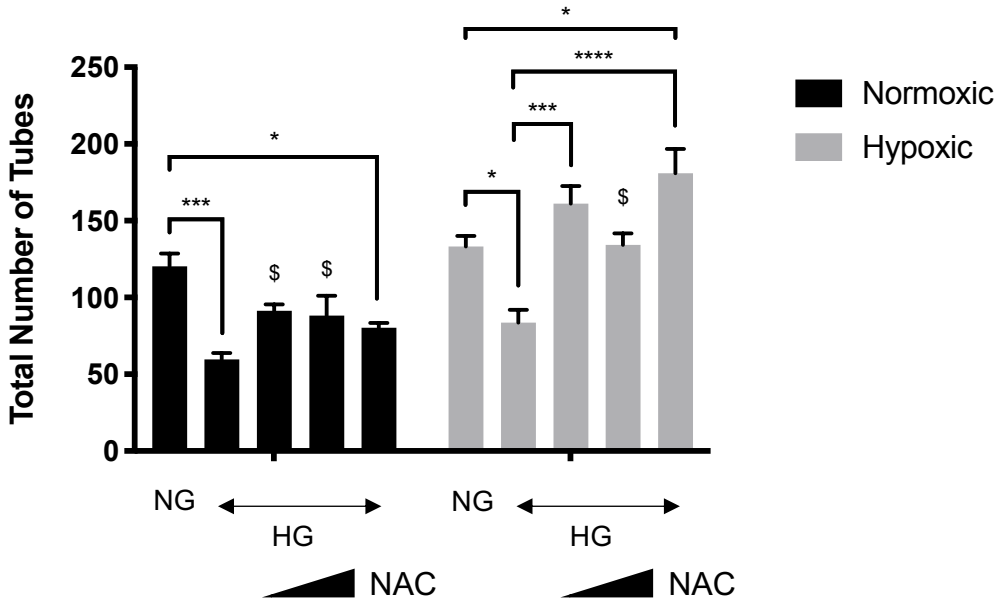
Total Number of Tubes
250
200
150
100
50
0
***
*
$
$
*
***
****
*
$
Normoxic
Hypoxic
NG
HG
NAC
NG
HG
NAC

4.3. HMVEC-C Expression of VEGF-A, VEGFR-2 and iNOS is Modulated by Hyperglycemia in Hypoxia

HMVEC-C monolayers were cultured in normoxia and hypoxia with normal (5.6 mM) or high (35 mM) glucose for 24 hours. After treatment, expression of VEGF-A, VEGFRs and cellular stress markers were analyzed by quantitative real time reverse transcription PCR (qPCR).

Autocrine VEGF-A and VEGFR-2 gene expression was significantly increased in hypoxic, normal glucose conditions compared to normoxic, normal glucose conditions (**Figure 11**). However, hypoxic, high glucose conditions blunted the significant increase of VEGF-A and VEGFR-2 expression compared to hypoxic, normal glucose conditions (**Figure 11**). iNOS expression was elevated in hypoxia compared to normoxia. Hypoxic, high glucose conditions elevated iNOS expression further ($p = 0.052$) when compared to normoxic, normal glucose conditions (**Figure 11**). No differences were observed for any of the genes analyzed between normal and high glucose in normoxia (**Figure 11**). VEGFR-1, CHOP, IL-1β and eNOS expression were not affected by any treatment group (**Figure 11**).

These results demonstrate a potential mechanism of reduced angiogenesis of HMVEC-Cs in hypoxic conditions. This could be explained by the effect of oxidative stress inhibiting the hypoxia-induced upregulation of VEGF-A and VEGFR-2 expression.

Figure 11. High glucose (35 mM) blunts hypoxia induced upregulations of VEGF-A and VEGFR-2. iNOS expression elevated in hypoxic, high glucose conditions. Change in gene expression of total VEGF-A, VEGFR-1, VEGFR-2, CHOP, iNOS, eNOS and IL-1β in monolayers of HMVEC-Cs treated with normal glucose (5 mM) or high glucose (35 mM) for 24 hours in a normoxic or hypoxic (1% O_2) environment. GAPDH used as a housekeeping control. Data expressed as an arbitrary unit in which the control group value equals 1.
n = 3 – 4 per group. Data expressed as mean ± SEM. Significance calculated using a two-way ANOVA followed by a multiple comparison test. *$p < 0.05$.

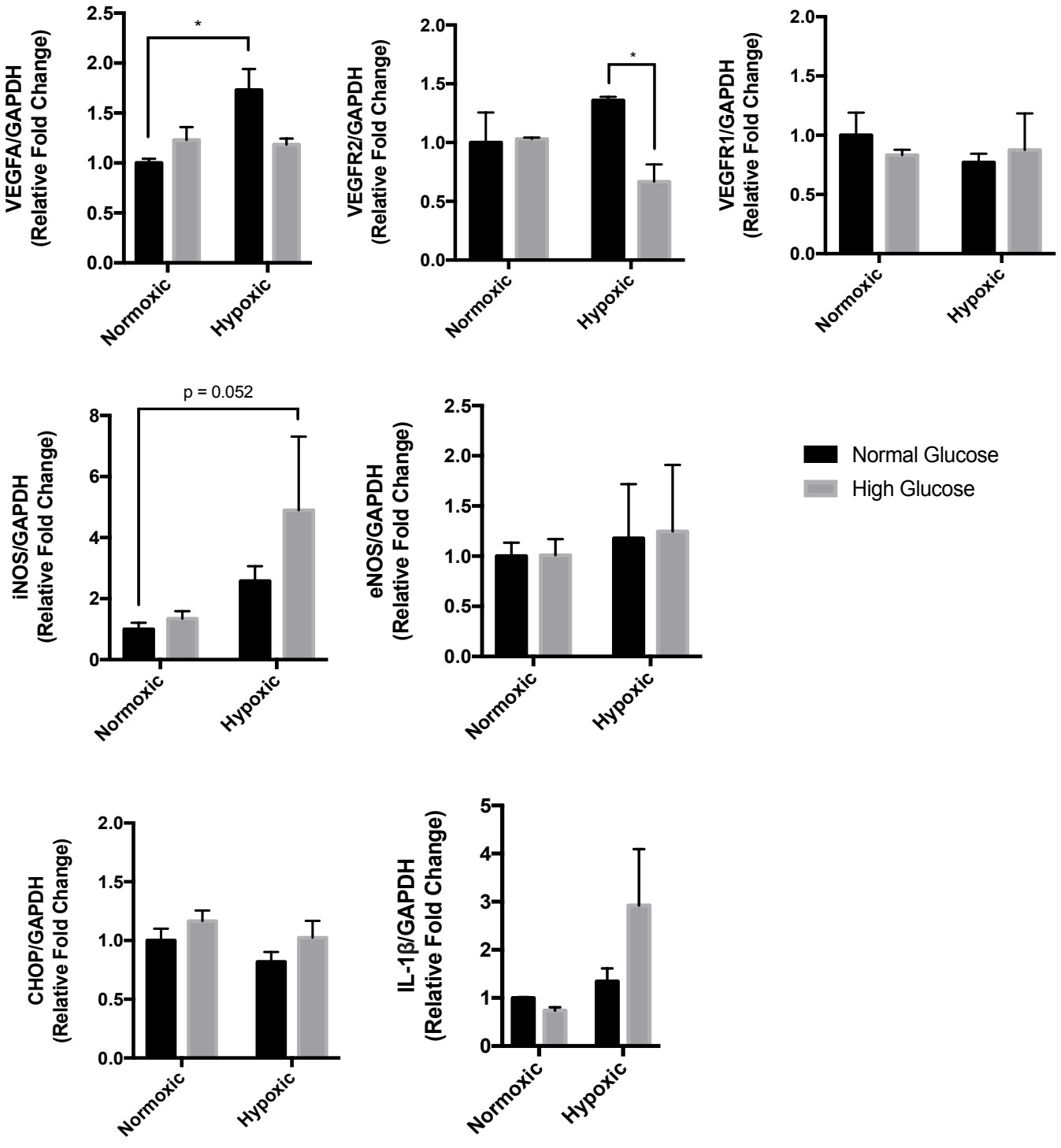
VEGFA/GAPDH (Relative Fold Change)
2.5
2.0
1.5
1.0
0.5
0.0
*
Normoxic
Hypoxic
VEGFR2/GAPDH (Relative Fold Change)
2.0
1.5
1.0
0.5
0.0
*
Normoxic
Hypoxic
VEGFR1/GAPDH (Relative Fold Change)
2.0
1.5
1.0
0.5
0.0
Normoxic
Hypoxic
iNOS/GAPDH (Relative Fold Change)
p = 0.052
8
6
4
2
0
Normoxic
Hypoxic
eNOS/GAPDH (Relative Fold Change)
2.5
2.0
1.5
1.0
0.5
0.0
Normoxic
Hypoxic
Normal Glucose
High Glucose
CHOP/GAPDH (Relative Fold Change)
2.0
1.5
1.0
0.5
0.0
Normoxic
Hypoxic
IL-1β/GAPDH (Relative Fold Change)
5
4
3
2
1
0
Normoxic
Hypoxic

4.3.1. Treatment with NAC or PX Rescues Hyperglycemic Induced Upregulation of VEGF-A in Hypoxia

Hypoxia induced upregulation of VEGF-A and VEGFR-2 gene expression was reduced in high glucose conditions (**Figure 11**). To examine the mechanisms associated with this reduction, HMVEC-Cs were treated with NAC (5 mM), PX (1 mM) or 4PBA (1 mM) for 24 hours in a normoxic or hypoxic (1% O_2) environment. qPCR was used to evaluate VEGF-A and VEGFR-2 gene expression after treatment. Treatment with NAC at 5 mM or PX at 1 mM seemed to elevate VEGF-A gene expression in hypoxic, high glucose conditions. However, the sample size needs to be increased to determine the significance of this trend. 4PBA did not rescue VEGF-A expression, maintaining normal glucose control expression levels (**Figure 12A**). None of the chemical interventions rescued hyperglycemic induced VEGFR-2 blunting (**Figure 12B**). These results suggest a role of hyperglycemia on autocrine VEGF-A production in hypoxic conditions, with respect to reducing *in vitro* angiogenesis in tube formation assays.

4.3.2. Treatment with NAC or PX Attenuates Hyperglycemic Increases of iNOS Expression In Hypoxia

As an extension of the previous experiment, iNOS gene expression was further examined. Treatment with NAC (5 mM) or PX (1 mM) was associated with decreased hyperglycemic elevations in iNOS gene expression in hypoxia (**Figure 12C**). However, this result was not statistically significant. Future experiments should be carried out with an increased sample size to determine the significance of this trend.

Figure 12. Treatment with PX or NAC in high glucose conditions rescues VEGF-A and iNOS expression back to levels similar to normal glucose controls in hypoxia. VEGFR-2 blunting in hypoxic, high glucose does not normalize with any treatment. Change in the gene expression of **(A)** total VEGF-A **(B)** VEGFR-2 and **(C)** iNOS in monolayers of HMVEC-Cs treated with normal glucose (5 mM) or high glucose (35 mM) + chemical interventions (4PBA = 1 mM, NAC = 5 mM or PX = 1 mM) for 24 hours in a hypoxic (1% O_2) environment. β-actin used as a housekeeping control and data expressed as an arbitrary unit in which the control group value equals 1. *n* = 3 to 4 per group. Data expressed as mean ± SEM. Significance calculated using a two-way ANOVA followed by a multiple comparison test. $^{\#}p < 0.05$, $^{\#\#}p < 0.01$ relative to normal glucose controls.

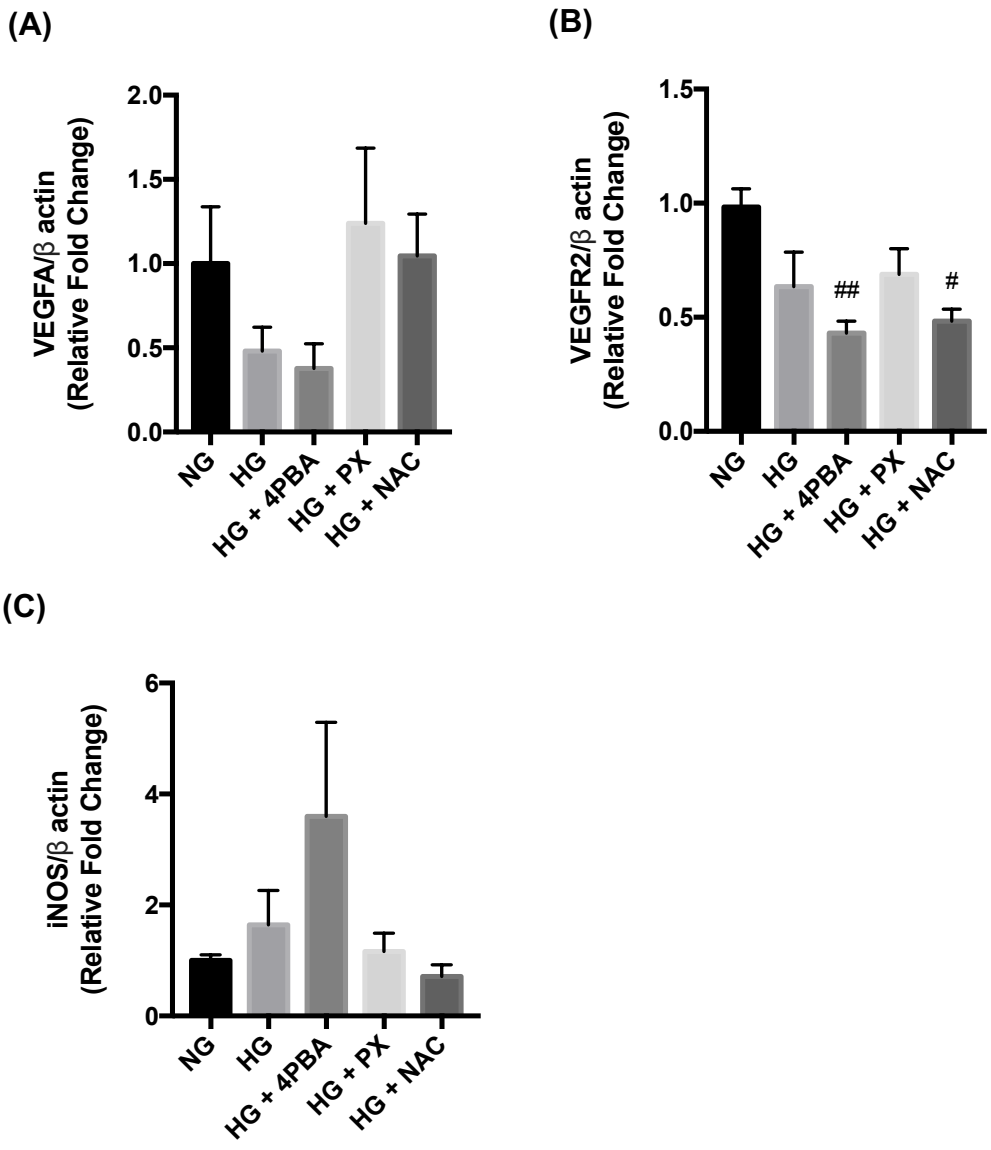
(A)
VEGFA/β actin
(Relative Fold Change)
2.0
1.5
1.0
0.5
0.0
NG
HG
HG + 4PBA
HG + PX
HG + NAC
(B)
VEGFR2/β actin
(Relative Fold Change)
1.5
1.0
0.5
0.0
##
#
NG
HG
HG + 4PBA
HG + PX
HG + NAC
(C)
iNOS/β actin
(Relative Fold Change)
6
4
2
0
NG
HG
HG + 4PBA
HG + PX
HG + NAC

To this point, *in vitro* data suggests that high glucose reduces HMVEC-Cs angiogenesis by attenuating VEGF-A and VEGFR-2 expression in response to hypoxic conditions. This interference is most likely a result of oxidative stress or AGEs, rather than ER stress, as treatment with PX or NAC was able to increase angiogenesis and VEGF-A expression in hypoxic conditions relative to normal glucose, control levels. Therefore, in order to confirm these effects *in vivo*, we completed a pilot study to test the efficacy and safety of 4PBA, NAC or PX supplementation in the drinking water of streptozotocin (STZ) APOE$^{-/-}$ mice. This included analysis of possible off target effects of STZ on metabolic parameters, body weight and organ size to eliminate potential confounding variables.

4.4. Effects of Hyperglycemia on Metabolic Parameters, Body Weight and Organ Size of STZ-APOE$^{-/-}$ Mice

Examining metabolic parameters, body weight and organ statistics are important to assess the safety of *in vivo* drug administration. Prior to that, STZ-induced effects without intervention treatments were first assessed to allow a direct comparison between STZ-hyperglycemic and STZ-hyperglycemic chemical intervention treated mice. STZ selectively targets and destroys pancreatic β cells, however possible off target interactions could implicate the functionality of other organs.

Metabolic parameter analysis shows elevated fasted blood glucose levels in 8, 12 and 16 week old hyperglycemic STZ-APOE$^{-/-}$ compared to normoglycemic APOE$^{-/-}$ controls (**Figure 13A**). This finding is similar to what was observed in the glucose tolerance data, where there is a significant increase in the area under the curve of STZ-APOE$^{-/-}$ mice compared to normoglycemic APOE$^{-/-}$ controls (**Figure 13C).**

Body weight analysis displays a reduced weight of STZ-APOE$^{-/-}$ mice compared to APOE$^{-/-}$ controls at 16 weeks of age (**Figure 13D**). Despite having reduced whole body weight, 16 week STZ-APOE$^{-/-}$ mice have significantly increased left kidney and liver weights compared to age matched APOE$^{-/-}$ controls (**Figure 14A-B**). Further, STZ-APOE$^{-/-}$ mice have significantly reduced perigonadal adipose, which is the visceral fat surrounding the gonads, at 16 weeks of age compared to age matched APOE$^{-/-}$ controls (**Figure 14D**). Although STZ selectively destroys pancreatic β cells, no significant difference in pancreas weight was observed in any of the experimental groups (**Figure 14C**).

4.5. Effects of Interventions on Metabolic Parameters, Body Weight and Organ Size of STZ-APOE$^{-/-}$ Mice

Treatment with 4PBA for 8 weeks increased endpoint glucose tolerance in hyperglycemic STZ-APOE$^{-/-}$ mice compared to hyperglycemic

STZ-APOE$^{-/-}$ mice without 4PBA treatment. These results were measured though an endpoint glucose tolerance test (**Figure 13B**) and area under the curve analysis of the glucose tolerance curves from 0 to 120 minutes post IP glucose injection (**Figure 13C**). Further, 16 week endpoint blood glucose level was significantly reduced in hyperglycemic STZ-APOE$^{-/-}$ mice treated with 4PBA compared to hyperglycemic STZ-APOE$^{-/-}$ mice without 4PBA treatment. However, the reduced values are still considered hyperglycemic (**Figure 13A**). NAC or PX administration had no effect on glycemia or glucose tolerance after 8 weeks of treatment (**Figure 13A-C**).

To observe if 4PBA, NAC or PX treatment could influence other organs beyond the vasculature, kidney weight, liver weight, pancreatic weight and perigonadal adipose weight was measured as a ratio relative to body weight in all experimental groups. Treatment with 4PBA or PX in hyperglycemic STZ-APOE$^{-/-}$ mice significantly reduced left kidney weight such that their weight were no different to normoglycemic APOE$^{-/-}$ mice or normoglycemic APOE$^{-/-}$ mice treated with 4PBA or PX. These ratios were reduced compared to hyperglycemic STZ-APOE$^{-/-}$ mice without treatment. Treatment with NAC had no effect on rescuing kidney weight in hyperglycemic STZ-APOE$^{-/-}$ mice (**Figure 14A**). None of the chemical interventions (4PBA, NAC or PX) were able to reduce liver weights or increase perigonadal weights back to normoglycemic control levels.

Figure 13. Glycemia, glucose tolerance and body weight analysis of 4PBA, NAC or PX treated and untreated APOE$^{-/-}$ and STZ-APOE$^{-/-}$ mice. (A) Fasted blood glucose measurements of all groups (normoglycemic, hyperglycemic, normoglycemic + chemical interventions and hyperglycemic + chemical interventions) at 5 weeks, 8 weeks, 12 weeks and 16 weeks of age. Chemical interventions started at 8 weeks of age (after STZ injections completed to induce hyperglycemia). ****$p < 0.0001$ relative to normoglycemic group. $^{\#\#\#\#}p < 0.0001$ relative to hyperglycemic group. **(B)** 16 week endpoint glucose tolerance test curves of all experimental groups. ****$p < 0.0001$ relative to normoglycemic group. $^{\#\#\#\#}p < 0.0001$ relative to hyperglycemic group. **(C)** Glucose tolerance test area under the curve calculated with a baseline set at y = 0. Area under the curve calculated using the trapezoidal method. ****$p < 0.0001$ relative to normoglycemic group. $^{\#\#\#\#}p < 0.0001$ relative to hyperglycemic group. **(D)** Body weight. Data expressed as mean ± SEM, *n* = 3 – 9 per group. Significance calculated using a two-way ANOVA followed by a multiple comparison test.

(A)

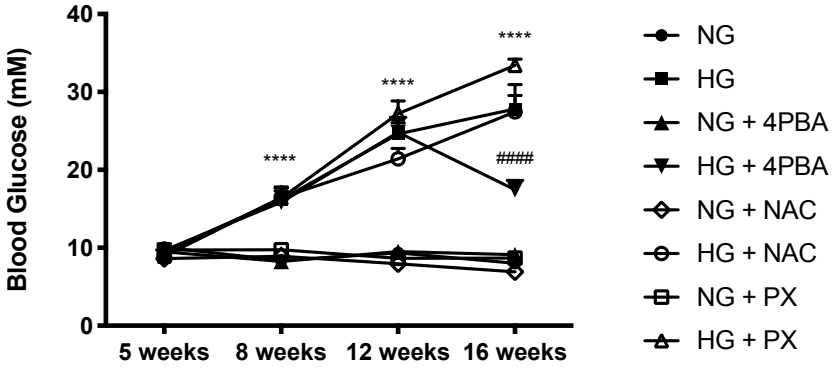

(B)

(C)

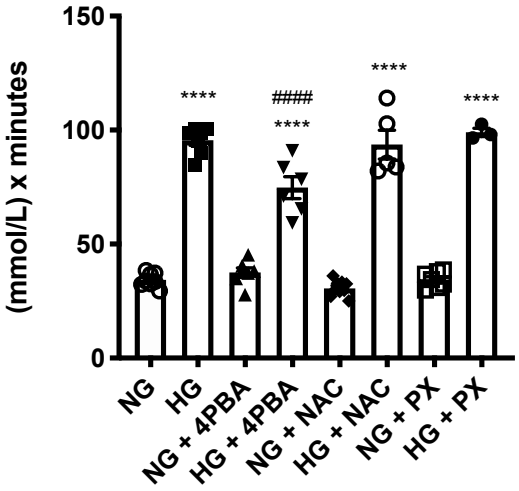

(D)

Glycemia	NG Body Weight (g)				HG Body Weight (g)			
Treatment	**NT**	**+4PBA**	**+NAC**	**+PX**	**NT**	**+4PBA**	**+NAC**	**+PX**
5 week	14.4 ± 0.4	16.0 ± 0.4	13.5 ± 0.5	15.3 ± 0.2	16.1 ± 0.9	14.0 ± 0.5	14.6 ± 0.5	15.1 ± 0.3
8 week	16.6 ± 0.6	15.8 ± 0.2	17.4 ± 0.4	17.6 ± 0.5	15.6 ± 0.7	15.1 ± 0.4	15.6 ± 0.4	14.9 ± 0.6
12 week	18.4 ± 0.7	18.5 ± 0.3	19.7 ± 0.4	19.7 ± 0.4	18.1 ± 0.9	17.5 ± 0.6	17.3 ± 0.7	16.8 ± 1.2
16 week	20.5 ± 0.5	18.3 ± 0.6	21.1 ± 0.3	21.0 ± 0.7	18.6 ± 0.9	18.4 ± 0.8	16.7 ± 1.0	16.8 ± 1.6

*NT = no treatment

Figure 14. Organ statistics of 16 week old hyperglycemic STZ-APOE$^{-/-}$ and normoglycemic APOE$^{-/-}$ controls treated with or without chemical interventions (4PBA, NAC or PX). (A) Left kidney **(B)** liver **(C)** pancreas and **(D)** perigonadal adipose weight (g) relative to the body weight of each mouse was recorded and calculated for each experimental group after sacrifice at 16 weeks of age. Data expressed as mean ± SEM, *n* = 2 – 9 per group. Significance calculated using a one-way ANOVA followed by a multiple comparison test. *p < 0.05, **p < 0.01, ***p < 0.001, ****p < 0.0001 relative to normoglycemic APOE$^{-/-}$ group. ####p < 0.0001 relative to hyperglycemic APOE$^{-/-}$ group.

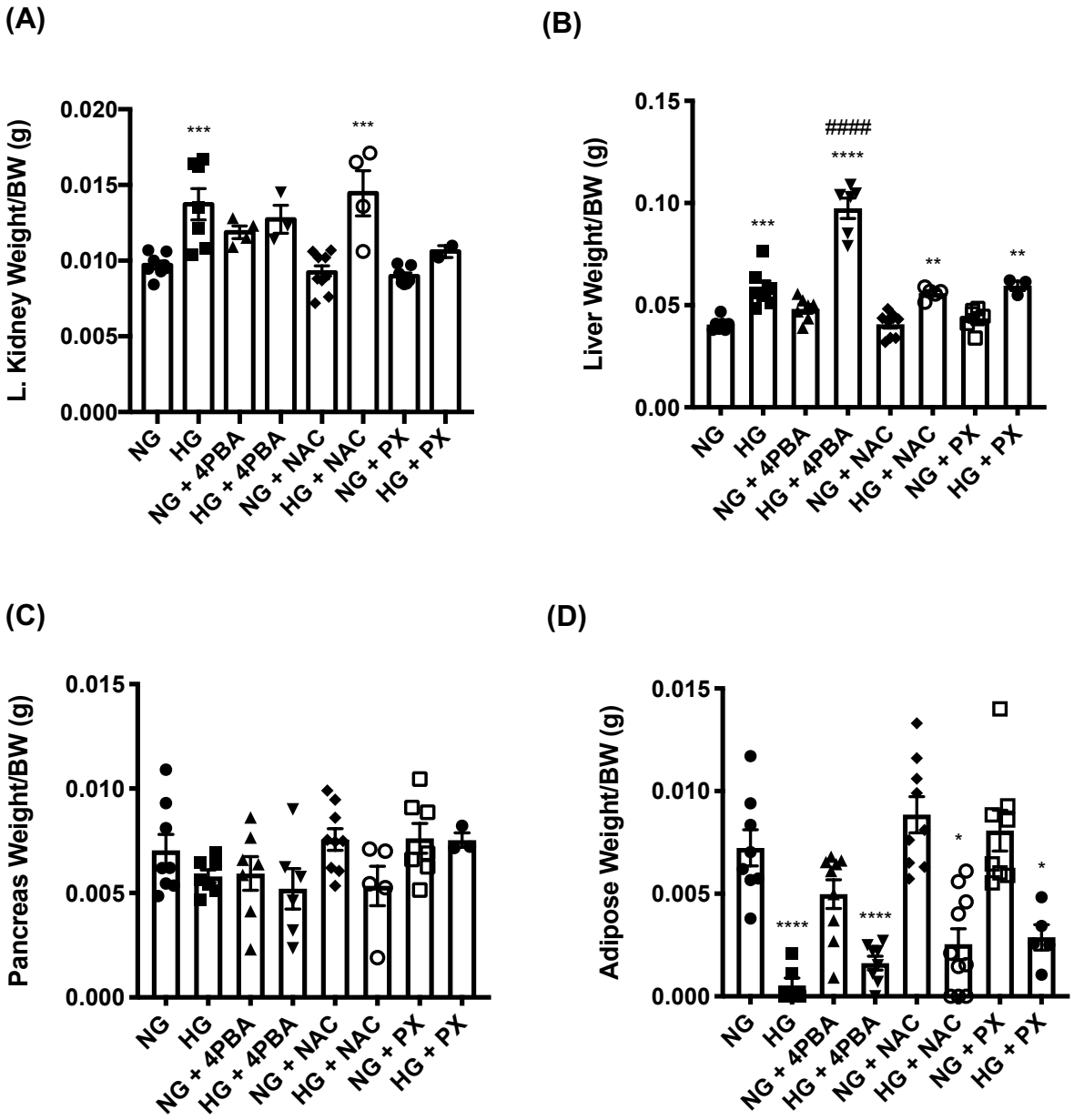
(A)
L. Kidney Weight/BW (g)
0.020
0.015
0.010
0.005
0.000
***
***
NG
HG
NG + 4PBA
HG + 4PBA
NG + NAC
HG + NAC
NG + PX
HG + PX
(B)
Liver Weight/BW (g)
0.15
0.10
0.05
0.00
####
****
***
**
**
NG
HG
NG + 4PBA
HG + 4PBA
NG + NAC
HG + NAC
NG + PX
HG + PX
(C)
Pancreas Weight/BW (g)
0.015
0.010
0.005
0.000
NG
HG
NG + 4PBA
HG + 4PBA
NG + NAC
HG + NAC
NG + PX
HG + PX
(D)
Adipose Weight/BW (g)
0.015
0.010
0.005
0.000
****
****
*
*
NG
HG
NG + 4PBA
HG + 4PBA
NG + NAC
HG + NAC
NG + PX
HG + PX

4.6. Hyperglycemia is Associated with Hypoxia in the Arterial Wall and Atherosclerosis Development

Despite a known relationship between hyperglycemia and reduced vasa vasorum density[31], it is still unclear whether hypoxia drives lesion development or if lesion development drives hypoxia. For this reason, we examined early hypoxia in 10 week old hyperglycemic STZ-APOE$^{-/-}$ mice and normoglycemic APOE$^{-/-}$ controls before significant lesion progression. Hypoxia was analyzed in the aortic sinus using two effective hypoxia markers, HIF-1α and hypoxyprobe. Hypoxyprobe, which is IP injected approximately 2 hours prior to sacrifice, uses pimonidazole hydrochloride which forms protein adducts inside hypoxic cells with an O_2 partial pressure < 10 mmHg. These adducts can be visualized through immunohistochemistry staining using a monoclonal antibody that binds pimonidazole hydrochloride.

Hyperglycemic STZ-APOE$^{-/-}$ mice had significantly elevated fasting blood glucose levels compared to age matched normoglycemic APOE$^{-/-}$ controls at 8 and 10 weeks of age (**Figure 15A**). Aortic sinus staining of 10 week old hyperglycemic STZ-APOE$^{-/-}$ and age matched normoglycemic APOE$^{-/-}$ mice demonstrated early lesion development in hyperglycemic STZ-APOE$^{-/-}$ mice. No lesions were detected in normoglycemic APOE$^{-/-}$ controls (**Figure 15B**). STZ-APOE$^{-/-}$ mice had increased hypoxyprobe (p =

0.24) and HIF-1α (p = 0.10) staining in the intima of aortic sinus serial sections compared to normoglycemic APOE$^{-/-}$ controls (**Figure 15**). These results suggest that hypoxia precedes significant atherosclerosis development and may accelerate the progression of atherosclerosis in the presence of DM. However, the small sample size needs to be elevated per group and significance reassessed to determine if $p < 0.05$.

Figure 15. **Hyperglycemia is associated with increased early hypoxia and atherosclerosis development at the aortic sinus of 10 week old female APOE$^{-/-}$ mice.** Female APOE$^{-/-}$ mice were enrolled at 5 weeks, injected with STZ for 2 consecutive weeks, confirmed as hyperglycemic with a blood glucose measurement > 15 mM at 8 weeks, followed by sacrifice at 10 weeks of age. **(A)** Metabolic parameters of hyperglycemic STZ-APOE$^{-/-}$ (STZ-HG) and normoglycemic APOE$^{-/-}$ (NG) mice at 5 weeks, 8 weeks and 10 weeks of age. *N* values indicated. **(B)** Masson's Trichrome representative staining for analysis of atherosclerotic development. Black arrows indicate regions of the aortic sinus with early plaque development. Scale bar = 100 μm. **(C)** Immunohistochemistry hypoxyprobe representative staining for hypoxic tissues (< 10 mmHg). Pimonidazole hydrochloride IP injected 2 hours prior to sacrifice. Black arrows indicate positive regions with early hypoxia. Scale bar = 100 μm**.** **(D)** HIF-1α immunofluorescent representative staining of the aortic sinus. White arrows indicate positive regions with early hypoxia. Scale bar = 100 μm**.** Percentage of intima stained quantification of **(E)** hypoxyprobe and **(F)** HIF-1α with corresponding p-value from a unpaired t-test. **(G)** Pre-immune IgG negative control images of the aortic sinus.

(A)	5 weeks	8 weeks		10 weeks	
	NG	**NG**	**STZ-HG**	**NG**	**STZ-HG**
Blood glucose (mM)	9.46 ± 0.42	7.68 ± 0.69	19.55 ± 2.05****	7.83 ± 0.88	21.63 ± 1.72****
Body weight (g)	13.70 ± 0.48	15.53 ± 0.62	14.45 ± 0.53	17.70 ± 0.56	15.25 ± 0.76*
Plasma					
Triglycerides (mM)	-	-	-	0.66 ± 0.07	0.51 ± 0.10
Cholesterol (mM)	-	-	-	5.92 ± 0.88	6.62 ± 1.03
n	8	4	4	4	4

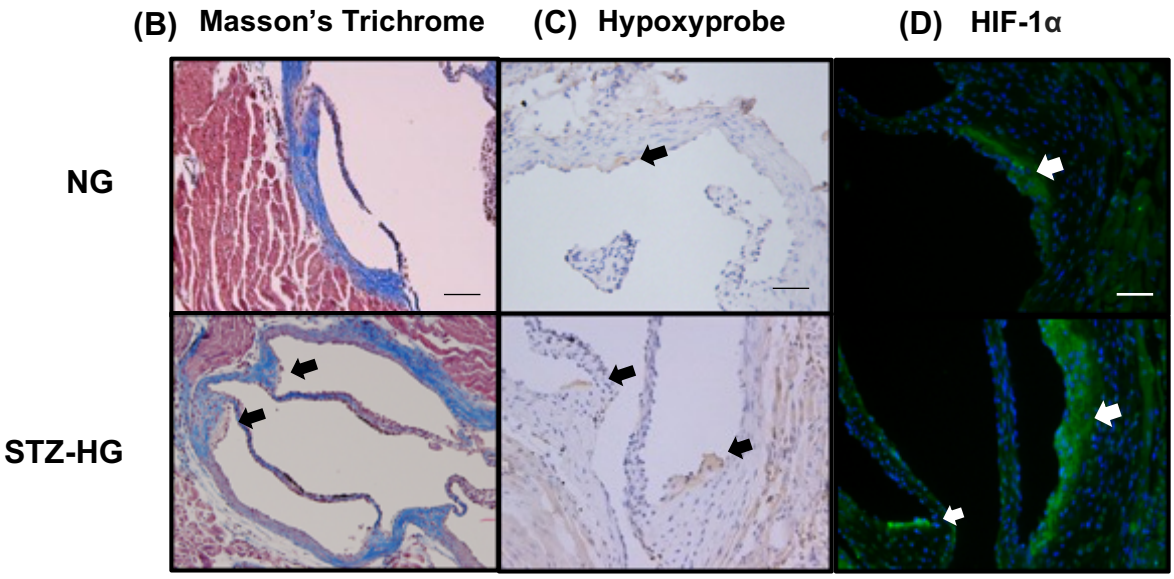

(E) Hypoxyprobe Quantification

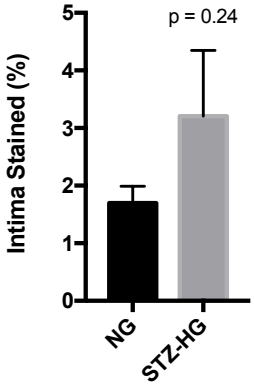

(F) HIF-1α Quantification

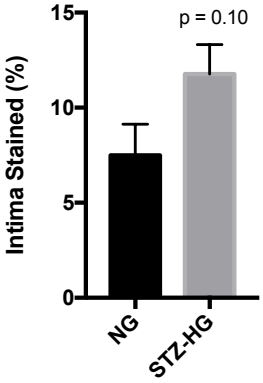

(G)

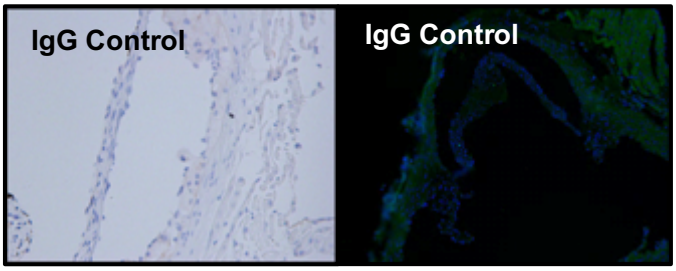

Hyperglycemic STZ-APOE$^{-/-}$ mice show increased early atherosclerosis development (**Figure 15B**) and elevated hypoxia staining (**Figure 15E-F**) in the intima compared to age matched normoglycemic APOE$^{-/-}$ controls. Staining appears to localize to macrophage foam cells in the subintima suggesting that hypoxia precedes atherosclerosis *in vivo*. To further examine subintimal macrophage recruitment, and the impact of hypoxia on macrophage physiology, we utilized qPCR on phorbol 12-myristate 13-acetate (PMA) differentiated THP-1 derived macrophages rested for 5 days (PMAr) and assessed angiogenic gene expression.

4.7.1. Hyperglycemia Causes Differential Splicing of VEGF-A in Hypoxia in PMAr THP-1 Derived Macrophages

To further examine subintimal macrophages and the impact of arterial hypoxia on macrophage physiology, gene expression of different VEGF-A splice variants in normal glucose (5 mM) or high glucose (35 mM) in normoxic or hypoxic conditions were analyzed by qPCR using PMAr THP-1 derived macrophages. Hypoxia caused a significant increase in total VEGF-A, VEGF-A_{165} and VEGF-A_{189} gene expression compared to normoxic controls (**Figure 16A-C**). No differences were seen in VEGF-A, VEGF-A_{165} or VEGF-A_{189} expression between normal and high glucose conditions in either hypoxia or normoxia (**Figure 16A-C**).

4.7.2. Hyperglycemia Causes Differential Splicing of VEGF-A_{165} in Hypoxia in PMAr THP-1 Derived Macrophages

Despite no differences between high glucose and normal glucose in hypoxia or normoxia for VEGF-A_{165}, it is important to examine further splice families of VEGF-A_{165}, including VEGF-A_{165}a (pro-angiogenic form) and VEGF-A_{165}b (anti-angiogenic form). These variants of VEGF-A_{165} can be utilized to study possible alterations to the balance between pro-angiogenic and anti-angiogenic forms of VEGF-A_{165}, specifically since VEGF-A_{165} gene expression appears unaffected under normal and high glucose conditions in both normoxia and hypoxia (**Figure 16B**).

Results showed no difference in VEGF-A_{165}a expression between normal and high glucose in normoxia. However, hypoxia elevated VEGF-A_{165}a expression in normal glucose, hypoxic conditions compared to normoxia (**Figure 17A**). This aligns with elevations in VEGF-A_{165} (**Figure 16B**). Further, high glucose conditions in hypoxia do not show the same trend of elevation. This suggests hyperglycemia interferes with the upregulation of VEGF-A_{165}a in hypoxic conditions, such that pro-angiogenic forms of VEGF-A_{165} are reduced (**Figure 17A).**

Results of VEGF-A_{165}b qPCR expression was variable with large SEM values. This could be due to the extreme specificity of this individual splice variant, meaning that despite using accurate primers, there may be

very limited VEGF-A_{165}b cDNA to bind the primers in the sample. Despite this variation, normal and high glucose conditions in hypoxia and high glucose in normoxia seem to elevate VEGF-A_{165}b expression compared to normal glucose, normoxic conditions (**Figure 17B**).

To examine the potential switch from pro-angiogenic splicing of VEGF-A_{165}a to anti-angiogenic splicing of VEGF-A_{165}b, VEGF-A_{165}a/ VEGF-A_{165}b was calculated before normalization (**Figure 17C**). Elevated expression of VEGF-A_{165}a compared to VEGF-A_{165}b would produce a ratio > 1. For example, a 2:1 ratio of VEGF-A_{165}a to VEGF-A_{165}b would yield a fold change of 2, representing double the amount of VEGF-A_{165}a to VEGF-A_{165}b. In contrast, reduced expression of VEGF-A_{165}a compared to VEGF-A_{165}b would produce a ratio < 1. For example, a 1:2 ratio of VEGF-A_{165}a to VEGF-A_{165}b would yield a fold change of 0.5, representing double the amount of VEGF-A_{165}b to VEGF-A_{165}a. Since large variation exists in VEGF-A_{165}b expression data (**Figure 17B),** ratio values also exhibit large variation. Nevertheless, these trends suggest reduced ratios of VEGF-A_{165}a to VEGF-A_{165}b in high glucose conditions in normoxia, and both normal and high glucose conditions in hypoxia compared to normal glucose conditions in normoxia. This suggests a switch from pro-angiogenic to anti-angiogenic forms in hyperglycemia, and hyperglycemia in hypoxia. Future experiments will aim to eliminate the large variation of

VEGF-A_{165}b expression as well as examine the significance of these trends by repeating the experiments with an increased sample size.

Figure 16. Hypoxia significantly increases the expression of total VEGF-A and differential splice variants of VEGF-A (VEGF-A_{165} and VEGF-A_{189}) in PMAr THP-1 derived macrophages. High glucose (35 mM) has no effect on total VEGF-A or VEGF-A splice variant expression. (A) Total VEGF-A **(B)** VEGF-A_{165} and **(C)** VEGF-A_{189} qPCR analysis of PMAr THP-1 derived macrophages in normoxic and hypoxic conditions in normal glucose (5 mM) or high glucose (35 mM). Relative amounts of VEGF-A, VEGF-A_{165} and VEGF-A_{189} were normalized to GAPDH and expressed as an arbitrary unit in which the control group value equals 1. n = 3 – 4 per group. Data expressed as mean ± SEM. Significance calculated using a two-way ANOVA followed by a multiple comparison test. *$p < 0.05$, **$p < 0.01$, ***$p < 0.001$ relative to normoxic, normal glucose group. $^{\#}p < 0.05$, $^{\#\#}p < 0.01$, $^{\#\#\#}p < 0.001$, $^{\#\#\#\#}p < 0.0001$ relative to normoxic, high glucose group.

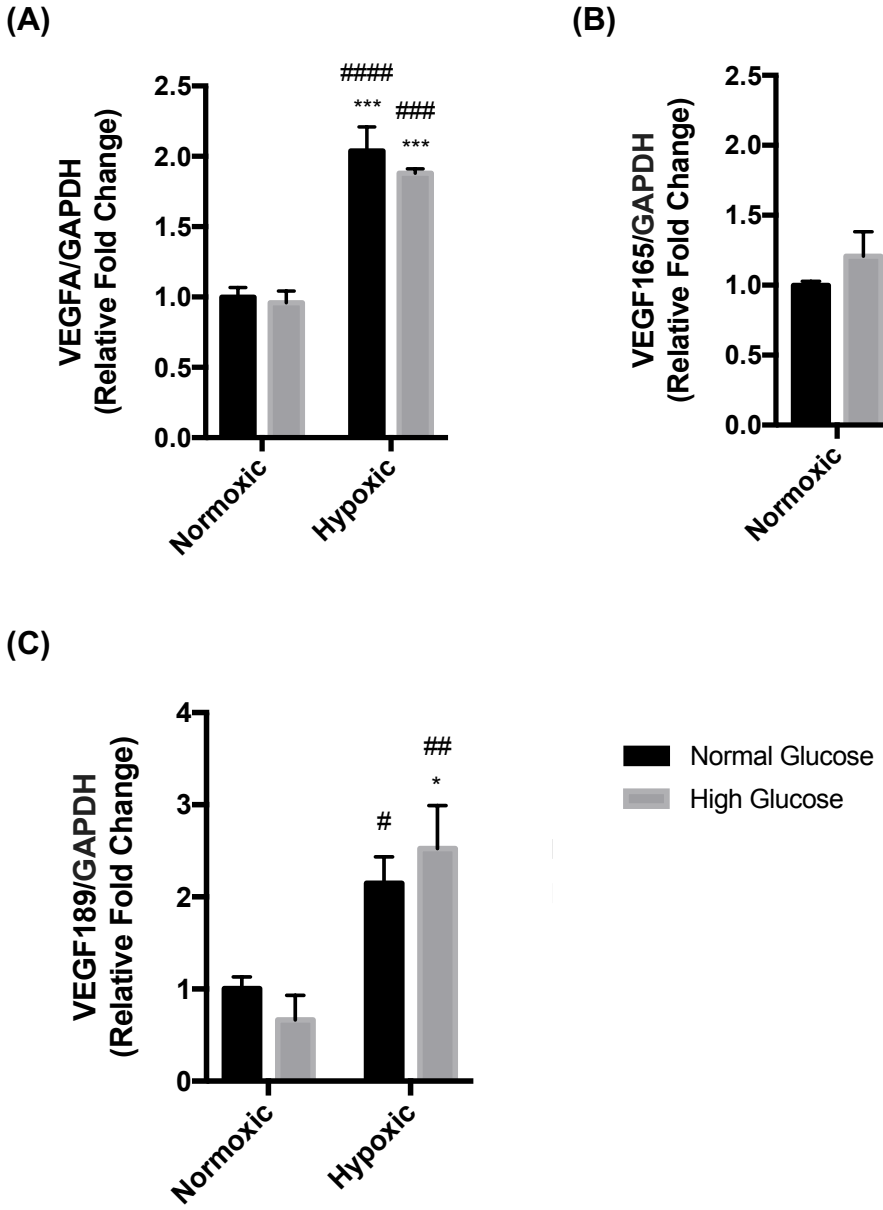
(A)
VEGFA/GAPDH
(Relative Fold Change)
2.5
2.0
1.5
1.0
0.5
0.0
####
***
###
***
Normoxic
Hypoxic
(B)
VEGF165/GAPDH
(Relative Fold Change)
2.5
2.0
1.5
1.0
0.5
0.0
#
**
###
**
Normoxic
Hypoxic
(C)
VEGF189/GAPDH
(Relative Fold Change)
4
3
2
1
0
#
##
*
Normoxic
Hypoxic
Normal Glucose
High Glucose

Figure 17. High glucose blunts the hypoxic mediated upregulation of the pro-angiogenic VEGF-A_{165} differential splice variant, VEGF-A_{165}a in PMAr THP-1 derived macrophages in hypoxia (1% O_2). (A) VEGF-A_{165}a **(B)** VEGF-A_{165}b and **(C)** VEGF-A_{165}a/VEGFA-$_{165}$b qPCR expression of PMAr THP-1 derived macrophages in normoxic and hypoxic conditions in normal glucose (5 mM) or high glucose (35 mM). Relative amounts of VEGF-A_{165}a and VEGF-A_{165}b were normalized to β-actin and expressed as an arbitrary unit in which the control group equals 1. *n* = 3 to 4 per group. Data expressed as mean ± SEM. Significance calculated using a two-way ANOVA followed by a multiple comparison test **$p < 0.01$ relative to normoxic, normal glucose group. $^{\#\#}p < 0.01$ relative to normoxic, high glucose group.

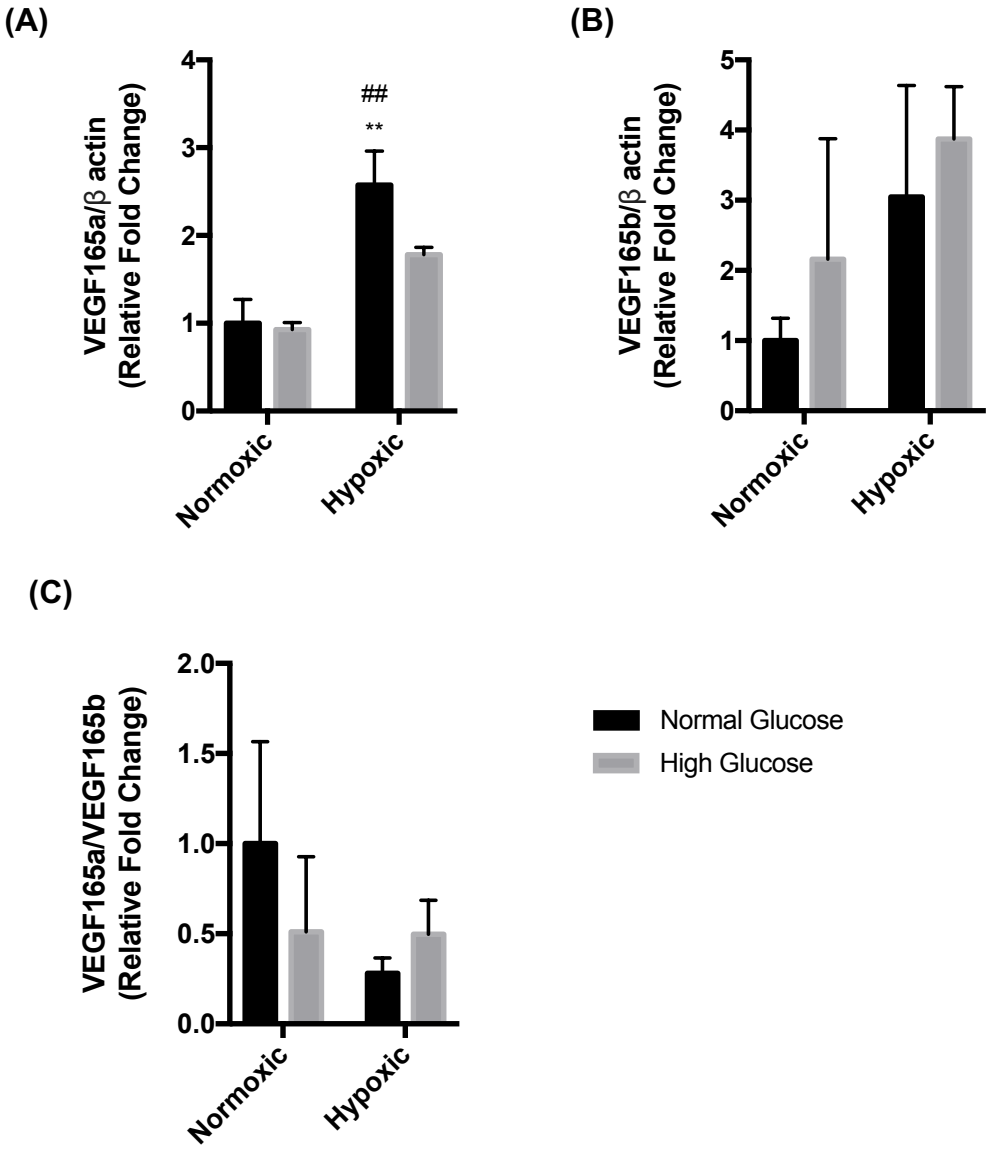
(A)
VEGF165a/β actin
(Relative Fold Change)
4
3
2
1
0
##
**
Normoxic
Hypoxic
(B)
VEGF165b/β actin
(Relative Fold Change)
5
4
3
2
1
0
Normoxic
Hypoxic
(C)
VEGF165a/VEGF165b
(Relative Fold Change)
2.0
1.5
1.0
0.5
0.0
Normoxic
Hypoxic
Normal Glucose
High Glucose

Increasing evidence suggests that hypoxia, through an imbalance between oxygen supply and demand, within the artery wall plays a role in the progression of atherosclerosis (**Figure 15**). We have previously shown that despite elevated arterial hypoxia in hyperglycemic APOE-deficient mice at 15 weeks of age, there is no corresponding increase in VEGF-A expression compared to normoglycemic APOE-deficient controls[31]. To further examine this disconnect, we have developed and characterized a novel transgenic mouse model to examine the effects of VEGF-A overexpression in macrophages, on oxygen imbalance and atherosclerosis progression. This mouse model utilizes the inducible cre-lox system, termed: **APOE$^{-/-}$ iCRE$^{+/-}$ ROSA26-FLOXSTOP-VEGF$_{164}$$^{+/-}$**.

4.8.1. Development of Novel Transgenic Mouse Model, Termed the APOE$^{-/-}$ iCRE$^{+/-}$ ROSA26-FLOXSTOP-VEGF$_{164}$$^{+/-}$

Development of this innovative and novel mouse model has taken approximately 1.5 years to complete. Original transgenic mice, ROSA26-FLOXSTOP-VEGF$_{164}$, were obtained from the Nagy Lab (*Nagy Lab*, Toronto, ON). These mice have a transgene inserted into the ROSA26 (*Gt(ROSA)26Sor*) gene locus. ROSA26 is a widely accepted gene locus for transgene insertion in animal research as the transgene integrates into a defined location on murine chromosome 6, rather than randomly

throughout the genome. This prevents possible gene disruption, and continually produces fertile and viable mice. FLOXSTOP-$VEGF_{164}$ is a transgene containing a STOP codon, flanked by two loxP sites, followed by $VEGF_{164}$, which codes for VEGF-A in mice.

These original mice were backcrossed 5 times onto a mouse strain with a C57Bl/6J genetic background. Backcrossing involves the breeding of two inbred strains to create hybrid generations (F1, F2 etc.) carrying the transgene of interest. This is important for transgenic strains with undefined genetic backgrounds. Backcrossing infers a genetic background almost genetically identical to C57Bl/6J mice. Control $APOE^{-/-}$ have a C57Bl/6J background. Therefore, backcrossing is vital for comparison.

C57Bl/6J ROSA26-FLOXSTOP-$VEGF_{164}$ were then crossed with $APOE^{-/-}$ to generate ROSA26-FLOXSTOP-$VEGF_{164}^{+/-}$ $APOE^{+/-}$ mice. These mice were crossed with cousins of the sample genotype to produce ROSA26-FLOXSTOP-$VEGF_{164}^{+/+}$ $APOE^{-/-}$ (6.25% of littermates).

To induce removal of the FLOXSTOP site, incorporation of an inducible cre recombinase is essential. For this project we selected Tg(Csf1r-cre/Esr1*)1Jwp/J mice (JAX, USA). These mice have a mutated murine estrogen receptor ligand domain which only binds synthetically injected tamoxifen. Therefore, when tamoxifen is IP injected into transgenic mice it binds to the mutated estrogen receptor domain allowing

cre recombinase to translocate into the nucleus and excise the STOP codon. These mice have cre recombinase controlled by colony stimulating factor 1 receptor (*Csf1r*) promoter. This *Csf1r* promoter is specific to macrophages. This allows for over expression of $VEGF_{164}$ specifically in macrophages and therefore, elevated total VEGF-A. Macrophage control was chosen to target VEGF-A overexpression in the atherosclerotic lesion of mice since plaques are high in macrophage content.

ROSA26-FLOXSTOP-$VEGF_{164}^{+/+}$ $APOE^{-/-}$ were then crossed with $APOE^{-/-}$ $iCRE^{+/-}$ to obtain $APOE^{-/-}$ $iCRE^{+/-}$ ROSA26-FLOXSTOP-$VEGF_{164}^{+/-}$ (50% of the littermates). Genotyping at each stage was essential to confirm genotype of interest for further breeding (**Figure 6**).

Figure 18. Crossing strategy to obtain $APOE^{-/-}$ $iCRE^{+/-}$ ROSA26-FLOXSTOP-$VEGF_{164}^{+/-}$ mice with a C57Bl/6J background.

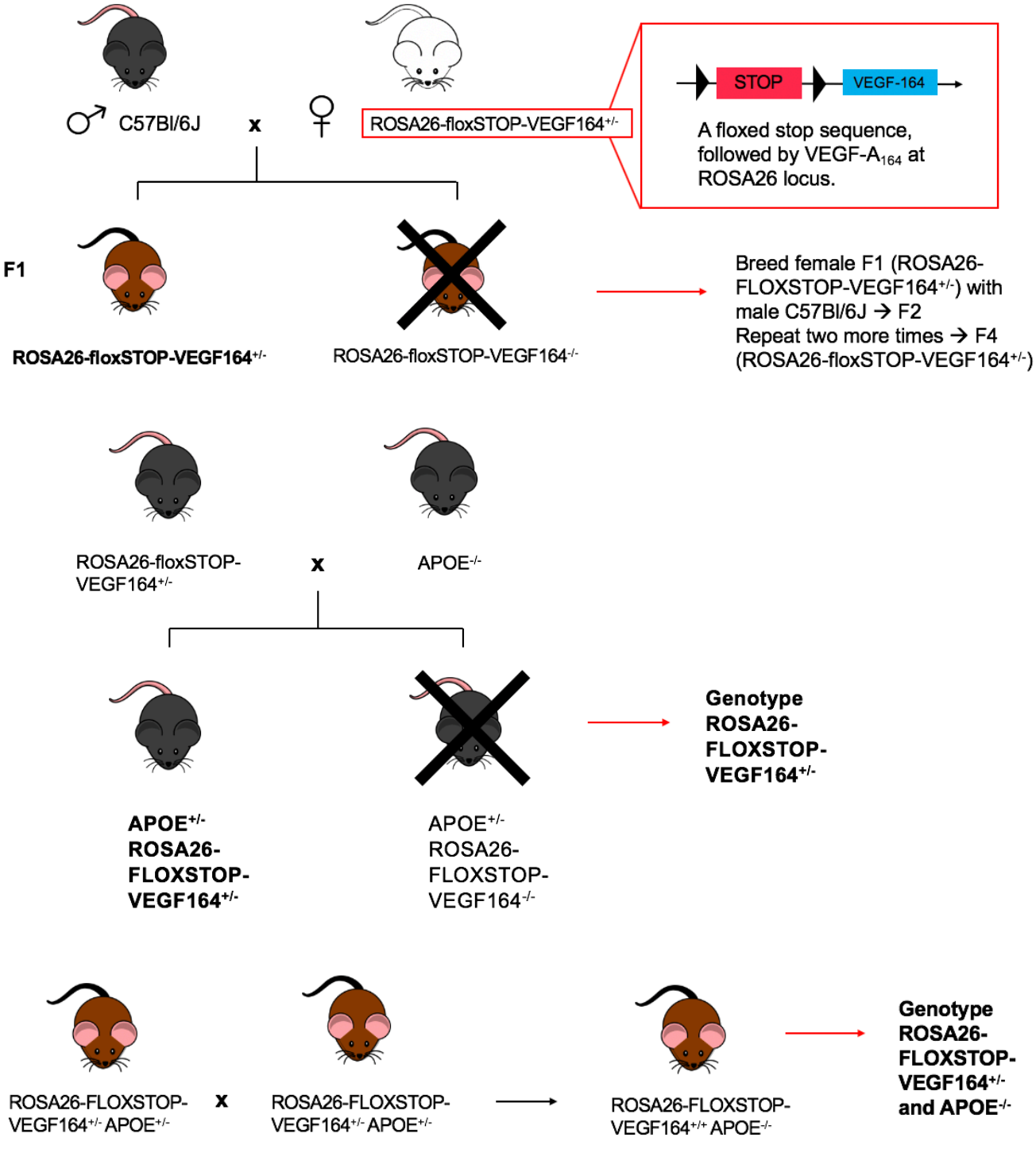
♂ C57Bl/6J
x
♀ ROSA26-floxSTOP-VEGF164+/-
STOP
VEGF-164
A floxed stop sequence, followed by VEGF-A164 at ROSA26 locus.
F1
ROSA26-floxSTOP-VEGF164+/-
ROSA26-floxSTOP-VEGF164-/-
Breed female F1 (ROSA26-FLOXSTOP-VEGF164+/-) with male C57Bl/6J → F2
Repeat two more times → F4 (ROSA26-floxSTOP-VEGF164+/-)
ROSA26-floxSTOP-VEGF164+/-
x
APOE-/-
APOE+/- ROSA26-FLOXSTOP-VEGF164+/-
APOE+/- ROSA26-FLOXSTOP-VEGF164-/-
Genotype ROSA26-FLOXSTOP-VEGF164+/-
ROSA26-FLOXSTOP-VEGF164+/- APOE+/-
x
ROSA26-FLOXSTOP-VEGF164+/- APOE+/-
ROSA26-FLOXSTOP-VEGF164+/+ APOE-/-
Genotype ROSA26-FLOXSTOP-VEGF164+/- and APOE-/-

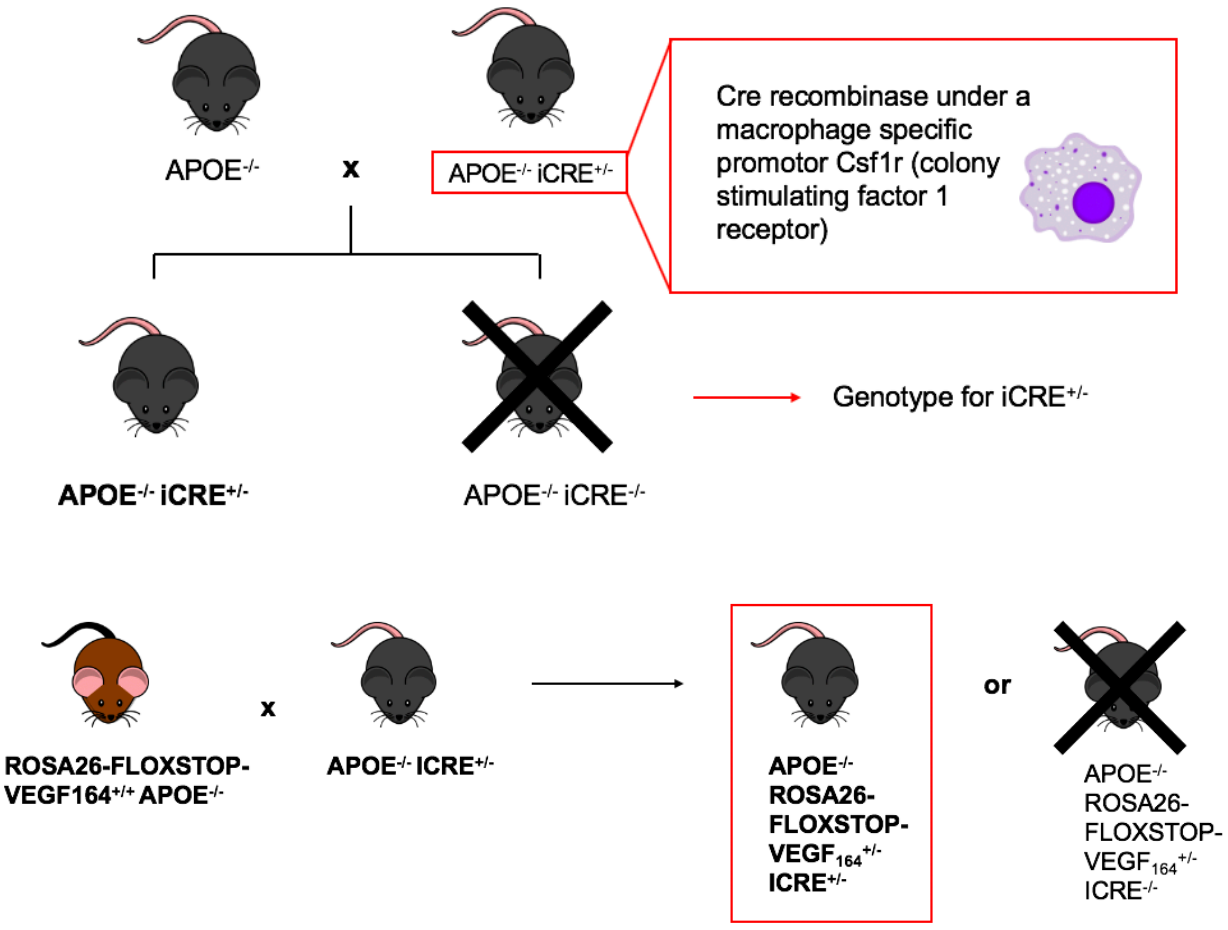
APOE-/-
x
APOE-/- iCRE+/-
Cre recombinase under a macrophage specific promotor Csf1r (colony stimulating factor 1 receptor)
APOE-/- iCRE+/-
APOE-/- iCRE-/-
Genotype for iCRE+/-
ROSA26-FLOXSTOP-VEGF164+/+ APOE-/-
x
APOE-/- ICRE+/-
APOE-/- ROSA26-FLOXSTOP-VEGF164+/- ICRE+/-
or
APOE-/- ROSA26-FLOXSTOP-VEGF164+/- ICRE-/-

4.8.2. Increased Macrophage VEGF-A Expression 1 Week After Tamoxifen Injection

VEGF-A gene and protein expression was analyzed in thioglycolate elicited peritoneal macrophages using qPCR and western blot 1 week after tamoxifen injection. Mice treated with tamoxifen had an approximate 3-fold, significant increase in VEGF-A gene expression compared to corn oil controls, without tamoxifen treatment (**Figure 19C**). VEGF-A protein expression was also increased in tamoxifen treated mice compared to corn oil controls (**Figure 19A-B**). Sample size needs to be increased to assess significance of this trend. Both control and tamoxifen treated mice had the same genotype.

Figure 19. Protein and gene expression analysis of cultured thioglycolate elicited peritoneal macrophages from ROSA26-FLOXSTOP-VEGF$_{164}^{+/-}$ iCRE$^{+/-}$ mice 1-week after IP injection of tamoxifen or corn oil. Protein concentration was determined by BCA and equal amounts of total macrophage protein was resolved by SDS-PAGE. Blots were probed with a rabbit polyclonal antibody for VEGF-A detection. **(A)** Representative western blot membrane showing single VEGF-A dimer (40 kD) used for quantification with (+) or without (-) tamoxifen injection. β-actin was used as a control. **(B)** Immunoblots were quantified by densitometry. All protein levels were normalized to β-actin and plotted relative to the control. **(C)** Total VEGF-A qPCR expression. Relative amounts of VEGF-A were normalized to β-actin and expressed as an arbitrary unit in which the control group equals 1. *n* = 3 – 5 per group. Data expressed as mean ± SEM. Significance calculated using an unpaired t-test. **p < 0.01 relative to no tamoxifen.

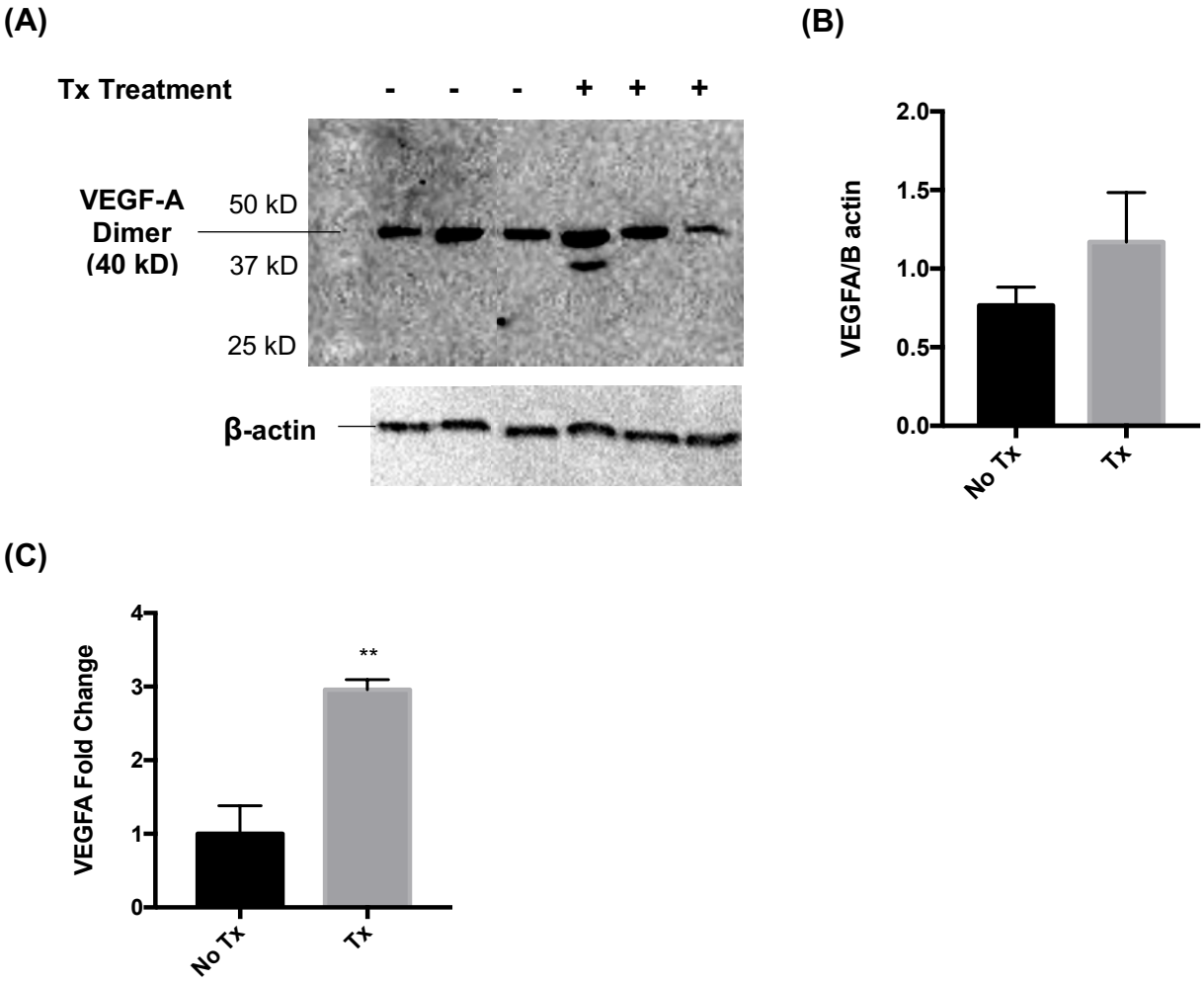
(A)
Tx Treatment
- - - + + +
VEGF-A
Dimer
(40 kD)
50 kD
37 kD
25 kD
β-actin
(B)
VEGFA/B actin
2.0
1.5
1.0
0.5
0.0
No Tx
Tx
(C)
VEGFA Fold Change
4
3
2
1
0
**
No Tx
Tx

5.0. DISCUSSION

5.1. Mechanisms Linking DM with Reduced Angiogenesis

Chronic hyperglycemia in DM is associated with microvascular and macrovascular pathologies, including reduced vasa vasorum angiogenesis and accelerated atherosclerosis development. Studies have identified detrimental, negative effects of high blood glucose levels on aortic vasa vasorum densities in hyperglycemic APOE-deficient mice[31] and in human left anterior descending coronary arteries of patients with DM[45]. However, the mechanisms underlying these differences are unknown. For this reason, we examined and elucidated the potential mechanisms associated with hyperglycemic induced reductions in vasa vasorum density *in vitro* and began to characterize possible *in vivo* interventions. These interventions included inhibitors of known vascular dysfunction pathways (**Figure 3**) such as 4PBA, NAC and PX.

Initial studies were completed to optimize a quantitative *in vitro* assay system, the tube formation assay. This assay involves seeding endothelial cells onto a matrix like basement membrane, allowing for endothelial cell migration and sprouting into tube-like capillary structures. This assay is frequently used in current research and is an established system for the study of angiogenesis *in vitro*[60-62]. Results demonstrated a

significant dose dependent reduction in the angiogenesis of HMVEC-Cs in hyperglycemic conditions up to 45 mM glucose compared to normoglycemic controls (**Figure 7**). This outcome suggests reduced HMVEC-C angiogenesis in hyperglycemia, not reduced viability, as glucose up to 45 mM in both normoxic and hypoxic environments had no effect on the survival of this cell type (**Figure 8**). These results are analogous to published *in vitro* tube formation data in the field [35-36, 60-62]. For example, assays seeded with HMVECs treated with 5 mM to 40 mM glucose show a significant dose dependent reduction in total tube length[60]. Further, assays seeded with human umbilical vein endothelial cells treated with 25 mM glucose showed a significant reduction in tube branch points[61]. These results are comparable to *in vivo* studies demonstrating reduced vasa vasorum and retinal microvascular density in diabetic mice[31]. Using these results, it is possible to predict increased levels of hypoxia around damaged microvessel densities, including large macro vessels that rely on oxygenation from microvessels, such as the aorta.

Although high glucose significantly reduces the angiogenesis of HMVEC-Cs (**Figure 8),** the mechanism remains unknown. Results show treatment with PX or NAC, but not 4PBA, mitigated the negative effects of high glucose on tube formation in hypoxia, indicating the ability of AGE inhibitors and antioxidants on preventing microvascular damage in

hyperglycemic conditions**.** However, none of the chemical interventions were able to rescue tube formation in normoxic environments (**Figure 10**).

To further elucidate the involvement of NAC or PX in elevating tube formation in high glucose conditions, gene expression of various angiogenic markers were examined. Analysis showed reduced VEGF-A and VEGFR-2 gene expression in high glucose, hypoxic environments compared to normal glucose, hypoxic environments (**Figure 11).** This implies that high glucose interferes with the normal upregulation of VEGF-A and VEGFR-2 under hypoxic conditions. VEGF-A and VEGFR-2 expression was unchanged in normoxia. The difference in normoxia and hypoxia may be explained by autocrine versus paracrine signalling. Generally, VEGF-A is not produced by endothelial cells under basal conditions, however studies using pulmonary artery endothelial cells show detectable VEGF-A expression in hypoxia[59]. This VEGF-A is secreted and acts on endothelial VEGFRs in an autocrine manner. Since this assay only includes HMVEC-Cs, VEGF-A can only be produced by this cell type.

Examination of reduced VEGF-A and VEGFR-2 expression in high glucose, hypoxic conditions was further examined with NAC, PX or 4PBA treatment. Analysis suggests that positive angiogenic outcomes using PX or NAC (**Figure 10**) may be attributed to protecting HMVEC-Cs from high glucose VEGF-A expression interference in hypoxia (**Figure 12**). VEGFR-

2 expression remained unchanged and low with 4PBA, NAC or PX treatment. However, increased VEGF-A expression with NAC or PX could act on existing VEGFRs to induce *in vitro* angiogenesis.

Interference of VEGF-A and VEGFR-2 expression in high glucose, hypoxic conditions was studied by examining markers of ER stress, oxidative stress and AGEs. These markers included 1) CHOP, an apoptotic UPR marker of ER stress, 2) eNOS and iNOS, markers of oxidative stress, reduced NO bioavailability and increased ROS and 3) IL-1β, a pro-inflammatory cytokine indicative of increased inflammation. qPCR experiments demonstrated increased iNOS gene expression in high glucose, hypoxic conditions (**Figure 11**) compared to other treatment groups ($p = 0.052$). Treatment with NAC or PX was able to reduce expression of iNOS back to normoglycemic control levels (**Figure 12**). CHOP, eNOS and IL-1β expression was not significantly affected by any treatment. These results suggest a major role of oxidative stress in hyperglycemic induced microvascular damage. Further investigations need to be completed to examine the correlation and positive or negative feedback of these pathways onto each other downstream of the group of genes assessed in this study to date.

5.2. Safety and Tolerance of 4PBA, PX and NAC *In Vivo*

Although *in vitro* tube formation assays are useful to elucidate mechanisms associated with hyperglycemic induced microvascular damage, there are many limitations to their use. For example, the assay only utilizes endothelial cells. Therefore, it is unable to recapitulate possible *in vivo* interactions with other cell types, tissues and organ systems. This is important since VEGF-A can be produced by a wide array of cell types, including macrophages, which induce paracrine angiogenesis signalling rather than autocrine signalling mechanisms. Further, although HMVEC-Cs are microvascular endothelial cells extracted from cardiac tissue they are not specific to the vasa vasorum, therefore the results of these experiments cannot be entirely compared to *in vivo* vasa vasorum plexuses. For these reasons, we completed a pilot study to test the efficacy and safety of *in vivo* supplementation and administration of 4PBA (1 g/kg bw/day), PX (250 mg/kg bw/day) or NAC (250 mg/kg bw/day) in the drinking water of streptozotocin (STZ) $APOE^{-/-}$ mice.

4PBA, NAC and PX dosing was selected using previous studies[48, 54, 63]. Although oral gavage treatment would be preferential to maintain equal dosing per mouse per day, we utilized supplemented drinking water to limit stress response and handling time that could interfere with the results of the experiment. Dosing was calculated based on the average

body weight of each mouse per cage, and the amount of water consumed per day (approximately 4 mL of water per day for a 25 g mouse). Therefore, 6.25 g of 4PBA or 1.56 g of NAC or PX was added to 1 L of sterile, buffered neutralized water. Pilot studies demonstrated a significantly reduced fasting blood glucose level in 16 week hyperglycemic STZ-APOE$^{-/-}$ mice treated with 4PBA compared to STZ-APOE$^{-/-}$ mice without 4PBA (**Figure 13A**). This reduction was not seen at the 12 week midpoint measurement suggesting that the effect of 4PBA occurred between 4 to 8 weeks of treatment (**Figure 13A**). This reduction is analogous to other findings[65]. For example, STZ rats treated with 4PBA for 20 days had significantly reduced blood glucose levels compared to DM controls[65]. This study also found elevated serum insulin levels, reduced β cell apoptosis and decreased pancreatic CHOP expression[65]. These results indicate a role of 4PBA in inhibiting pancreatic ER stress by reducing CHOP expression and resulting in attenuated β cell apoptosis via the UPR pathway[65]. Another potential mechanism could involve 4PBA increasing microvascular health within the pancreas. For example, STZ mice develop pancreatic islet dysfunction, including increased permeability and vascular leakage, one hour after STZ injection[74]. Therefore, future studies using our models could measure circulating insulin and C-peptide to analyze pancreatic health and assess β cell regeneration or vascular

protection with 4PBA. In addition, 4PBA significantly increased glucose recovery after 120 minutes in a glucose tolerance test and significantly reduced glucose tolerance test area under the curve (**Figure 13B-C**). Data showed no effect of NAC or PX on glucose tolerance in these mice.

Organ analysis of 16 week hyperglycemic STZ-APOE$^{-/-}$ mice treated with or without each chemical intervention was completed. Results demonstrate a 41% increase in left kidney weight to body weight ratio in hyperglycemic versus normoglycemic mice (**Figure 14).** Renal hypertrophy has been identified in other STZ models and may be attributed to extracellular matrix accumulation and glomerular mesangial cell expansion[64]. Treatment with 4PBA or PX in STZ-APOE$^{-/-}$ mice reduced left kidney weight back to values similar to the control group (**Figure 14A**). Further, liver weight to body weight ratio was elevated in all hyperglycemic groups with or without treatment compared to normoglycemic controls (**Figure 14B**). These results are comparable to other STZ models exhibiting hypertrophy of the liver due to triglyceride accumulation[64]. Perigonadal adipose tissue, a subset of visceral fat surrounding the gonads, was significantly reduced in hyperglycemic versus normoglycemic mice (**Figure 14D**). 4PBA, NAC or PX treatment had no effect on elevating adipose content. Pancreatic weight to body weight ratio remained stable in all experimental groups (**Figure 14C**).

The findings of this pilot study demonstrate that the selected doses of 4PBA, PX and NAC were well tolerated in our STZ-APOE$^{-/-}$ model. Future experiments will be completed to examine the effects of each of the chemical interventions on vasa vasorum density, vascular inflammation and atherosclerosis development. These experiments are crucial to confirm our *in vitro* findings of reduced angiogenesis, and decreased VEGF-A and VEGFR-2 levels in high glucose conditions.

5.3. Hypoxia Precedes Atherosclerosis Development

Scientific evidence clearly suggests that atherosclerosis and hypoxia are tightly linked through the anoxemia theory[31]. However, it is still unclear whether lesion progression in atherosclerosis stimulates arterial hypoxia or if arterial hypoxia stimulates lesion growth. To answer this question, we examined early arterial hypoxia in 10 week old hyperglycemic STZ-APOE$^{-/-}$ mice and normoglycemic APOE$^{-/-}$ controls. A 10 week end point was selected as very limited atherosclerosis is present at this time. Hypoxia was analyzed in aortic sections by staining for two known hypoxia markers, HIF-1α and hypoxyprobe. Findings demonstrated increased early atherosclerosis, elevated HIF-1α ($p = 0.10$) and elevated hypoxyprobe ($p = 0.24$) staining in the tunica intima of STZ-APOE$^{-/-}$ mice compared to age matched APOE$^{-/-}$ controls (**Figure 15**). This staining

appeared to localize to macrophage foam cells in the subintima. Future studies need to be completed to increase sample size, and reassess significance to confirm this trend. However, hypoxia seems to precede atherosclerosis.

5.4. Alternative Splicing in Glucose Treated THP-1 Derived Macrophages in Hypoxic Environments

To further examine subintimal macrophage recruitment and the impact of hypoxia on macrophage physiology, we utilized qPCR on PMAr THP-1 derived macrophages to assess angiogenic gene expression. Hypoxia increased total VEGF-A expression by approximately 100% compared to normoxia (**Figure 16A**). These results were expected, as HIF complex binding to HREs is increased in hypoxia, leading to increased transcription of hypoxia inducible genes such as VEGF (**Figure 4**). Analysis of VEGF-A alternative splice variants (VEGF-A_{165} and VEGF-A_{189}) demonstrated analogous results (**Figure 16B-C**). High glucose conditions had no effect on interfering the upregulation of VEGF-A in hypoxic conditions, demonstrating a distinct difference between endothelial cell and macrophage physiology (**Figure 11**).

Recent angiogenic research has examined the differential splice variants of VEGF-A_{165} acting as pro-angiogenic (VEGF-A_{165}a) and anti-

angiogenic (VEGF-A_{165}b) stimuli. VEGF-A_{165}b binds VEGFR-2, but has insufficient tyrosine phosphorylation, leading to weaker downstream angiogenic signalling compared to VEGF-A_{165}a. Further, binding of VEGF-A_{165}b takes up VEGFR-2, preventing VEGF-A_{165}a binding. qPCR analysis demonstrated a significant, 250% increase in VEGF-A_{165}a expression in hypoxic, normal glucose conditions compared to normoxia controls (**Figure 17A**). However, pro-angiogenic VEGF-A_{165}a expression was reduced in hypoxic, high glucose conditions compared to hypoxic, normal glucose conditions (**Figure 17A**). In contrast, VEGF-A_{165}b expression was elevated in hypoxia versus normoxia (**Figure 17B**). These findings suggest a potential switch from pro-angiogenic to anti-angiogenic forms of VEGF-A_{165} in high glucose that could help to explain decreased vasa vasorum density in DM *in vivo* (**Figure 17C**).

5.5. Development and Characterization of a Novel Transgenic Model to Study Vasa Vasorum Angiogenesis

Studies in our lab have identified a discrepancy between hypoxia and VEGF-A in STZ-APOE$^{-/-}$ mice such that despite elevations in HIF-1α, there is no corresponding increase in VEGF-A expression[31]. To further examine this difference, we developed and characterized a novel transgenic mouse model for the study of vasa vasorum angiogenesis and

atherosclerosis development in mice (**Figure 18**). Characterization of this model, by extracting peritoneal macrophages from transgenic mice injected with tamoxifen, demonstrated an elevated gene and protein expression of VEGF-A (**Figure 19**). We hope to utilize this model in future experiments to determine the effects of increasing vasa vasorum angiogenesis, by upregulating VEGF-A around the lesion, on atherosclerosis development in both normoglycemia and hyperglycemia. We hope our studies will help to assemble a working model that will ultimately help to slow the progression of CVD in patients with DM.

Figure 20. Pathways Associated with Hyperglycemic Induced Reductions in Angiogenesis and Accelerated Atherosclerosis.

Hyperglycemia results in significantly reduced HMVEC-C angiogenesis in both normoxic and hypoxic environments. Hypoxic outcomes may be attributed to reduced endothelial expression of vascular endothelial growth factor A (VEGF-A), reduced endothelial expression of vascular endothelial growth factor receptor 2 (VEGFR-2) and/or increased endothelial expression of inducible nitric oxide synthase (iNOS). Reduced macrophage expression of pro-angiogenic VEGFA-$_{165}$a (and VEGFA-$_{165}$a to anti-angiogenic VEGFA-$_{165}$b ratios) may also contribute to reduced paracrine VEGF secretion. Treatment with NAC or PX mitigates the negative effect of hyperglycemia on endothelial angiogenesis, VEGF-A and iNOS expression in hypoxic conditions. These results suggest that hyperglycemic induced oxidative stress and advanced glycation end product production interferes with physiologic VEGF-A, iNOS and VEGFA$_{165}$a gene expression in response to hypoxia.

Hyperglycemic Effects:

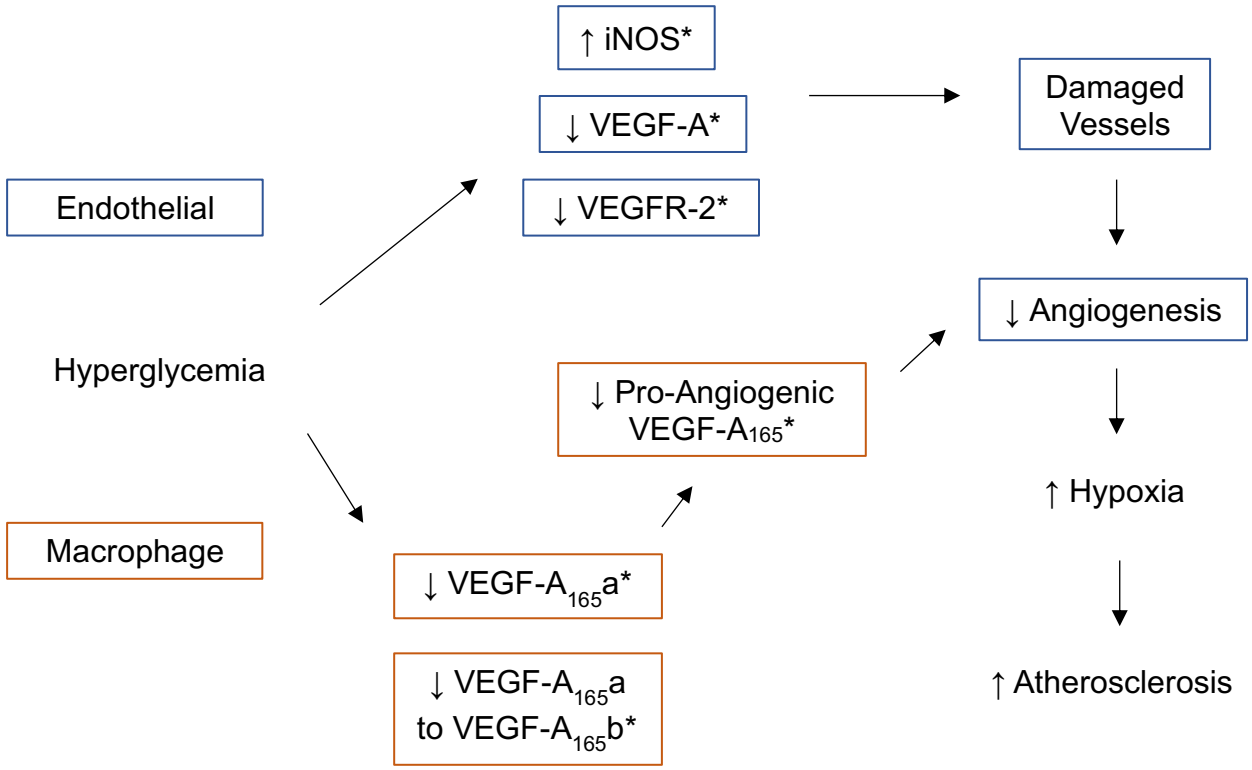

Potential Mechanism:

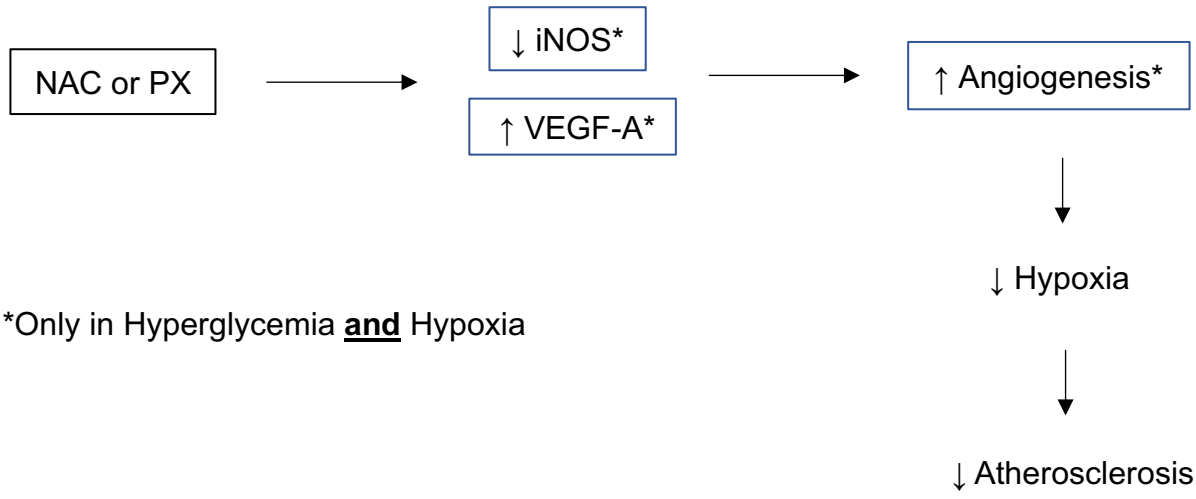

*Only in Hyperglycemia **and** Hypoxia

5.6. Future Directions

In addition to increasing the sample size for some of the experiments completed to date, there are a number of other experiments that would be useful to gather more information into this non-canonical field of atherosclerosis development.

5.6.1. Effect of VEGF-A or VEGFR-2 Agonists on HMVEC-C Angiogenesis using Tube Formation Assays

Data to this point suggests high glucose interferes with normal VEGF-A expression and tube angiogenesis in response to hypoxia. To further confirm this finding, it is important to assess the effect of VEGF-A or VEGFR-2 agonists by adding them to existing tube formation assays. If both supplements do increase angiogenesis in high glucose, it will help to confirm the hypothesis we have developed throughout this report.

5.6.2. Effect of *In Vivo* Supplementation of 4PBA, PX or NAC on Atherosclerosis Development and Vasa Vasorum

As previously mentioned, it is necessary for future studies to examine the *in vivo* link between each of the chemical interventions used in this study (4PBA, NAC or PX) on atherosclerosis and vasa vasorum density. These studies will not only confirm existing *in vitro* data, but will

highlight important differences or similarities between *in vitro* angiogenesis assays and physiological *in vivo* angiogenesis.

5.6.3. Effect of VEGF-A Upregulation in Macrophages on Atherosclerosis Development and Vasa Vasorum

A future long term project should utilize the developed transgenic mouse model to examine the effects of VEGF-A overexpression on atherosclerosis development and vasa vasorum angiogenesis. This experiment should include a wide variety of controls, including mice with the transgene without tamoxifen, mice without the transgene with tamoxifen, and mice without the transgene but with cre recombinase. These controls will confirm that any positive results are due to the experimental treatment of overexpressed VEGF-A, and not due to the potential cardioprotective role of tamoxifen or the potential disruptive effects of cre genetic insertion.

5.7. Limitations

Aside from the limitations already mentioned throughout this report, there are several other important factors to consider.

STZ Model: Although the streptozotocin (STZ) mouse model is a widely used and well accepted model for DM, it has various limitations to its use. Firstly, STZ is a small molecule and therefore, may induce toxic effects on other organs other than the pancreas. This is important to consider when analyzing organ statistics (**Figure 14**) and determining the difference between 1) effects of hyperglycemia or 2) influence of STZ toxicity. Secondly, STZ is generally a model of T1DM, an autoimmune disorder that destroys pancreatic β cells. This model fails to consider other forms of DM including T2DM, which involves insulin insufficiency and insulin resistance in peripheral tissues. Due to these limitations, it is important to complete follow up experiments with other mouse models of DM, including the $Ins2^{Akita}$ mouse, as well as DM models fed a HFD to induce metabolic dysfunction, similar to that seen in T2DM.

Hypoinsulinemia: These studies have a large focus on hyperglycemia, a key feature of DM. However, it is important to acknowledge that the hyperglycemic mouse models used in these studies also have low insulin concentrations, termed hypoinsulinemia. This condition results from reduced pancreatic β cells, cells that produce the peptide hormone insulin. Examining the balance between glucose and insulin levels *in vivo* is

important to distinguish effects due to 1) high glucose concentrations or 2) low insulin concentrations.

6.0. CONCLUSIONS

Individuals with DM have a 2 to 4-fold increased risk of CVD compared to those without DM. A major contributing factor to the development of CVD is atherosclerosis, a chronic inflammatory disease causing plaque build-up in medium to larger arteries. Increasing evidence suggests that hypoxia within the arterial wall is known to promote atherosclerosis, however the underlying mechanisms remain unclear. In these studies we examined reductions in aortic vasa vasorum oxygen supply, by utilizing an *in vitro* angiogenic assay on human cardiac microvascular endothelial cells (HMVEC-Cs). Results demonstrate a detrimental, negative effect of high glucose on HMVEC-C angiogenesis. This negative effect seems to be correlated with low VEGF-A and VEGFR-2 expression in response to hypoxia. Treatment with NAC and PX in hypoxic conditions increases angiogenesis and VEGF-A expression *in vitro*, suggesting a negative effect of oxidative stress and AGEs, more than ER stress, in this microvascular damage. Results also demonstrate hypoxia precedes atherosclerosis *in vivo* in an STZ atherosclerotic prone mouse model suggesting hypoxia drives accelerated atherosclerosis development in DM. Further, *in vitro* examination of macrophage physiology shows differential splicing of VEGF-A in hypoxic conditions,

such that the balance of VEGF-A_{165} shifted from pro-angiogenic (VEGF-A_{165}a) to anti-angiogenic (VEGF-A_{165}b) forms. An overall understanding of the non-canonical pathways linking DM and atherosclerosis will facilitate the development of new and more effective treatments for this epidemic.

7.0. REFERENCES

[1] Silva, D. G., Daley, S. R., Hogan, J., Lee, S. K., Teh, C. E., Hu, D. Y., . . . Vinuesa, C. G. (2011). Anti-Islet Autoantibodies Trigger Autoimmune Diabetes in the Presence of an Increased Frequency of Islet-Reactive CD4 T Cells. *Diabetes, 60*(8), 2102-2111. doi:10.2337/db10-1344

[2] Punthakee, Z., Goldenberg, R., & Katz, P. (2018). Definition, Classification and Diagnosis of Diabetes, Prediabetes and Metabolic Syndrome. *Canadian Journal of Diabetes, 42*. doi:10.1016/j.jcjd.2017.10.003

[3] Diabetes 360°: A Framework for a Diabetes Strategy for Canada. (n.d.). https://www.diabetes.ca/DiabetesCanadaWebsite/media/Advocacy-and-Policy/Diabetes-360-Executive-Summary-EN_1.pdf

[4] Tarr, J. M., Kaul, K., Chopra, M., Kohner, E. M., & Chibber, R. (2012). Pathophysiology of Diabetic Retinopathy. *ISRN Ophthalmology, 2013,* 1-13. doi: 10.1155/2013/343560.

[5] Yagihashi, S., Mizukami, H., & Sugimoto, K. (2010). Mechanism of diabetic neuropathy: Where are we now and where to go? *Journal of Diabetes Investigation, 2*(1), 18-32. doi:10.1111/j.2040-1124.2010.00070.x

[6] Haffner, S. M., Lehto, S., Rönnemaa, T., Pyörälä, K., & Laakso, M. (1998). Mortality from Coronary Heart Disease in Subjects with Type 2 Diabetes and in Nondiabetic Subjects with and without Prior Myocardial Infarction. *New England Journal of Medicine, 339*(4), 229-234. doi:10.1056/nejm199807233390404

[7] Beckman, J. A., Creager, M. A., & Libby, P. (2002). Diabetes and Atherosclerosis. *Jama, 287*(19), 2570. doi:10.1001/jama.287.19.2570

[8] Klein, R. (1996). Relation of Glycemic Control to Diabetic Microvascular Complications in Diabetes Mellitus. *Annals of Internal Medicine,124*(1_Part_2), 90. doi:10.7326/0003-4819-124-1_part_2-199601011-00003

[9] Kramer, C. K., et al. “Diabetic Retinopathy Predicts All-Cause Mortality and Cardiovascular Events in Both Type 1 and 2 Diabetes: Meta-

Analysis of Observational Studies." *Diabetes Care*, vol. 34, no. 5, 2011, pp. 1238–1244., doi:10.2337/dc11-0079.

[10] Theodorou, K., & Boon, R. A. (2018). Endothelial Cell Metabolism in Atherosclerosis. *Frontiers in Cell and Developmental Biology, 6*. doi:10.3389/fcell.2018.00082

[11] Lusis A. J. (2000). Atherosclerosis. *Nature*, *407*(6801), 233-41.

[12] Rafieian-Kopaei, M., Setorki, M., Doudi, M., Baradaran, A., & Nasri, H. (2014). Atherosclerosis: process, indicators, risk factors and new hopes. *International journal of preventive medicine*, *5*(8), 927-46.

[13] Getz, G. S., & Reardon, C. A. (2012). Animal models of atherosclerosis. *Arteriosclerosis, thrombosis, and vascular biology*, *32*(5), 1104-15.

[14] Cholesterol, Lipoproteins and the Liver. (n.d.). Retrieved from https://courses.washington.edu/conj/bess/cholesterol/liver.html

[15] Fernández-Friera, L., Fuster, V., López-Melgar, B., Oliva, B., García-Ruiz, J. M., Mendiguren, J., … Sanz, J. (2017). Normal LDL-Cholesterol Levels Are Associated With Subclinical Atherosclerosis in the Absence of Risk Factors. *Journal of the American College of Cardiology*, *70*(24), 2979–2991. doi: 10.1016/j.jacc.2017.10.024

[16] Ritman, E., & Lerman, A. (2007). The dynamic vasa vasorum. *Cardiovascular Research, 75*(4), 649-658. doi:10.1016/j.cardiores.2007.06.020

[17] Kwon, T., Lerman, L. O., & Lerman, A. (2015). The Vasa Vasorum in Atherosclerosis. *Journal of the American College of Cardiology, 65*(23), 2478-2480. doi:10.1016/j.jacc.2015.04.032

[18] Sedding, D. G., Boyle, E. C., Demandt, J. A., Sluimer, J. C., Dutzmann, J., Haverich, A., & Bauersachs, J. (2018). Vasa Vasorum Angiogenesis: Key Player in the Initiation and Progression of Atherosclerosis and Potential Target for the Treatment of Cardiovascular Disease. *Frontiers in Immunology, 9*. doi:10.3389/fimmu.2018.00706

[19] Zeiher, A. M., Drexler, H., Wollschläger, H., & Just, H. (1991). Endothelial dysfunction of the coronary microvasculature is associated with coronary blood flow regulation in patients with early

atherosclerosis. *Circulation, 84*(5), 1984-1992. doi:10.1161/01.cir.84.5.1984

[20] Wright, E., Scism-Bacon, J. L., & Glass, L. C. (2006). Oxidative stress in type 2 diabetes: The role of fasting and postprandial glycaemia. *International Journal of Clinical Practice, 60*(3), 308-314. doi:10.1111/j.1368-5031.2006.00825.x

[21] Giacco, F., & Brownlee, M. (2010). Oxidative stress and diabetic complications. *Circulation research*, *107*(9), 1058-70.

[22] Krock, B. L., Skuli, N., & Simon, M. C. (2011). Hypoxia-Induced Angiogenesis: Good and Evil. *Genes & Cancer, 2*(12), 1117-1133. doi:10.1177/1947601911423654

[23] Dainin, K., Ide, R., Maeda, A., Suyama, K., & Akagawa, M. (2017). Pyridoxamine scavenges protein carbonyls and inhibits protein aggregation in oxidative stress-induced human HepG2 hepatocytes. *Biochemical and Biophysical Research Communications, 486*(3), 845-851. doi:10.1016/j.bbrc.2017.03.147

[24] Stitt, A., Gardiner, T. A., Anderson, N. L., Canning, P., Frizzell, N., Duffy, N., . . . Thorpe, S. R. (2002). The AGE Inhibitor Pyridoxamine Inhibits Development of Retinopathy in Experimental Diabetes. *Diabetes, 51*(9), 2826-2832. doi:10.2337/diabetes.51.9.2826

[25] Dludla, P. V., Dias, S. C., Obonye, N., Johnson, R., Louw, J., & Nkambule, B. B. (2018). A Systematic Review on the Protective Effect of N-Acetyl Cysteine Against Diabetes-Associated Cardiovascular Complications. *American Journal of Cardiovascular Drugs, 18*(4), 283-298. doi:10.1007/s40256-018-0275-2

[26] Kolb, P., Ayaub, E., Zhou, W., Yum, V., Dickhout, J., & Ask, K. (2015). The therapeutic effects of 4-phenylbutyric acid in maintaining proteostasis. *The International Journal of Biochemistry & Cell Biology, 61*, 45-52. doi:10.1016/j.biocel.2015.01.015

[27] Goodsell, D. S. (2002). The Molecular Perspective: VEGF and Angiogenesis. *The Oncologist, 7*(6), 569-570. doi:10.1634/theoncologist.7-6-569

[28] Bruce, D. The Role of VEGF in Angiogenesis. Retrieved January 22, 2019, from https://www.abcam.com/cancer/the-role-of-vegf-in-angiogenesis

[29] Polin, R. A., Abman, S. H., Rowitch, D. H., Benitz, W. E., & Fox, W. W. (2017). *Fetal and Neonatal Physiology*. Philadelphia: Elsevier.

[30] Langheinrich, A. C., Michniewicz, A., Sedding, D. G., Walker, G., Beighley, P. E., Rau, W. S., . . . Ritman, E. L. (2006). Correlation of Vasa Vasorum Neovascularization and Plaque Progression in Aortas of Apolipoprotein E −/− /Low-Density Lipoprotein −/− Double Knockout Mice. *Arteriosclerosis, Thrombosis, and Vascular Biology, 26*(2), 347-352. doi:10.1161/01.atv.0000196565.38679.6d

[31] Veerman, K., Venegas-Pino, D., Shi, Y., Khan, M., Gerstein, H., & Werstuck, G. (2013). Hyperglycaemia is associated with impaired vasa vasorum neovascularization and accelerated atherosclerosis in apolipoprotein-E deficient mice. *Atherosclerosis, 227*(2), 250-258. doi:10.1016/j.atherosclerosis.2013.01.018

[32] DeCicco-Skinner, K. L., Henry, G. H., Cataisson, C., Tabib, T., Gwilliam, J. C., Watson, N. J., Bullwinkle, E. M., Falkenburg, L., O'Neill, R. C., Morin, A., … Wiest, J. S. (2014). Endothelial cell tube formation assay for the in vitro study of angiogenesis. *Journal of visualized experiments : JoVE*, (91), e51312. doi:10.3791/51312

[33] Daigneault, Marc & Preston, Julie & Marriott, Helen & Whyte, Moira & Dockrell, David. (2010). The Identification of Markers of Macrophage Differentiation in PMA-Stimulated THP-1 Cells and Monocyte-Derived Macrophages. *PloS one*. 5. e8668. 10.1371/journal.pone.0008668.

[34] Ribatti, D., & Crivellato, E. (2012). “Sprouting Angiogenesis”, a Reppraisal. *Developmental Biology*, *372*(2), 157-165. doi:10.1016/j.ydbio.2012.09.018

[35] Prisco, A. R., Bukowy, J. D., Hoffmann, B. R., Karcher, J. R., Exner, E. C., & Greene, A. S. (2014). Automated quantification reveals hyperglycemia inhibits endothelial angiogenic function. *PloS one*, *9*(4), e94599. doi:10.1371/journal.pone.0094599

[36] Lee, C.-H., Shieh, Y.-S., Hsiao, F.-C., Kuo, F.-C., Lin, C.-Y., Hsieh, C.-H., & Hung, Y.-J. (2016). High glucose induces human endothelial

dysfunction through an Axl-dependent mechanism. *Diabetes Research and Clinical Practice*, *120*. doi: 10.1016/s0168-8227(16)31097-x

[37] Zheng, F., Xing, S., Gong, Z., Mu, W., & Xing, Q. (2014). Silence of NLRP3 Suppresses Atherosclerosis and Stabilizes Plaques in Apolipoprotein E-Deficient Mice. *Mediators of Inflammation*, *2014*, 1–8. doi: 10.1155/2014/507208

[38] Pinhas-Hamiel, O., & Zeitler, P. (2007). Acute and chronic complications of type 2 diabetes mellitus in children and adolescents. *The Lancet, 369*(9575), 1823-1831. doi:10.1016/s0140-6736(07)60821

[39] Rosival, V. (2014). Management of adult diabetic ketoacidosis. *Diabetes, Metabolic Syndrome and Obesity: Targets and Therapy,* 571. doi:10.2147/dmso.s73896

[40] Wang, W., & Lo, A. (2018). Diabetic Retinopathy: Pathophysiology and Treatments. *International Journal of Molecular Sciences*, *19*(6), 1816. doi: 10.3390/ijms19061816

[41] Cooper ME, Gilbert RE, Epstein M. Pathophysiology of diabetic nephropathy. *Metabolism*. 1998;47(12 Suppl 1):3–6. doi:10.1016/s0026-0495(98)90362-6

[42] Tucker WD, Mahajan K. Anatomy, Blood Vessels. [Updated 2018 Nov 10]. In: StatPearls [Internet]. Treasure Island (FL): StatPearls Publishing; 2018 Jan-. Available from: https://www.ncbi.nlm.nih.gov/books/NBK470401/

[43] Barger, A. C., Beeuwkes,Reinier, I.,II, Lainey, L. L., & Silverman, K. J. (1984). Hypothesis: Vasa vasorum and neovascularization of human coronary arteries: A possible role in the pathophysiology of atherosclerosis. *The New England Journal of Medicine, 310*(3), 175-177.

[44] Kwon, T.-G., Lerman, L. O., & Lerman, A. (2015). The Vasa Vasorum in Atherosclerosis. *Journal of the American College of Cardiology*, *65*(23), 2478–2480. doi: 10.1016/j.jacc.2015.04.032

[45] Gerstein, H. C., Nair, V., Chaube, R., Stoute, H., & Werstuck, G. (2019). Dysglycemia and the Density of the Coronary Vasa Vasorum. *Diabetes Care*, *42*(5), 980–982. doi: 10.2337/dc18-2483

[46] Prasad A, Bekker P, Tsimikas S. Advanced glycation end products and diabetic cardiovascular disease. *Cardiol Rev*. 2012;20(4):177–183. doi:10.1097/CRD.0b013e318244e57c

[47] Nin, J. W., Jorsal, A., Ferreira, I., Schalkwijk, C. G., Prins, M. H., Parving, H.-H., … Stehouwer, C. D. (2011). Higher Plasma Levels of Advanced Glycation End Products Are Associated With Incident Cardiovascular Disease and All-Cause Mortality in Type 1 Diabetes: A 12-year follow-up study. *Diabetes Care*, *34*(2), 442–447. doi: 10.2337/dc10-1087

[48] Watson, A. M. D., Soro-Paavonen, A., Sheehy, K., Li, J., Calkin, A. C., Koitka, A., … Jandeleit-Dahm, K. J. A. (2010). Delayed intervention with AGE inhibitors attenuates the progression of diabetes-accelerated atherosclerosis in diabetic apolipoprotein E knockout mice. *Diabetologia*, *54*(3), 681–689. doi: 10.1007/s00125-010-2000-9

[49] Kaneto, H., Katakami, N., Matsuhisa, M., & Matsuoka, T.-A. (2010). Role of Reactive Oxygen Species in the Progression of Type 2 Diabetes and Atherosclerosis. *Mediators of Inflammation*, *2010*, 1–11. doi: 10.1155/2010/453892

[50] Förstermann, U., Xia, N., & Li, H. (2017). Roles of Vascular Oxidative Stress and Nitric Oxide in the Pathogenesis of Atherosclerosis. *Circulation Research*, *120*(4), 713–735. doi: 10.1161/circresaha.116.309326

[51] Shimada, K., Murayama, T., Yokode, M., Kita, T., Uzui, H., Ueda, T., … Kishimoto, C. (2009). N-Acetylcysteine Reduces the Severity of Atherosclerosis in Apolipoprotein E-Deficient Mice by Reducing Superoxide Production. *Circulation Journal*, *73*(7), 1337–1341. doi: 10.1253/circj.cj-08-1148

[52] Kaga, A. K., Barbanera, P. O., Carmo, N. O. L. D., Rosa, L. R. D. O., & Fernandes, A. A. H. (2018). Effect of N-Acetylcysteine on Dyslipidemia and Carbohydrate Metabolism in STZ-Induced Diabetic Rats. International Journal of Vascular Medicine, 2018, 1–7. doi: 10.1155/2018/6428630

[53] Sage, A. T., Walter, L. A., Shi, Y., Khan, M. I., Kaneto, H., Capretta, A., & Werstuck, G. H. (2010). Hexosamine biosynthesis pathway flux promotes endoplasmic reticulum stress, lipid accumulation, and

inflammatory gene expression in hepatic cells. *American Journal of Physiology-Endocrinology and Metabolism*, *298*(3). doi: 10.1152/ajpendo.00507.2009

[54] Huang, A., Young, T. L., Dang, V. T., Shi, Y., Mcalpine, C. S., & Werstuck, G. H. (2017). 4-phenylbutyrate and valproate treatment attenuates the progression of atherosclerosis and stabilizes existing plaques. *Atherosclerosis*, *266*, 103–112. doi: 10.1016/j.atherosclerosis.2017.09.034

[55] Ratcliffe, P. J. (2007). HIF-1 and HIF-2: working alone or together in hypoxia? *Journal of Clinical Investigation*, *117*(4), 862–865. doi: 10.1172/jci31750

[56] Koh, M. Y., & Powis, G. (2012). Passing the baton: the HIF switch. *Trends in Biochemical Sciences*, *37*(9), 364–372. doi: 10.1016/j.tibs.2012.06.004

[57] Harper, S. J., & Bates, D. O. (2008). VEGF-A splicing: the key to anti-angiogenic therapeutics?. *Nature reviews. Cancer*, *8*(11), 880–887. https://doi.org/10.1038/nrc2505

[58] Gelfand, M. V., Hagan, N., Tata, A., Oh, W. J., Lacoste, B., Kang, K. T., Kopycinska, J., Bischoff, J., Wang, J. H., & Gu, C. (2014). Neuropilin-1 functions as a VEGFR2 co-receptor to guide developmental angiogenesis independent of ligand binding. *eLife*, *3*, e03720. https://doi.org/10.7554/eLife.03720

[59] Liu, Y., Cox, S. R., Morita, T., & Kourembanas, S. (1995). Hypoxia Regulates Vascular Endothelial Growth Factor Gene Expression in Endothelial Cells. *Circulation Research*, *77*(3), 638–643. doi: 10.1161/01.res.77.3.638

[60] Lee, C.-H., Shieh, Y.-S., Hsiao, F.-C., Kuo, F.-C., Lin, C.-Y., Hsieh, C.-H., & Hung, Y.-J. (2014). High glucose induces human endothelial dysfunction through an Axl-dependent mechanism. *Cardiovascular Diabetology*, *13*(1), 53. doi: 10.1186/1475-2840-13-53

[61] Wang, X., Ackermann, M., Neufurth, M., Wang, S., Li, Q., Feng, Q., … Müller, W. (2017). Restoration of Impaired Metabolic Energy Balance (ATP Pool) and Tube Formation Potential of Endothelial Cells under “high glucose”, Diabetic Conditions by the Bioinorganic

Polymer Polyphosphate. *Polymers*, *9*(11), 575. doi: 10.3390/polym9110575

[62] Zhou, Jian & Ni, Xiaotian & Huang, Xiaojie & Yao, Julei & He, Qizhi & Wang, Kai & Duan, Tao. (2016). Potential Role of Hyperglycemia in Fetoplacental Endothelial Dysfunction in Gestational Diabetes Mellitus. Cellular Physiology and Biochemistry. 39. 1317-1328. 10.1159/000447836.

[63] Ma, Y., Gao, M., & Liu, D. (2016). N-acetylcysteine Protects Mice from High Fat Diet-induced Metabolic Disorders. *Pharmaceutical Research*, *33*(8), 2033–2042. doi: 10.1007/s11095-016-1941-1

[64] Zafar, M., & Naqvi, S. N.-U.-H. (2010). Effects of STZ-Induced Diabetes on the Relative Weights of Kidney, Liver and Pancreas in Albino Rats: A Comparative Study. *International Journal of Morphology*, *28*(1). doi: 10.4067/s0717-95022010000100019

[65] Zhu, M., Guo, M., Fei, L., Pan, X.-Q., & Liu, Q.-Q. (2013). 4-Phenylbutyric acid attenuates endoplasmic reticulum stress-mediated pancreatic β-cell apoptosis in rats with streptozotocin-induced diabetes. *Endocrine*, *47*(1), 129–137. doi: 10.1007/s12020-013-0132-7

[66] Wenger, R. H., Kurtcuoglu, V., Scholz, C. C., Marti, H. H., & Hoogewijs, D. (2015). Frequently asked questions in hypoxia research. *Hypoxia (Auckland, N.Z.)*, *3*, 35-43. doi:10.2147/HP.S92198

[67] Thurston, G., & Kitajewski, J. (2008). VEGF and Delta-Notch: Interacting signalling pathways in tumour angiogenesis. *British Journal of Cancer, 99*(8), 1204-1209. doi:10.1038/sj.bjc.6604484

[68] Kota, S. K., Meher, L. K., Jammula, S., Kota, S. K., Krishna, S. V., & Modi, K. D. (2012). Aberrant angiogenesis: The gateway to diabetic complications. *Indian journal of endocrinology and metabolism*, *16*(6), 918-30.

[69] Pizzorno J. (2014). Glutathione!. *Integrative medicine (Encinitas, Calif.)*, *13*(1), 8–12.

[70] Wallert, M., Schmölz, L., Galli, F., Birringer, M., & Lorkowski, S. (2014). Regulatory metabolites of vitamin E and their putative relevance for

atherogenesis. *Redox Biology*, *2*, 495–503. doi: 10.1016/j.redox.2014.02.002

[71] Björnheden T., Levin, M., Evaldsson, M., & Wiklund, O. (1999). Evidence of Hypoxic Areas Within the Arterial Wall In Vivo. *Arteriosclerosis, Thrombosis, and Vascular Biology*, *19*(4), 870–876. doi: 10.1161/01.atv.19.4.870

[72] Tahergorabi, Z., & Khazaei, M. (2012). A review on angiogenesis and its assays. *Iranian journal of basic medical sciences*, *15*(6), 1110–1126.

[73] Jenkins, N. (2019, March 29). The Vasa Vasorum. Retrieved May 18, 2020, from https://www.crossfit.com/essentials/vasa-vasorum-part-1

[74] Medarova, Z., Castillo, G., Dai, G., Bolotin, E., Bogdanov, A., & Moore, A. (2007). Noninvasive Magnetic Resonance Imaging of Microvascular Changes in Type 1 Diabetes. *Diabetes*, *56*(11), 2677–2682. doi: 10.2337/db07-0822